Seasonal cycle of phytoplankton at Drøbak with emphasis on *Skeletonema*

Louise Valestrand

Master of Science thesis

Department of Biosciences
Section for Aquatic Biology and Toxicology

UNIVERSITY OF OSLO

February 2018

Seasonal cycle of phytoplankton at Drøbak with emphasis on *Skeletonema*

Louise Valestrand
lvalestrand@gmail.com
+47 978 90 292

Supervisors
Wenche Eikrem
wenche.eikrem@nhm.uio.no

Bente Edvardsen
bente.edvardsen@ibv.uio.no

Dag Øystein Hjermann
dag.hjermann@niva.no

Section for Aquatic Biology and Toxicology
Department of Biosciences
University of Oslo
2018

Year: 2018

Title: Seasonal cycle of phytoplankton at Drøbak with emphasis on *Skeletonema*

Author: Louise Valestrand

http://www.duo.uio.no

Printed: Reprosentralen, Universitetet i Oslo

Abstract

This study aimed to investigate the seasonal variation of phytoplankton at Drøbak in relation to environmental parameters. The genus *Skeletonema* was of particular interest due to its significant role in the spring bloom, and uncertainty regarding its identity in Oslofjorden. Monthly cruises were conducted with RV Trygve Braarud. A CTD and a Secchi disk provided the hydrographical data. Water samples for phytoplankton analysis were gathered by net hauls and Niskin bottles. Taxa and species identifications were achieved in a light microscope and a scanning electron microscope (SEM), and cell enumeration was done under an inverted light microscope at the University of Oslo. Historical net samples from Drøbak from the UiO Grethe Hasle Diatom Collection and a culture (strain NIVA-Bac 1) isolated at Drøbak during the summer of 1962 were studied in SEM to investigate earlier occurring species of *Skeletonema*. The present study uncovered a seasonal dynamic phytoplankton growth, finding the same trends as previously documented by NIVA and IMR monitoring programs. However, the cell counts were lower and the number of taxa was higher compared to samples collected at Drøbak between 1957 – 1958 by Hasle and Smayda. This difference might be due to a eutrophication in Oslofjorden in the 1950s, which illustrates how phytoplankton growth varies according to the surrounding environment. Only one species of *Skeletonema* was detected at Drøbak from the samples collected in the present study and from the NHM: *S. marinoi*. However, the strain NIVA-Bac 1 was assigned to *S. pseudocostatum*, which implies that other species of *Skeletonema* may appear in Oslofjorden, presumably due to different water currents that carry various species of phytoplankton. Yet, *S. marinoi* was observed in every season in the present study, illustrating that it is adapted to different environmental conditions. Observed variations in *S. marinoi* cell size and chain morphology correlated with changing environmental parameters. Larger cells and chains arose during the spring at a salinity around 24 and temperature at 9°C, correlating with timing of the highest cell abundance. Smaller cells and chains occurred under assumingly more unfavorable conditions during the winter and summer with the lowest and highest values of salinity and temperature. The cell counts of *Skeletonema* sp. decreased when these unfavorable conditions arose, which suggest that some cells remained in surface waters, whereas others sedimented, forming resting stages that will germinate during better circumstances. The variation in cell and chain morphology may be strategies to increase survival of *S. marinoi* and may be explanations to its success in Oslofjorden.

Acknowledgement

The work presented in this master thesis was accomplished at the Section for Aquatic Biology and Toxicology at the Department of Bioscience in the University of Oslo in collaboration with the Norwegian Institute of Water Research under the supervision of associate professor Wenche Eikrem (UiO/NIVA), professor Bente Edvardsen (UiO), and researcher scientist Dag Øystein Hjermann (NIVA).

This thesis would not have been accomplished without the help and guidance of many people of whom I am grateful. First, I would like to thank my supervisors Wenche Eikrem and Bente Edvardsen. Their shared joy for algae has been contagious, and their dedication, patience and kindness have made this project an unforgettable and educational experience.

I would also like to thank Dag Øystein Hjermann. Without his help, I would still be working with R. His help has been crucial for the project, and I am very thankful. At the same time, I would like to give a huge appreciation to Mats Huserbråten, Professor Karl Inne Ugland and Kim Aalborg, whom have all helped me with R and other statistical problems.

A huge thanks to the crew at RV Trygve Braarud. Sindre Holm, Tom Opsahl and Tor Egil Wold have always been available for questions and made the cruises unforgettable. Also, a lot of thanks to Luka Supraha who has guided me through the complicated world of genetics, both in the lab and with the later analysis. I would like to thank Jacquelyn Diamond and Julie Sørlie Paus-Knudsen for the thorough proofreading and guidance in writing.

Lastly, I would like to say thanks to all the students in room 4405 where many a discussion and laughter have occurred, and all my thanks to family and friends who have never stopped to believe in me and whom have made this master project a fun and memorable experience.

Table of contents

1 Introduction

Phytoplankton are primary producers found at the bottom of the aquatic food web. They have a short and fast life cycle that is generated by physical and biological parameters. With the right conditions, they may bloom into extremely high numbers, and die out just as fast with unfavorable conditions. Life in the aquatic environment in the temperate sea has been adapted around the annual phytoplankton cycle. It is normal to find a peak in zooplankton shortly after the peak in phytoplankton. Fish larvae, which depend on the zooplankton as a food source, tend to spawn at the same time. A change in the timing of blooming may have an impact on higher trophic levels. Understanding the study of annual recurring life cycle events, the phenology, can give insight into potential environmental changes.

A trend during the last decade is that the surface temperature is increasing, in addition to heavier rainfall (Füssel et al., 2017). An increase in rainfall alters the salinity and nutrient concentration in the top layer of the sea. Phytoplankton are in the surface layer, as that is where there is sunlight for photosynthesis. Changes in freshwater supply and surface temperature may have an impact on the phytoplankton phenology. In Oslofjorden phytoplankton composition and seasonal dynamics have been studied for almost a century. Gran and Gaarder with their students at the University of Oslo started these studies in the 1920s (Gaarder & Gran, 1927). Further studies have been done by several other researchers (Braarud & Bursa, 1939; Hasle & Smayda, 1960; Paasche & Kristiansen, 1982; Throndsen et al., 2007). During the last decade, there have been annual reports from monitoring programs organized by, e.g., NIVA, DNV, and IMR which focus on physical parameters such as oxygen and nutrient concentration, as well as the phytoplankton composition (Aure et al., 2014; Dragsund et al., 2006; Walday et al., 2015). Because of these studies, it is possible to observe if there have been changes in the phytoplankton composition and the timing of the blooming, and which parameters may influence growth and death.

Within the phytoplankton, the diatoms have a significant role and are responsible for 40% of the oceanic primary production (Nelson et al., 1995). A genus within the diatoms, *Skeletonema* (Greville), is documented as an essential group of algae in Oslofjorden, especially during the spring bloom (Braarud & Bursa, 1939; Walday et al., 2011, 2015). Despite this, little is known about *Skeletonema*'s lifecycle and life strategies in Oslofjorden. Earlier it was believed that *Skeletonema costatum* was the *Skeletonema* species found in Oslofjorden (Hasle & Smayda,

1960; Walday et al., 2015) There have been no later species investigations concerning *Skeletonema* in Oslofjorden. Suspicion about the *Skeletonema* diversity in Oslofjorden increased after *Skeletonema marinoi* was found along the Swedish west coast by Godhe et al. (2006). The suspicion was further amplified after a geographical investigation of *Skeletonema* species where *S. marinoi* was the only species found in Skagerrak (Kooistra et al., 2008). Yet, no later research has been performed on the *Skeletonema* in Oslofjorden.

The lack of knowledge about *Skeletonema* in Oslofjorden and the necessity to investigate phytoplankton phenology lead to this thesis. There is a possibility to compare results with earlier findings because of monitoring research and due to the investigation of seasonal cycle at Drøbak between 1957 – 1958 performed by Hasle and Smayda (1960).

1.1 Oslofjorden

It is essential to understand the topography and physical conditions in Oslofjorden to understand the phytoplankton phenology further. The fjord runs into Skagerrak at Færder in the south and stretches 100 km up into to the country of Norway. The fjord divides into the inner and the outer part of Oslofjorden where the Drøbak sill marks the separation point. This sill is the shallowest in the fjord, with a mean of 20 meters depth. The depth in inner Oslofjorden varies between 160 – 50 meters, whereas in outer Oslofjorden outside the Drøbak sill the depth drops down to 200 meters (Aure et al., 2014; Baalsrud & Magnusson, 2002).

In addition to topography, freshwater, wind conditions and different water masses may influence the properties and movement of water in Skagerrak and Oslofjorden. Atlantic water arrives from the North Sea through the south of the Norwegian trench. It is high-density cold-water with a salinity of 35‰ and high nutrient concentration. From the south, water arrives from the German Bight along the coast of Denmark. These water masses are mainly wind driven when there are southern winds during the summer. From the western coast of Denmark and the coast of Sweden, water arrives from the Baltic Sea and the Kattegat. These are the water masses that dominate the Skagerrak surface water, as it has a lower salinity than the heavy Atlantic water (Sætre, 2007). The different currents in the Skagerrak create a counter clock-wise circulation that favors an upwelling of nutrient-rich water (Lange et al., 1992). The water in the Skagerrak is the water that enters Oslofjorden. In outer Oslofjorden freshwater is added through two main rivers: Drammenselva which empties at Drammen and Glomma which

empties in the area around Fredrikstad (Figure 1). These two rivers transport high amounts of nutrients, especially during the spring when there is snow melting and heavy rainfall.

Figure 1*: Map of Oslofjorden, with arrow pointing at the Drøbak sill and the river mouth of Glomma and Drammenselva (Oslofjorden.no)*

Oslofjorden has been going through tremendous changes during the last century. The input of nutrients into the fjord started to increase with the population and industry growth and was further amplified by sewage that ran into the fjord after the introduction of the water closet in the early 1900s. The increase of nutrients lead to eutrophication that peaked in the 1970s. Eutrophication can lead to high algal growth, but can also create anoxic conditions with time. Due to the unfavorable consequences of the eutrophication, actions were taken to reduce the nutrient input. As a result, organisms in the fjord have adapted to different environmental conditions over the last century (Aure et al., 2014; Baalsrud & Magnusson, 2002). Later reports have also documented an increase in nutrients in Oslofjorden from agricultural land use and due to the continued increase in population (Walday et al., 2016; Walday et al., 2017).

1.2 Seasonal cycle of phytoplankton in Oslofjorden – earlier studies

The phytoplankton in Oslofjorden have been studied for almost a century (Braarud & Bursa, 1939; Throndsen et al., 2007; Walday et al., 2017). These studies have focused on the environmental conditions that initiate algal bloom.

Between 1957 and 1958, Hasle and Smayda examined the changes in phytoplankton communities at Drøbak (Hasle & Smayda, 1960). They investigated how the wind conditions and the topography of Oslofjorden could result in different phytoplankton compositions. They discovered that there was an annual minimum of phytoplankton from November to February followed by a maximum in March-May. This phytoplankton maximum was first dominated by a *Thalassiosira-Chaetoceros* community followed by a *Skeletonema* community. They also found a second maximum from September to October, which was dominated by *Cerataulina-Lauderia*.

Later monitoring data from outer Oslofjorden contains some of the same results as were found at Drøbak by Hasle and Smayda. Data from 1999 – 2011 indicates that in outer Oslofjorden there was a bloom in March and a late autumn bloom in October (Aure et al., 2014). In 2009, there were two blooms during the spring, one in late February-early March, and then a second one in May. The spring bloom in 2010 was in January, which is earlier than previous years suggesting that the timing of the spring bloom varies. Although the time of the bloom is varying, the dominating phytoplankton remained the same with diatoms being the most abundant group (Naustvoll et al., 2010; Walday et al., 2011). Table 1 illustrates the dominating species found in Oslofjorden between 2007 – 2011 (Walday et al., 2012)

***Table 1**: The most dominating species in the outer part of Oslofjorden between 2007 – 2011.*

Diatoms	Dinoflagellates
Dactyliosolen fragilissimus	*Tripos* spp. (*previously Ceratium* spp.)
Leptocylidrus danicus	*Gymnodinium* spp.
Ceratulina pelagica	*Prorocentrum micans*
Pseudo-nitzschia spp.	*Scripsiella trochoidea*
Skeletonema costatum	

Monitoring programs have also looked at the hydrographical and physical conditions which influence algal growth. Variations in temperature, salinity, density, light and available nutrients among others, favor different algal production. These variations are seasonally dependent in temperate seas (Table 2).

***Table 2**: Variation of abiotic factors with different seasons.*

Season	Light	Freshwater	Temperature	Nutrient
Winter	Low	Low	Low	High
Spring	Low/High	High	Low	High
Summer	High	Low	High	Low
Autumn	High/Low	High	High	High

A two-layered sea can occur in temperate oceans due to water with different densities and temperatures depending on season. During the winter, the water has almost the same density and temperature, allowing vertical mixing in the entire water column. Due to the mixing during winter, previously sedimented nutrients are transported back to the surface. A pycnocline develops in the spring due to an increase of freshwater. At this time nutrient concentration is high above the pycnocline because of the freshwater input and the prior mixing. Together these parameters create favorable conditions for algal growth, and a bloom may occur (Figure 2). A bloom is when there is a rapid growth of phytoplankton that peaks above an average abundance. The same conditions that occur in the spring might reoccur during the autumn due to the increase in runoff from land, and a reduced pycnocline and mixing of deep water, and a second bloom develops.

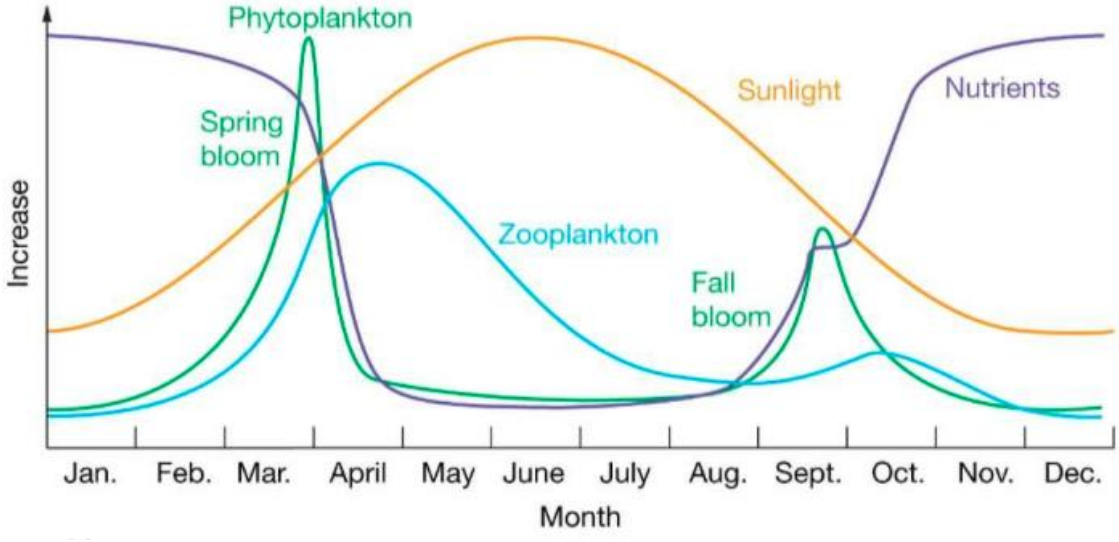

***Figure 2**: Graph showing the seasonal cycle of phytoplankton and the annual variation of sunlight, nutrients and zooplankton in temperate sea (copyright 2004 Pearson Prentice Hall, Inc.)*

Phytoplankton have adaptations and life history strategies to exploit different environmental conditions. These strategies might be to alter the population size, the timing and duration of resting spores, and change in reproductive/developmental status (Ji et al, 2010). The study of phytoplankton phenology can provide sensitive indications of climate changes. Temperate marine environments may be particularly vulnerable to changes because the recruitment success of higher trophic levels is dependent on the bottom-up regulation (Edwards & Richardson, 2004). As a coping mechanism, intraspecific variation in diatoms might be a response to altering environmental conditions. In addition, diatoms are fast dividing organisms which may enable them to respond to potential environmental changes (Godhe & Rynearson, 2017).

1.3 Genus *Skeletonema*

1.3.1 Historical investigations

Skeletonema costatum was first described by Greville (1866) as *Melosira costata.* Later, in 1873, it was identified as a species of *Skeletonema* by Cleve due to the similarity to *Skeletonema barbadense*. Until then, *S. barbadense* was the only described *Skeletonema* species (Cleve, 1873). *Skeletonema costatum* was later regarded as a cosmopolitan species. It was also recorded in surveys from Oslofjorden and was known as an annual blooming species that dominated the spring bloom (Braarud & Bursa, 1939; Hasle & Smayda, 1960; Lange et al., 1992; Walday et al., 2012). Its morphology and taxonomy were described in 1973 by Hasle where it was characterized as an "[…] extremely variable species in size as well as in shape" (1973, p. 109).

Skeletonema costatum was regarded as synonymous with *Skeletonema.* In 1982, Gallagher investigated physiological variations and electrophoretic banding patterns in *S. costatum* (Gallagher, 1982). It was from this investigation that a high diversity in allozymes between different strains of *S. costatum* were discovered. These results lead up to believe that there might be several distinct species of *Skeletonema* hidden under *S. costatum*. Later analysis has shown that what was considered as *S. costatum* might be several distinct species. In 1991 Medlin *et al.,* argued for a new species, *Skeletonema pseudocostatum* from a culture of *S. costatum* based on genetic variance (Medlin et al, 1991). The morphological differences that are between *S. costatum* and *S. pseudocostatum* were earlier believed to be intraspecific

variations. Furthermore, in 2005 Sarno *et al.,* argued that what was earlier identified as *S. costatum* could be several different species. By examining strains of *S. costatum*, in LM, SEM, TEM and by DNA analysis, eight distinct entities were identified. Four of these identified species were new: *S. dornii* Sarno et Kooistra, *S. grethae* Zingone et Sarno, *S. japonicum* Zingone et Sarno, and *S. marinoi* Sarno et Zingone (Sarno et al, 2005).

After the newly described species of *Skeletonema*, the geographical distributions of different species were investigated (Kooistra et al., 2008). According to this study, *S. costatum* has a stricter distribution than earlier believed (Figure 3). Furthermore, only two species were located close to Oslofjorden. *Skeletonema marinoi* was identified in Skagerrak (Figure 4), and *Skeletonema pseudocostatum* was identified in the Baltic Sea (Figure 5).

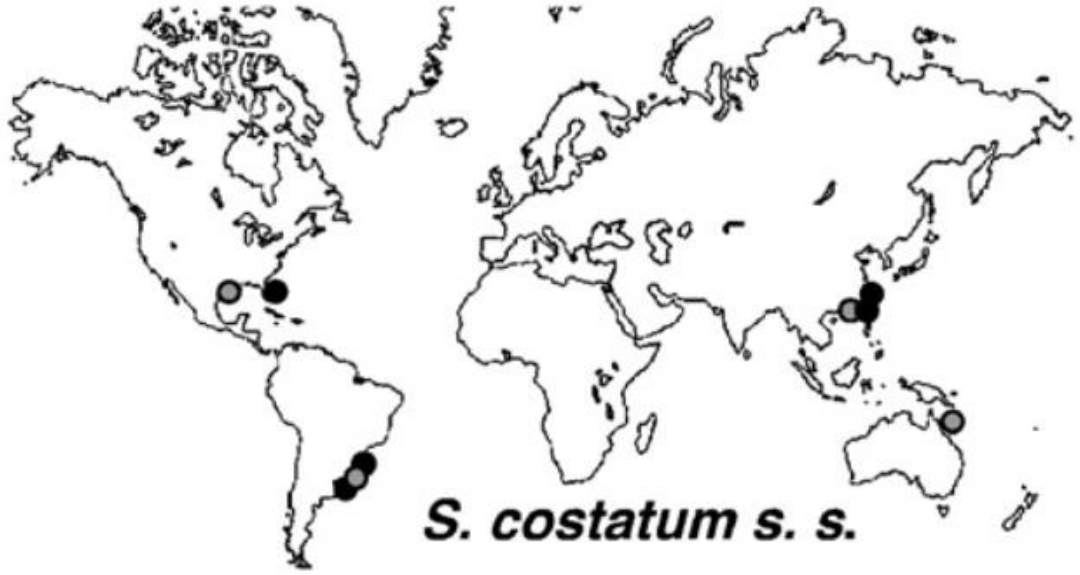

Figure 3*: Geographical distribution of* S. costatum *(Kooistra et al., 2008).*

Figure 4*: Geographical distribution of* S. pseudocostatum - *note that the dot between Sweden and the Netherlands represent the Baltic Sea (Kooistra et al., 2008).*

Figure 5*: Geographical distribution of* S. marinoi *(Kooistra et al., 2008).*

Skeletonema marinoi has been found in later investigations from Skagerrak (Skjevik, 2012). A similar study had not been performed in Oslofjorden, and up until recently *S. costatum* has been the recorded *Skeletonema* species (Walday et al., 2015)

1.3.2 Taxonomy and morphological features

Today there are 24 described species of *Skeletonema* and 21 of them are accepted taxonomically (algeabase.org). Sarno et al. constructed a maximum-likelihood tree of the 24 species (Figure 6; Sarno et al, 2007).

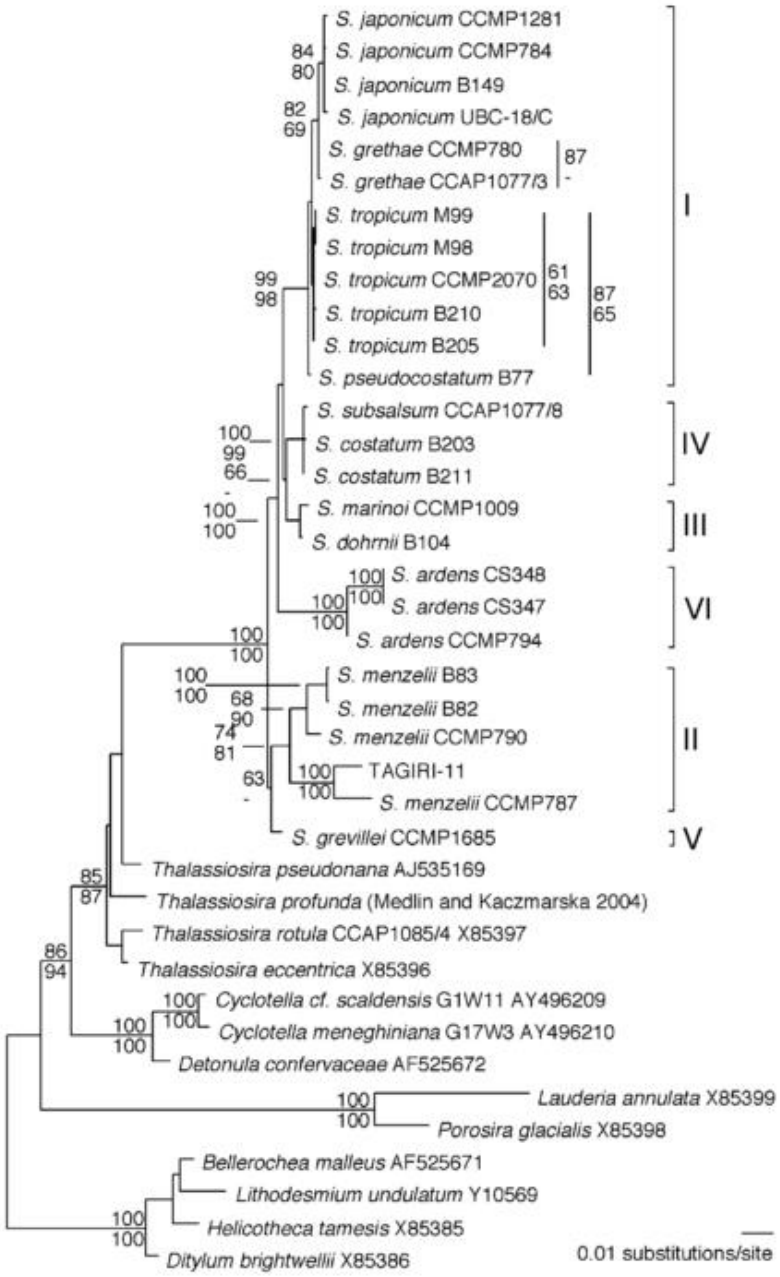

***Figure 6**: Maximum-likelihood tree of* Skeletonema *species constructed on alignment of SSU in rDNA sequences (Sarno et al., 2007).*

Skeletonema belongs to the phylum *Bacillariophyta*, commonly known as diatoms, a group of silicified algae. *Skeletonema* is further confined to the class *Mediophyceae*, which consists of bipolar and multipolar centric diatoms (Medlin & Kaczmarska, 2004). Its cells occur in chains,

connected by strutted processes organized in a marginal ring. The genus is easily recognized in a light microscope where it looks like pearls on a chain in addition to the meeting point between the strutted processes that forms a firm line (Figure 7). The cells vary in shape from square to more cylindrical, consisting of an epitheca and a hypotheca (valves), and measure between 2 – 38 µm. They may contain one, two, or many chloroplasts and occur in predominately chains or solitary.

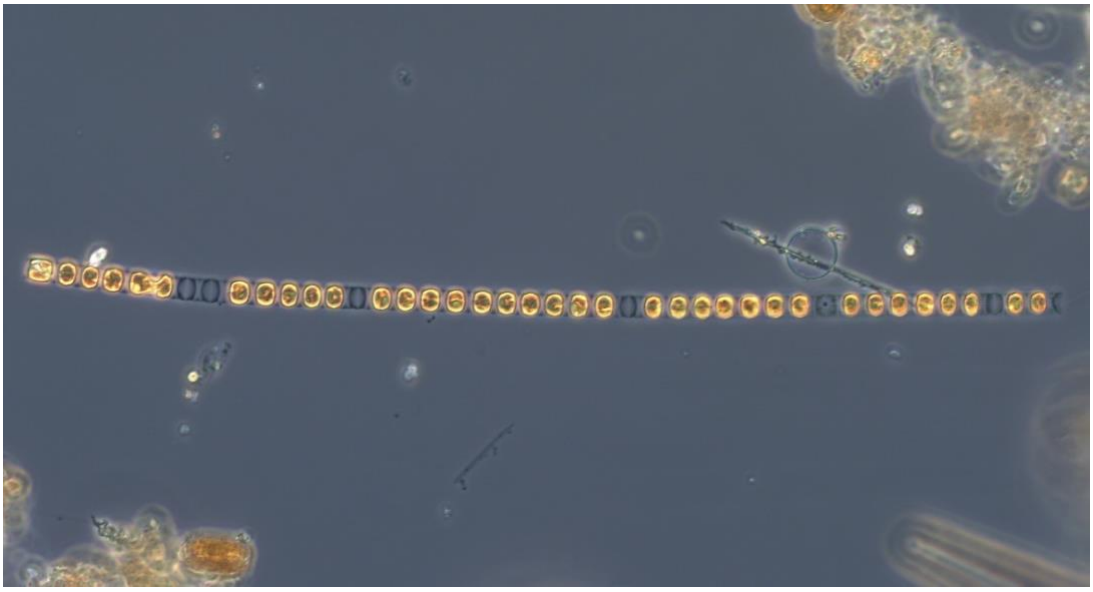

Figure 7*: Picture of* Skeletonema *sp. in LM from January 2017.*

Detailed morphological structures used in species identification of *Skeletonema* are visible in a scanning electron microscope (Figure 8 – 9). The terminology to describe these structures is the same as used by Sarno et al. (2005; Table 3).

Table 3*: Terminology used in describing morphological features in* Skeletonema.

Strutted process	Terminal fultoportula process Intercalary fultoportula process
Labiate process	Terminal rimoportula process Intercalary rimoportula process

The outer wall called the frustule is composed of two silica valves with species-specific ornaments. When in chains, the strutted processes connect the valves. Strutted processes, also known as fultoportula processes, are aligned in a marginal ring perpendicularly to the valve face. The strutted processes of opposite valves link at the ends, either 1:1 or 1:2. This linking may vary in form and construction. Additionally, each valve possesses a labiate process, the rimoportula process. It is positioned either sub-centrally or marginally in terminal valves and marginally in intercalary valves.

The way that the strutted processes are connected might be used in species identification (Figure 8). *Skeletonema costatum* have strutted processes in a 1:2 linkage creating a zigzag formation (Figure 8A). The interlocking between the strutted processes is a plain joint. The same formation is found in *S. marinoi.* The difference is that the connection might also be in a 1:1 linkage (Figure 8B). Whereas in *Skeletonema pseudocostatum* the connection between the processes is usually 1:1 and the interlocking is a fork joint, or a knot/knuckle-like joint (Figure 8C; Sarno et al., 2007, 2005).

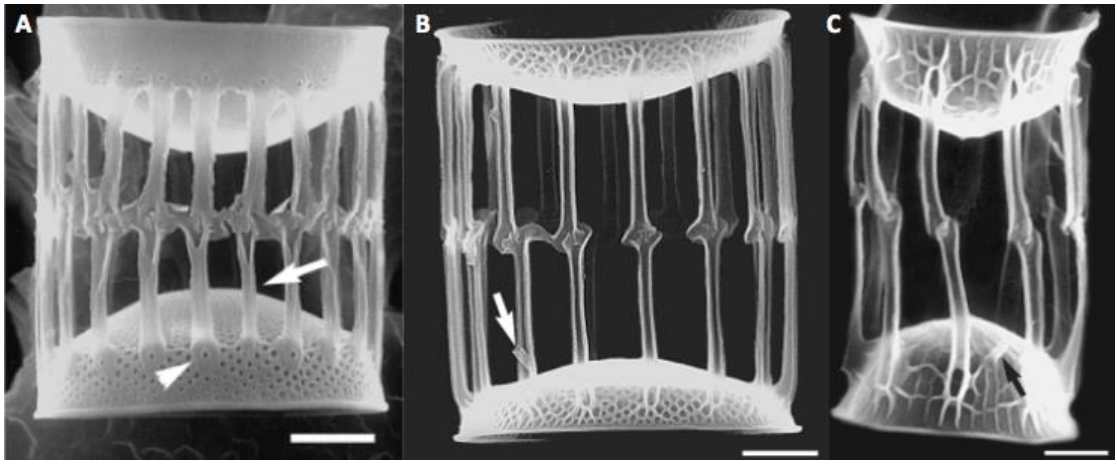

Figure 8*: Picture of connecting processes in A:* S. costatum. *B:* S. marinoi. *C.* S. pseudocostatum. *A,B,C: Arrows points at the intercalary labiate process* (Sarno et al., 2007, 2005).

The morphology of the terminal strutted processes and the location of the terminal labiate process is also used in species identification. In *S. costatum*, the terminal strutted processes are split tubes with a claw-like ending (Figure 9 A-B). In the case of *S. marinoi*, the terminal strutted processes are flattened and flared with a dental-like ending (Figure 9 C-D). The terminal strutted processes in *S. pseudocostatum* have a narrow tip that can either be spiny, truncated or claw-like (Figure 9 E-F). The terminal labiate process is sub-central in *S. marinoi* and *S. pseudocostatum*, and marginal in *S. costatum*.

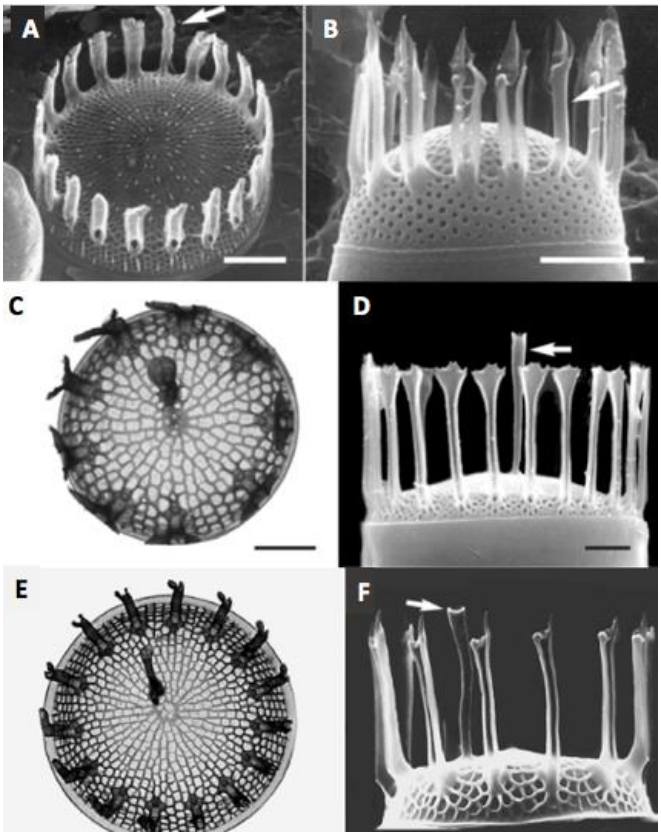

Figure 9*:Picture of the terminal valves in A-B:* S. costatum. *C-D:* S. marinoi. *E-F:* S. pseudocostatum. *In all: arrows points at the terminal labiate process (Sarno et al., 2007, 2005.)*

1.3.3 Life cycle and life strategies

The life cycle in diatoms is mainly asexual. The division happens within the valves, as hypotheca and epitheca separate and new wall elements are created within the separated valves, resulting in a smaller wall element (Figure 10). For each cell division, the new daughter cells decrease in size until a threshold reaches. Beyond this threshold, the cells are too small to divide any further. The restitution to initial cell size occurs by two different methods. One is by vegetative cell enlargement, the other by auxosporulation. The latter is the most common, which usually happens through sexual reproduction. In the case of diatoms belonging to *Mediophyceae*, the sexual reproduction is in the form of oogamy where one cell becomes an egg and another cell starts to produce uniflagellate spermatozoids. After fertilization, an auxospore develops. A auxospore may start to expand and reach the initial cell size where vegetative division may start again (Hasle et al., 1996).

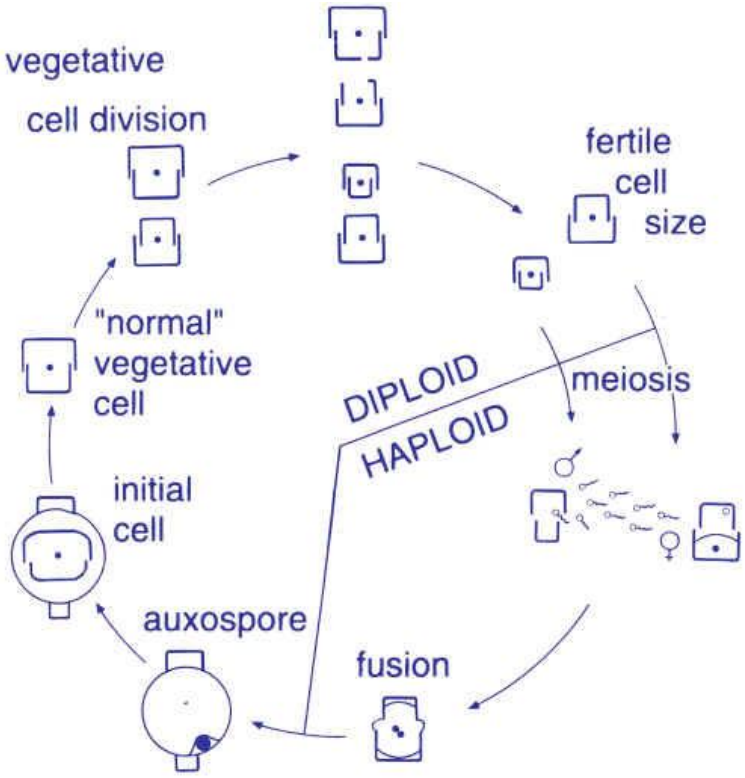

***Figure 10**: Illustration of the life cycle of centric diatoms* (Hasle et al., 1996)

Investigations have shown that environmental factors such as temperature, light, and salinity may initiate auxosporulation (Armbrust et al., 1990). For instance, cells of *Skeletonema marinoi* became sexualized by changing the strains from low salinity to high salinity (Saravanan & Godhe, 2010)

Resting spores and cells are other life strategies found in diatoms. These spores and cells have earlier been mixed up with the term auxospore, as an auxospore on some rare occasions may become a resting spore (Kaczmarska et al., 2013). Resting cells and spores have a specialized cell structure that enables them to survive harsh conditions. They are believed to sink down to the sediment where they remain at a benthic stage. If vertical mixing occurs along with more favorable conditions, the cells may germinate and increase in number again (McQuoid & Hobson, 1996).

1.4 Objectives

This research aimed to investigate the seasonal occurrence of pelagic phytoplankton in the size range 20 – 200 μm of Drøbak, Oslofjorden, with a special focus on the genus *Skeletonema* from September 2016-August 2017. The present study aimed to compare phytoplankton data from 2016 – 2017 with the data from a seasonal investigation of phytoplankton performed by Hasle & Smayda in 1957 – 1958 (Hasle & Smayda, 1960) and reports of monitoring investigations performed by NIVA and IMR. Objectives during the present research were thus:

1. Reveal the seasonal cycle of phytoplankton at Drøbak between September 2016 and August 2017 by focusing on:
    - Variations in hydrographical conditions
    - Variations in species composition, number of counted cells and biovolume correlating with the observed hydrographical conditions, and compare with earlier observations from Oslofjorden.
2. Reveal differences in phytoplankton composition between the present study with those of Hasle & Smayda (1960) in terms of timing and abundance of observed taxa.
3. Obtain new knowledge on the genus *Skeletonema*:
    - Identify *Skeletonema* species from selected samples collected at Drøbak in the 1930s and up to the present year.
    - Assess the role of *Skeletonema* in the seasonal cycle of phytoplankton from September 2016 to August 2017, and compare with the study of Hasle & Smayda (1960).
    - Elucidate possible life cycle strategies of *Skeletonema* in a seasonally changing environment.

2 Material and Methods

2.1 Sampling area

The study area was outside of the city Drøbak, located in outer Oslofjorden, Norway (Figure 11). The field work was organized in monthly visits from September 2016 until August 2017 at the monitoring station Elle (59°37’29.91’’N, 10°37’70.75’’E). Also, there were two cruises in February as an attempt to cover a predicted spring bloom.

***Figure 11**: Map of Oslofjorden with star at Elle*

The cruises were carried out from the UiO research vessel Trygve Braarud (Figure 12).

Figure 12: *Picture of the RV Trygve Braarud (Photo: Tom Opsahl)*

2.2 Sampling procedures

2.2.1 Water quality

Hydrographical data were collected on every cruise with an SBE 9plus CTD (Sea-Bird Scientific, USA) that measured conductivity (a measure for salinity), temperature, and depth in addition to density (Figure 13). The CTD was unavailable in January, February, March and July. An STD (SD204, SAIV A/S, Norway) was then used instead as a replacement for the CTD. It measures the same parameters as the CTD except for density. The STD is also smaller and thus lacks a rosette for Niskin bottles, and cannot be used to collect water. To collect hydrographical measurements, water was pumped through different sensors throughout the water column. The measurements were logged when the CTD/STD was lowered to 100 m depth.

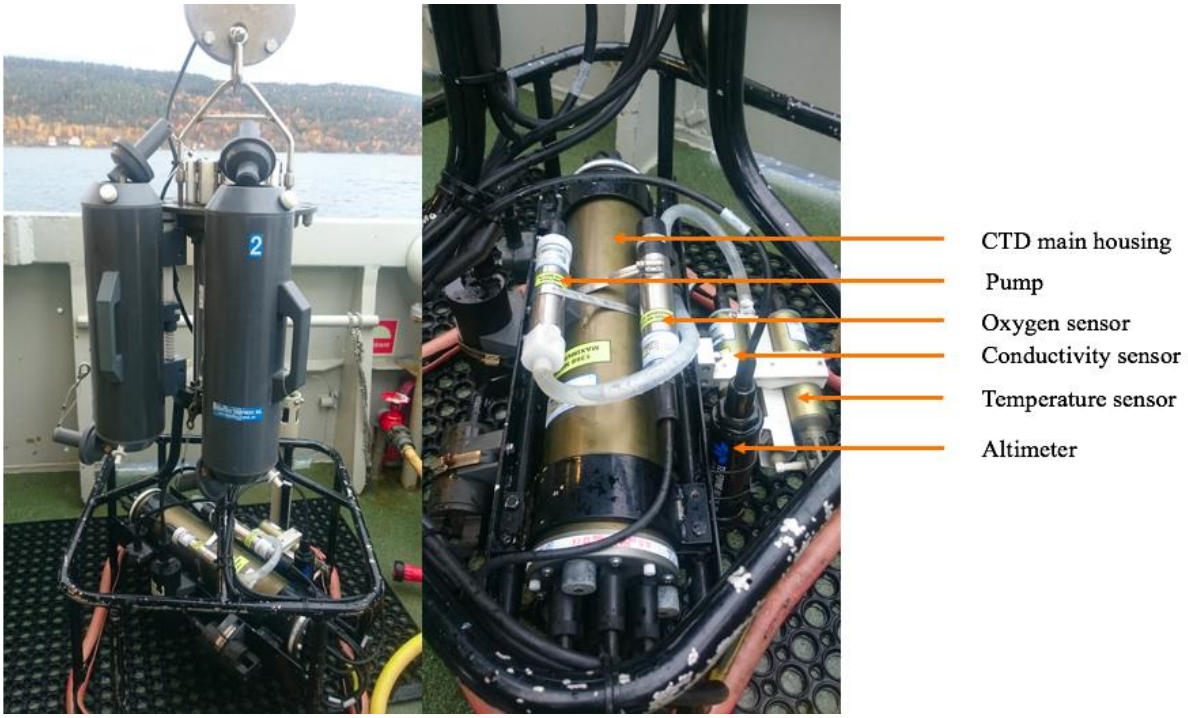

***Figure 13**: Picture of the CTD attached with two 5L niskin bottles attached (left) and a close up to the different sensors (right).*

A sensor that measures fluorescence was also located on the CTD. The sensor emits blue light which phytoplankton can either use in the photosynthesis, or the chlorophyll molecules emit the excess energy as red light. The sensor captures this red radiation, and it gives an indication of the amount of chlorophyll (photosynthesizing organisms) and the distribution in the water column. Fluorescence was not measured during the months where the STD was used instead of the CTD.

In addition to the CTD/STD, a Secchi disk was used to gather information about the water transparency. The Secchi disk is a white disk that is lowered down to the depth where it is no longer visible. This depth can be used in a formula to estimate 1% light depth (Equation 1).

Equation 1: $$D = f * S$$

D is the 1% light depth, f is a given factor that is about 3 in Oslofjorden, and S is the measured Secchi depth (Paasche, 2005).

2.2.2 Phytoplankton sampling

On each cruise, water samples and net haul samples were collected for later analyses. The sampled water was designated for different analyses (Table 4). Many of the samples were collected in triplets, as the cruises were a collaboration between three separate master-projects.

***Table 4**: Information about the sampled water from the cruises*.

Sampling Method	Amount of water	Preservation	Microscope/ analysis
Water sample with CTD/Ruttner	100 mL x3	1mL of Lugol's solution x3	Inverted microscope
Water sample with CTD/Ruttner	1 L x3	Non	SEM
	1 L x3	Non	DNA analysis
Vertical net haul	100 mL	1 mL of Lugol's solution	LM
	100 mL	1 mL of formalin	SEM
Horizontal net haul	100 mL	1 mL of Lugol's solution	LM
	100 mL	1 mL of formalin	SEM

Net hauls

Vertical- and horizontal net hauls (mesh size 20 μm) were used to collect water for qualitative analysis. The vertical net haul sampled from 20 m depth to the surface, and the horizontal net haul was dragged behind the vessel for 5 – 10 minutes at the surface (1 – 2 m depth). Half of both the horizontal and the vertical net haul samples were preserved in 1% Lugol's solution

and the other half was preserved in 3% aqueous solution of CH_2OH-CHO, formalin (Throndsen, 1978).

Water samples

For each cruise, around 6.3 L of water were collected in two 5 L Niskin bottles (PWS, Hydro-Bios, Germany) that were attached to the CTD. During the cruises where the CTD was unavailable, water was collected with aid of a Ruttner water sampler (KC, KC Denmark A/S, Denmark). Water was sampled from the subsurface at 1 – 2 m depth. From the collected water, 100 mL was preserved in 1% Lugol's solution for later quantitative analysis and 1 L was pre-filtrated through 200 μm mesh *in situ* to eliminate bigger organisms.

2.3 Investigation of the phytoplankton composition and abundance

To identify and quantify the phytoplankton, three different methods were used: Light microscope (LM), inverted light microscope, and scanning electron microscope (SEM). All microscopes belong to the University of Oslo and are located at the Department of Biosciences.

2.3.1 Light microscope – qualitative analysis

The net hauls preserved with Lugol's solution were qualitatively analyzed in a light microscope (Nikon eclipse TE300, Japan). The goal was to identify microplankton to the lowest practical level. Identification was conducted with aid from the flora by Throndsen and co-workers (Throndsen et al., 2007). For each new species or genus, photos were taken as documentation with a Nikon camera (model D-5000). Further, sizes of the counted algae were measured. These measurements are usually done from water samples under an inverted microscope, but in this case, it was the net hauls that were investigated in a light microscope. Both length and width of the cells were measured. In the case of S*keletonema* sp., the length of the chains was measured and the number of cells per chain were recorded. Also, the variations found in chain and cell morphology of the genus *Skeletonema* were documented and photographed.

2.3.2 Inverted microscope – quantitative analysis

The Utermöhl method was used for the quantitative analysis (Utermöhl, 1958). The advantage with this method is that it allows both enumeration and identification. The Utermöhl method requires an inverted microscope (Nikon eclipse TE305, Japan) where the objectives are underneath the sample. This microscope is crucial for the identification as the method is based on sedimentation of algae that falls down to the bottom of the sedimentation chamber. To exclude air bubbles in the sedimentation chambers the sample was adapted to room temperature for ca. 8 hours. Next it had to be mixed thoroughly, but gently, so it became homogenized before sedimentation. Two different sized sedimentation chambers were used, depending on the algal concentration (10 mL and 25 mL). The sedimentation is based on gravity, where the algae will fall down at the bottom of the chamber after some time between 16 to 24 h (Horner, 2002). Preserving a sample in Lugol's solution may increase the weight of the algae. An increase in weight might lead to faster sinking rate. Thus, the samples in this project had a setting time of ca. 16 h. In order to count the algae the oculars were equipped with a stage micrometer and grids in form of three squares (Figure 14).

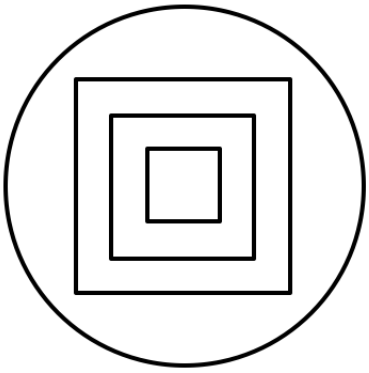

***Figure 14**: Grids used as counting aid in the eyepiece*

The phytoplankton were identified and enumerated after successful sedimentation. The identification was at the lowest taxonomic level possible. To make the enumeration easier, all the net haul samples had been looked at and identified in a light microscope before quantitative analysis. Additionally, two fellow students will count the same water sample enabling later comparison between results as a quality assurance.

2.3.3 Biovolume

The biovolume was calculated with the program Phytoplankton toolbox 1.2.1. (www.nordicmicroalgae.org/tools). This is a program constructed by Nordic Microalgae and is open and free for everyone to use. The program needs information about the sample to perform the calculations. It requires knowing the observed taxa and the amount of counted cells as well as the size of the taxon (length and width). Hillebrand et al. (1999) illustrated how the volume of different geometric structures gives an estimate of the cell volume of a taxon. The phytoplankton toolbox calculates the cell volume by the same method. Furthermore, the

program asks for the volume of the sedimentation chamber and preservation solution. In the present research, whole chambers were counted. The exception was the May sample where *Pseudo-nitzschia* spp. cells were counted in 5 field of views and later calculated to get an estimate of cells per liter (Appendix 1). Also, the preservation volume was so little (1%) that it did not alter the sample concentration significantly. The counted chambers were either 10 mL or 25 mL, resulting in that on had to multiply with either 100 or 40 to get an estimate of cells/L and μm^3/L.

2.3.4 Statistical approach for the phytoplankton analysis

Results from the cell count and biovolume were illustrated logarithmically as some of the values were of several orders of magnitude higher than other numbers. In the case of biovolume it was calculated with log(x+1) in order to get positive values in the bar chart.

2.3.5 Phytoplankton composition reported from Drøbak and the outer part of Oslofjorden

Results gathered about phytoplankton abundance and composition were compared with earlier findings from available monitoring data sampled at Drøbak and the outer part of Oslofjorden. Trends about timing of blooms and visible seasonal occurrence of taxa and their composition were investigated as extensively as possible. The annual study of phytoplankton at Drøbak performed by Hasle & Smayda (1960) was used, as well as reports from the outer part of Oslofjorden delivered by NIVA and IMR, e.g., Naustvoll et al. (2013) and Walday et al. (2015).

2.4 Investigation of *Skeletonema*

2.4.1 Preparation of water samples from 2016-2017, and analysis using scanning electron microscope

The pre-filtrated water samples from the Niskin bottles/Ruttner water sampler were further filtrated *in vivo* at the University of Oslo (Figure 15). There were six 1 L bottles, two bottles for the three-master project, collected on each cruise. The water was filtered on to a polycarbonate filter with 0.8 μm pore size (Nuclepore/Whatman, GE Healthcare, USA) using a peristaltic pump (Easy-load II Masterflex, Cole-Parmer, USA), preventing smaller cells of *Skeletonema* from being dragged through the filter, but rather stick to it. Subsequently, the

filters were placed upon stubs with 8 mm carbon tape after successful filtration. The stubs were prepared for later analysis in a scanning electron microscope.

***Figure 15**: **A**: Picture of the pre-filtration of the water with water from the Ruttner water sampler. **B**: Picture of the filtration setup with a peristaltic pump at the lab.*

To remove organic material from the samples, the net haul samples were acid cleaned. The acid cleaning consisted of 30% hydrogen peroxide and 37% hydrochloric acid (Appendix 2; Adil Al Handal, personal communication). After the cleaning, stubs for SEM were prepared. Two stubs were prepared for each sample: one with only 8 mm of carbon tape and another with 8 mm carbon tape and a poly-L-lysine covered glass (Merck, Germany). The two different stubs were prepared to determine the most efficient method to examine essential features of *Skeletonema* in SEM.

The stubs prepared from water samples and net hauls were coated with 6 nm of platinum in a sputter coater (Cressington 308UHR, Ted Pella Inc., USA). A scanning electron microscope (Hitachi S-4800, Hitachi Ltd., Japan) with a field emission gun was used to analyze the stubs for species of *Skeletonema.* Pictures of essential features for species identification of *Skeletonema* (described in the introduction) were taken as documentation. In addition, photos were taken of the different chain formation and cell morphology of *Skeletonema.*

2.4.2 SEM analysis of historical samples from Drøbak

At the Natural History Museum, UiO in Oslo, there is the Hasle collection, a collection of Grethe Hasle's own samples and colleagues at UiO. In this collection, there are formalin preserved water samples from Drøbak. A selection of Hasle's samples (04.04.1930; 22.03.1936; 21.05.1951; 15.11.1971; 01.12.1987) were acid cleaned and analyzed in SEM. The samples were acid cleaned with 30% hydrogen peroxide and 37% hydrochloric acid (Appendix 2) before they were mounted on stubs. The exception was the samples collected in 1930 and 1951 which were already acid cleaned, and were instead directly mounted onto stubs. The stubs contained both carbon tape and poly-L-lysine glass, and were further coated with 4.5 nm of platinum. The samples were further analyzed in SEM and photographs were taken as documentation. Also, the *Skeletonema* enumeration results from 2016-2017 (section 2.3.2) were compared with the *Skeletonema* cell counts of Hasle & Smayda (1960).

2.4.3 Analysis of cultured *Skeletonema pseudocostatum*

From the Norwegian Culture Collection of Algae, NORCCA, we received a culture of *Skeletonema pseudocostatum* (NIVA-Bac 1) that was isolated by NORCCA from the Drøbak area during the summer of 1962 by Eystein Paasche. To be certain about the identification, both morphological and genetic analysis were performed.

Morphological analysis of the culture NIVA BAC-1

The morphological analysis was conducted in a SEM. The samples were first acid cleaned as the net haul samples (Appendix 2) before it was mounted on a stub. The stub contained both carbon tape and poly-L-lysine glass and was further coated with 4.5 nm of platinum. Identification was performed by following described morphological features from papers by Medlin et al. (1991) and Sarno et al. (2005). Photographs were taken as presentation of the results.

Genetic analysis of the culture NIVA BAC-1

The first step in the genetic analysis was to perform DNA extraction. The 2 mL of dense culture was transferred to an Eppendorf tube and centrifuged at 4000 rpm for 10 minutes (Eppendorf Centrifuge 5810R, Germany). The supernatant was discarded and the remaining pellet containing the culture material was kept frozen at -20°C. Next, the DNA from the culture was extracted using the DNeasy Blood & Tissue Kit (Qiagen, Germany). The isolation followed

the protocol included in this kit (Appendix 3). The concentration of the extracted DNA was measured with a Quibit reader to be 13.5 ng/µl. The DNA was stored at -20°C.
The 601bp-long segment of 28S (LSU) region of nuclear ribosomal DNA was amplified by PCR (polymerase chain reaction) using the D1R and D2C primer (Scholin et al., 1994). The reaction was run with a total volume of 25 µl. This amount included 2.5 µl of the template (extracted DNA), 12.5 µl GoTaq Green Master Mix and 1.5 µl of forward (D1R) and reverse (D2C) primer each. The PCR reaction was conducted in a mastercycler (Eppendorf mastercycle EP gradient, Germany) with the following program: initiation at 94°C for 3 min, then 35 cycles of denaturation at 94°C for 45 s, annealing at 55°C for 45 s and extension at 72°C for 1 min. After a completed cycle, the extension was continued at 72°C for 7 min.

After completed PCR the amplified product was loaded onto a 0.8% agarose gel. The gel was made of 0.4 g agarose powder (Merck, Germany) mixed with 50 ml of 1xTAF buffer (Tris-acetate-EDTA). There were five wells in the gel where one was loaded with 1 µl of size marker, one with 1 µl of loading dye + 5µL of the LSU PCR product, and one with 1 µl loading dye + a PCR reaction with H_2O instead of the template (negative control). The gel electrophoresis was conducted with an Electrophoresis Power Supply (EPS 301, GE Healthcare, USA) at 80 V for 40 min. After completed gel electrophoresis, the gel was observed under UV-transillumination (GeneGenius bio-imaging system, Synge; Appendix 4). Finally, the PCR products were purified using ExoSAP-IT PCR Product Cleanup Reagent (Thermo Fisher Scientific, USA) and sequenced in both directions using the same primers as in the PCR using Sanger sequencing method at GATC Biotech (Germany).

The obtained forward and reverse sequences were analyzed using Geneious software v. R11 (Biomatters, New Zealand). Uncertain flanking bases were cut from the sequences and the remaining high-quality sequences were aligned to obtain a 601-bp long consensus sequence. The sequence was further used in nuclear BLAST from the GenBank molecular database of National Center of Biotechnology Information (NCBI) to search for the best related match. By using accession numbers (Appendix 5) from related *Skeletonema* species and for *Thalassiosira rotula* as outgroup identified by Sarno *et al.* (2005; 2007), a phylogenetic tree was constructed with the obtained sequences and reference sequences. The tree was generated by neighbor joining with 100 replicates.

2.4.4 Variation in *Skeletonema* cell size and chain length

The variation of *Skeletonema* cell size and chain length from the LM analysis (section 2.3.1) were statistically investigated using the statistical software R (version 3.3.2, the R Foundation for Statistical Computing 2016). A generalized additive model (GAM) was used, a type of generalized linear model that include nonlinear and linear relationships. With GAM, the variation in *Skeletonema* size was analyzed together with the hydrographical data. GAMs were fitted using R's mgcv package (Wood, 2011), a penalized regression approach that fits smooth terms to the data and automatically select the complexity (the "wiggliness") of these terms. First, trends in the cell variation were checked by examining length with variating months, temperature and salinity. The same was performed for both the number of cells in chain and chain length. Note that we treated time as sampling month using January= 1 and November= 11, that is, the graphs follow the calendar year instead of following the chronology of the sampling (the sampling began in September 2016 and was completed in August 2017). Also, the y-scale on the plots which illustrates the cell size or chain length shows the deviance from the mean values. To get the appropriate cell size and chain length it is necessary to add an estimated standard deviation value for each point (table 8 – 9).

3 Results

3.1 Hydrographical data

3.1.1 Variation in temperature and salinity

Most of the collected data concerning the phytoplankton was sampled from the surface layer. The CTD/STD logged down to 100 m depth (Appendix 6), however values were extracted from 2 m depth as a mean to simplify the variation in salinity and temperature (Figure 16).

The temperature was decreasing from September to February before it increased again up to August (Figure 16). The salinity varied more than the temperature, peaking in January and March and declining in February and June.

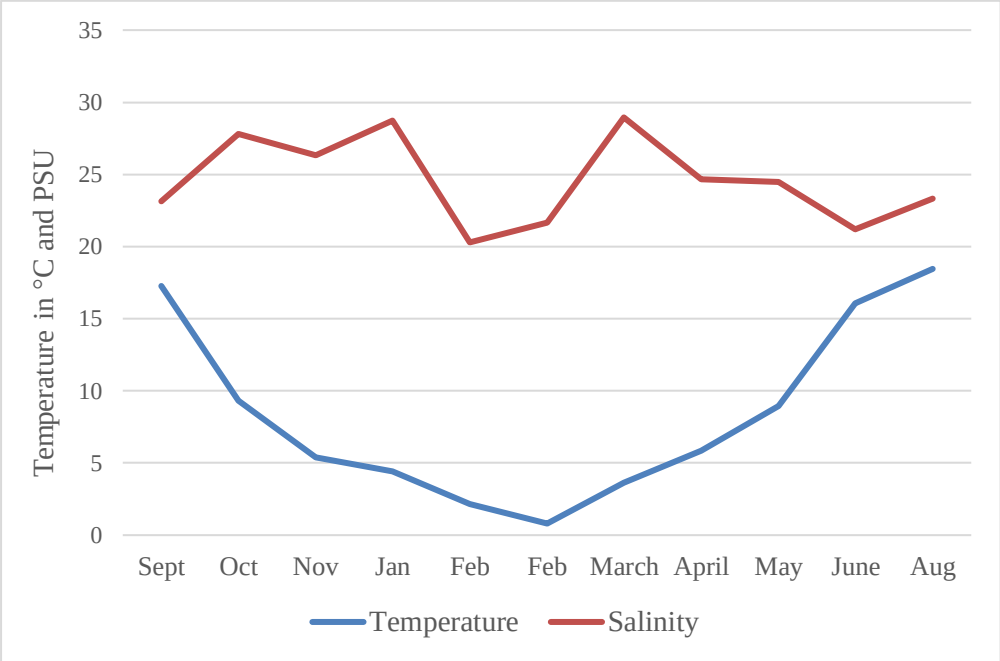

***Figure 16**: The variation of temperature (℃) and in salinity (PSU) over the sampling year at 2 m depth. The blue line is the temperature and the red line is the salinity.*

There was little difference between the temperature measured at Drøbak in 2017 and those recorded by Hasle & Smayda in 1957 (Figure 17).

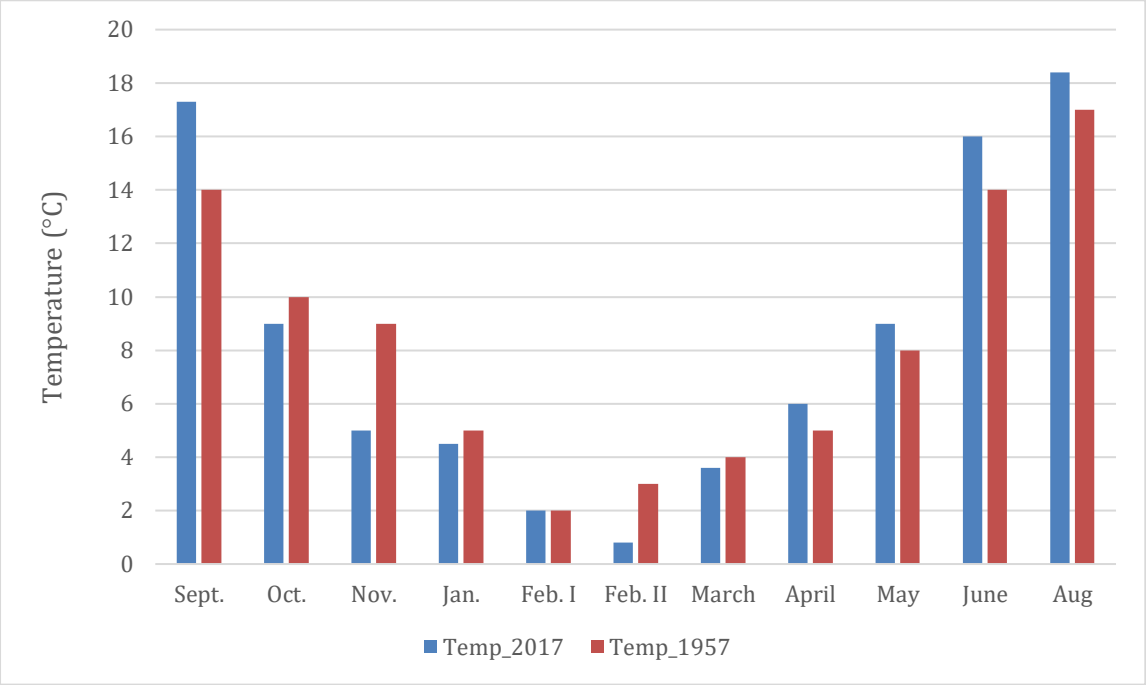

***Figure 17**: The difference between temperature in 2017 (blue) and 1957(red).*

There was a difference between the measured salinity in 2017 and 1957, with slightly higher values in 1957 except for October, March, and June (Figure 18).

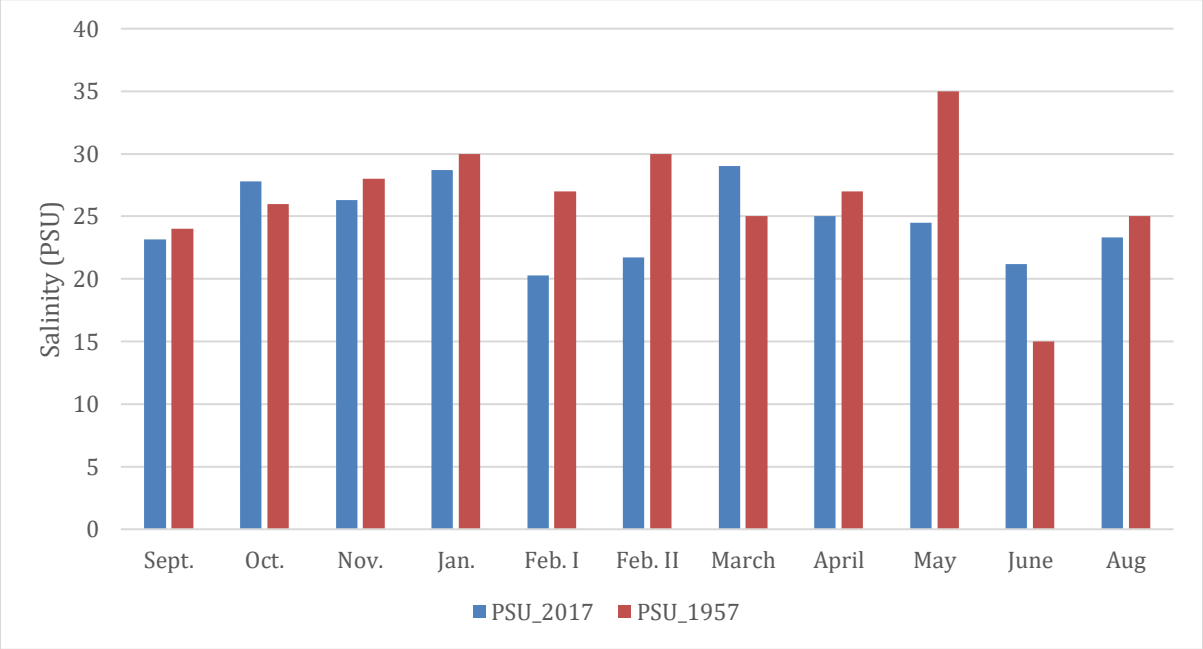

***Figure 18**: Difference of measured salinity in 2017 (blue) and in 1957 (red).*

3.1.2 Water transparency

The values from the Secchi measurements were between 6 m depth and 9 m depth most of the sampling year (Figure 19). The shallowest measurements were in April and May where the Secchi depths were at 3.5 m and 4.5 m depth.

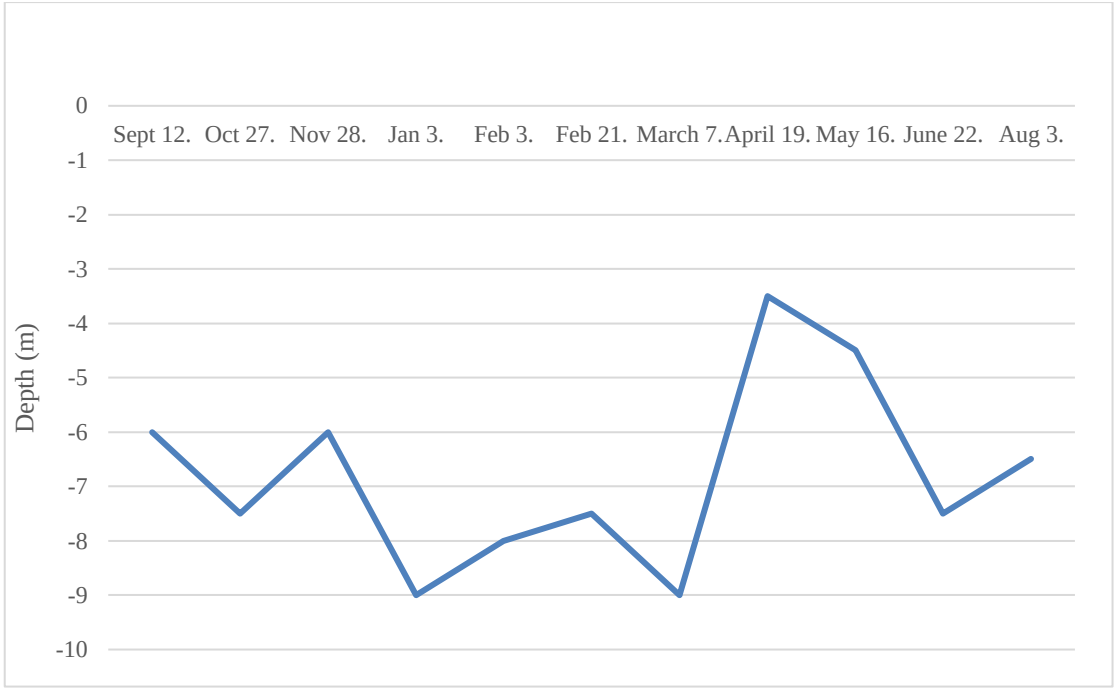

***Figure 19**: The variation of Secchi depth at Drøbak from September 2016 to August 2017*

The 1 % light depth, calculated from the Secchi depth varied between 11 and 27 m (Figure 20).

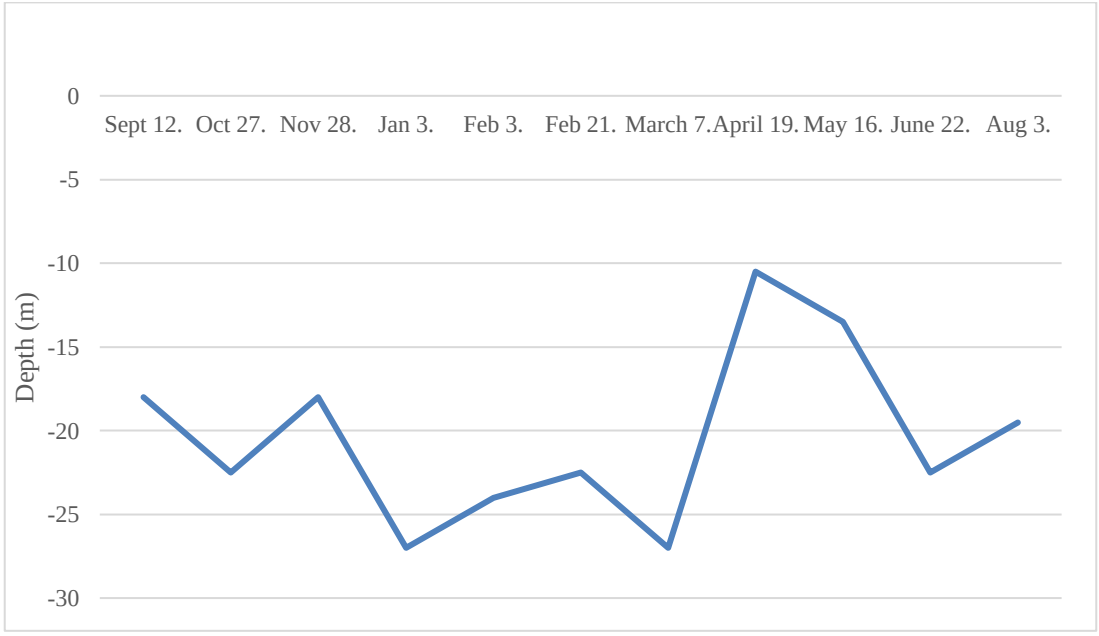

***Figure 20**: The calculated 1% light depth from the Secchi measurements.*

3.2 Phytoplankton observations

3.2.1 Taxa identified from net samples

In the net hauls, 34 different diatoms and 39 different dinoflagellates were identified. In addition, four phytoplankton taxa were classified under the category "others" (Table 5). These taxa included *Dictyocha speculum* (Class *Dictyochophyceae)*, *Dictyocha fibula* (Class *Dictyochophyceae)*, *Dinobryon* sp. (Class *Chrysophyceae)*, and *Eutreptiella* sp. (Class *Euglenophyceae*). The formal taxonomy follows Algaebase (algaebase.org).

Table 5*: Phytoplankton taxa recorded in net samples at Drøbak from September 2016 to August 2017.*

Sampling months	Sept. 12.	Oct. 27.	Nov. 28.	Jan. 3.	Feb. 3.	Feb. 21	Marc h 7.	April 19.	May 16.	June 22.	Aug. 7.
DIATOMS											
Ceratulina pelagica (Cleve) Hendey									x		x
Chaetoceros cf. *diadema* (Ehrenberg) Gran									x		
Chaetoceros curvisetus Cleve		x	x					x		x	
Chaetoceros debilis Cleve				x			x				
Chaetoceros decipiens Cleve		x		x							
Chaetoceros sp. Ehrenberg	x	x		x		x	x	x		x	x
Chaetoceros tenuisimus Meunier	x										
Coscinodiscus radiatus Ehrenberg				x							
Coscinodiscus sp. Ehrenberg		x	x	x							

Cylindrotheca closterium (Ehrenberg) Reimann & J.C. Lewin	x	x	x	x	x	x	x	x	x	x	x
Dactyliosolen fragilissimus (Bergon) Hasle	x			x				x	x	x	x
Ditylum brightwellii (T. West) Grunow		x	x	x		x	x				
Fragilariopsis sp. Hustedt									x	x	
Guinardia delicatula (Cleve) Hasle							x			x	
Leptocylindrus sp. Cleve							x		x		x
Leptocylindrus danicus Cleve		x	x	x					x		x
Licmorphora sp. C. Agardh									x		
Melosira cf. *moniliformis* (O.F. Müller) C. Agardh		x									
Melosira nummuloides C. Agardh							x				
Navicula sp. Bory				x		x	x	x	x		
Odontella aurita (Lyngbye) C. Agardh							x				
Cf. *Pleurosigma normanii* Rarlfs			x								
Proboscia alata (Brightwell) Sundström		x	x	x	x	x	x	x	x	x	x

Pseudo-nitzschia sp. H. Peragallo	x	x	x	x	x		x	x	x	x	x
Rhizosolenia cf. *Punges* A. Cleve-Euler						x	x				
Rhizosolenia cf. *setigera* Brightwell								x			
Rhizosolenia hebetata Bailey		x									
Rhizosolenia hebetata f. hebetata Bailey	x					x	x				
Rhizosolenia hebetata f. semispina (Hensen) Gran		x		x		x		x	x		
Rhizosolenia sp. Brightwell	x										
Skeletonema sp. Greville	x	x	x	x	x	x	x	x	x	x	
Striatella unipunctata (Lyngbye) C. Agardh										x	
Thalassionema nitzschioides (Grunow) Mereschkowsky				x	x	x	x	x	x	x	
Thalassiosira angustelineata (A. Schmidt) G. Fryxell & Hasle				x			x				
Thalassiosira nordenskioldii Cleve				x			x				
Thalassiosira rotula Meunier		x	x	x			x				

Thalassiosira sp. Cleve		x	x		x	x	x	x			
DINOFLAGELLATA											
Akashiwo sanguinea (K. Hirasaka) G. Hansen & Moestrup		x	x	x	x						
Tripos furca (Ehrenberg) F. Gómez	x								x		
Tripos fusus (Ehrenberg) F. Gómez				x					x	x	x
Tripos horridum (Cleve) F. Gómez		x	x	x	x					x	x
Tripos lineatus (Ehrenberg) F. Gómes	x	x	x	x	x		x				
Tripos longipes (J.W. Bailey) F. Gómez		x	x	x	x				x		
Tripos macroceros (Ehrenberg) F. Gómez		x	x						x	x	
Tripos muelleri Bory	x	x	x						x	x	x
Dinophysis acuminata Claparèd & Lachmann	x	x	x	x	x			x	x	x	
Dinophysis norvegica Claparèd & Lachmann			x	x	x				x	x	
Dinophysis rotundata Claparèd & Lachmann	x		x				x				

Dinophysis sp. Ehrenberg											x
Dinophysis acuta Ehrenberg	x	x	x	x						x	
Gymnodiniales sp. Apstein		x	x	x	x			x		x	x
Gymnodinium vestifici Schütt								x			
Gyrodinium fusiforme Kofoid & Swezy	x	x	x		x						
Gyrodinium sp. Kofoid & Swezy	x										
Katodinium glaucum (Lebour) Loeblich II								x			
Phalacroma rotundatum (Claparèd & Lachmann) Kofoid & Michener										x	
Polykrikos kofodii Chatton	x										
Protoperidinium curtipes (Jørgensen) Balech				x							
Prorocentrum micans Ehrenberg	x	x								x	x
Prorocentrum minimum (Pavillard) J. Schiller	x						x	x			x
Prorocentrum sp. Ehrenberg					x			x			
Protoperidinium brevis										x	

Protoperidinium cf. *leonis* (Pavillard) Balech										x	
Protoperidinium cf. *pallidum* (Ostenfeld) Balech				x							
Protoperidinium cf. *bipes* (Paulsen) Balech				x					x		
Protoperidinium cf. *cerasus* (Paulsen) Balech				x							
Protoperidinium cf. *conicoides* (Paulsen) Balech		x									
Protoperidinium conicum (Gran) Balech		x									
Protoperidinium depressum (Bailey) Balech		x							x		
Protoperidinium divergens (Ehrenberg) Balech				x							
Protoperidinium granii (Ostenfeld) Balech	x	x		x	x						
Protoperidinium oblongum (Aurivillius) Parke & Dodge	x										
Protoperidinium pellucidum Bergh	x						x		x	x	

Protoperidinium sp. R.S. Bergh		x		x	x				x	x	x
Protoperidinium steinii (Jørgensen) Balech	x	x								x	x
Scripsiella sp. Balech ex A.R. Loeblich III	x					x				x	x
OTHERS											
Dictyocha fibula Ehrenberg		x									
Dictyocha speculum Ehrenberg	x	x	x	x	x		x				
Dinobryon sp. Ehrenberg	x								x		x
Eutreptiella A. da Cunha					x	x				x	

Some of the identified taxa were recorded in almost every month, for example *Cylindrotheca closterium* was documented in all samples. *Skeletonema* sp. was not observed in the September sample and *Pseudo-nitzschia* spp. was not observed in the late February sample. Within the dinoflagellates, it was the genus *Tripos* and *Dinophysis* that occurred most frequently. The rest of the observed taxa were either seasonally dependent or appeared to be randomly occurring.

The variation in taxa over the sampling year is illustrated season by season (Table 6).

***Table 6**: Designated seasons to the sampling months*

Season	Sampling period
Autumn	September 12. – October 27.
Winter	November 25. – February
Spring	February 21. – May 16.
Summer	June 22. – August 7.

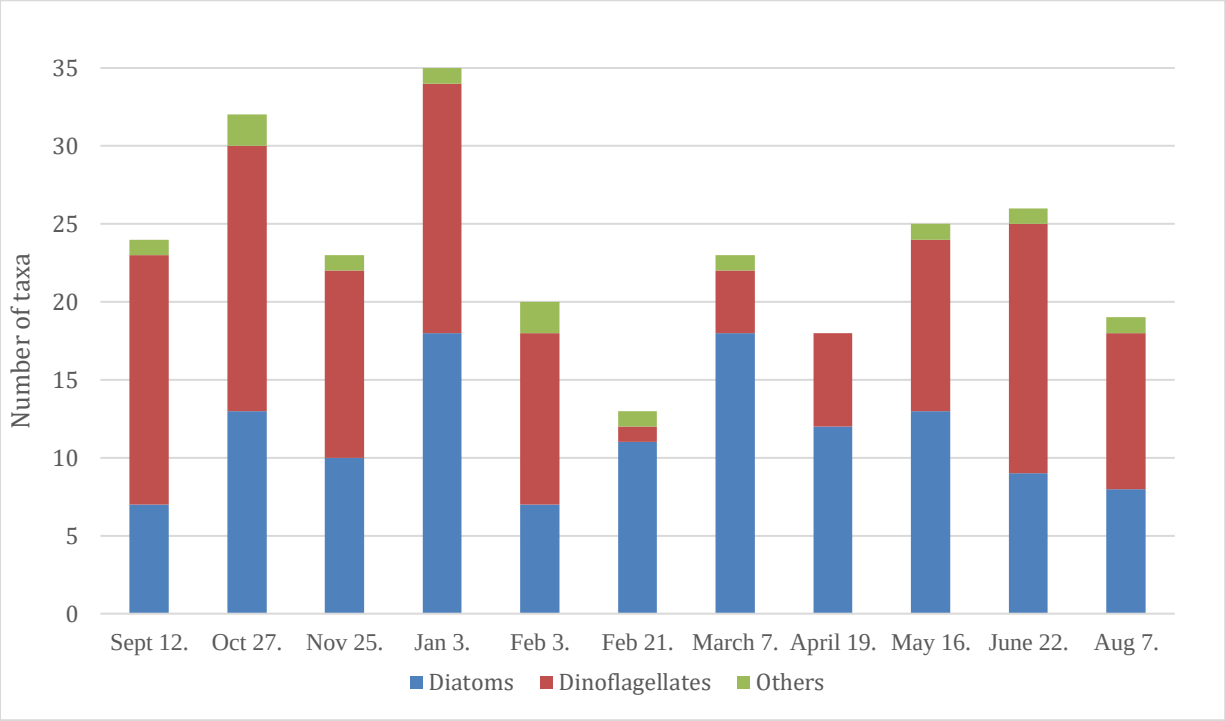

***Figure 21**: The variation in number of identified taxa over the sampling year. The blue areas correspond to the number of diatom taxa, red is the number of dinoflagellate taxa and green is the number of other taxa.*

The number of observed taxa was at its highest the 3rd of January with 35 taxa and the 27th of October with 32 taxa (Figure 21). The lowest observed number of taxa occurred the 21st of February. The remaining months fluctuated between 17 to 26 observed taxa.

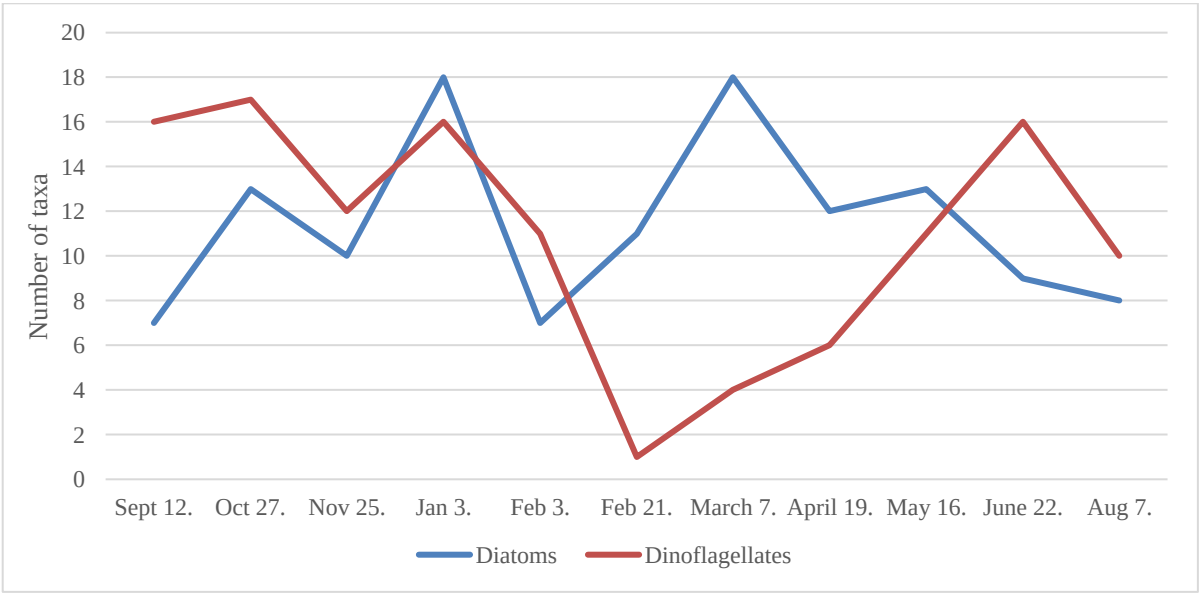

***Figure 22**: The variation in numbers of diatoms (blue line) and dinoflagellates (red line) taxa over the sampling year.*

In the autumn there were 47 described taxa, of which 25 were dinoflagellates. In September there were 16 observed dinoflagellate taxa and 7 diatom taxa (Figure 22). In October, there was a peak in observed taxa, where there were 17 taxa of dinoflagellates and 13 taxa of diatoms. Within the diatoms, *Skeletonema* sp., *Pseudo-nitzschia* spp., *Cylindrotheca closterium*, *Chaetoceros* spp., and various species of *Tripos* were observed. Several species of *Protoperidinium* occurred only in this season e.g., *Protoperidinium cf. conicoides, P. oblongum*, and *P. conicum*.

In November, there were 23 described taxa before an increase up to 35 different taxa in January. Regarding the observed taxa, 16 belong to dinoflagellates and 17 to diatoms, with several species observed within the same genus e.g., *Thalassiosira nordenskioldii* and *T. rotula.* In early February, the number of taxa dropped down to 20, with only 7 observed diatoms.

During the spring months, 66 taxa were observed. There was only one observed dinoflagellate taxon in late February belonging to the *Scripsiella* group. The number of dinoflagellate taxa increased up to 11 in May. For the diatoms, 11 taxa were observed in February, 17 taxa in March and 10-12 taxa in April-May.

During the summer season, it was the dinoflagellates that were the dominating group above the diatoms with 17 observed taxa. Several species of *Protoperidinium, Tripos*, and *Dinophysis* contributed to this increase. The number of observed diatom taxa were between 7 – 9.

3.2.2 Taxa abundance

A total of 44 different species were identified and counted (Table 7). Of these 22 were diatoms, 17 were dinoflagellates, and 4 were under the category "others". These were *Dictyocha speculum, Dictyocha fibula, Dinobryon* spp., and *Eutreptiella* spp.

***Table 7**: Phytoplankton cell counts at Drøbak between September 2016 and August 2017.*

Species	**Sept. 12.**	**Oct. 27.**	**Nov. 28.**	**Jan. 3.**	**Feb. 3.**	**Feb. 21**	**March 7.**	**April 19.**	**May 16.**	**June 22.**	**Aug. 7.**
Diatoms											
Chaetoceros socialis	0	0	0	0	0	0	106400	0	0	0	0
Chaetoceros curvisetus	0	350	0	0	0	0	0	0	0	0	0
Chaetoceros tenuisimus	0	0	0	0	0	0	0	25000	0	0	0
Chaetoceros decipiens	0	1350	0	0	0	0	5320	45600	0	0	0
Chaetoceros sp.	5720	4430	120	160	320	168	10640	26000	6200	26500	4000
Coscinodiscus spp.	0	0	0	0	0	0	200	0	0	0	0
Cylindrotheca closterium	8880	4000	160	360	480	80	2300	12400	0	2500	1200
Dactyliosolen fragilissimus	200	0	0	160	0	0	0	0	12200	67800	246300
Ditylum brightwellii	0	120	240	80	0	80	0	0	0	0	0
Guinardia delicatula	0	1400	0	0	0	0	0	0	1100	0	0
Leptocylindrus danicus	0	5400	3480	4520	200	0	0	0	0	4300	0
Leptocylindrus minimus	0	0	0	0	0	0	0	0	0	0	49600

Leptocylindrus spp.	0	0	0	0	0	0	1500	66600	0	0	0
Licmorphora spp.	0	0	0	0	0	0	300	800	0	500	0
Melosira moniliformis	0	80	0	0	0	0		0	0	0	0
Navicula spp.	0	1720	160	480	560	480	3000	0	0	400	0
Odontella aurita	0	0	0	0	0	0	200	0	0	0	0
Proboscia alata	0	0	320	0	0	0	500	1000	0	1600	1700
Pseudo-nitzschia spp.	20320	22960	4520	3280	800	0	11200	1023100	1234596734	166200	0
Rhizosolenia hebetata f. hebetata	420	800	0	80	0	1520	3000	0	0	0	0
Skeletonema spp.	0	1600	200	520	3560	70840	330900	800300	173100	12300	0
Thalassionema nitzschioides	0	0	0	0	0	3840	8300	32600	53900	400	0
Thalassiosira spp.	0	280	80	800	0	1680	14800	0	0	0	0
Dinoflagellates											
Akashiwo sanguinea	0	0	800	0	640	0	400	0	0	0	0
Tripos fusus	0	0	0	0	0	0	0	0	200	0	0

Tripos horridum	0	0	0	0	0	0	0	0	0	700	0
Tripos lineatus	160	80	360	0	0	0	200	0	0	0	0
Tripos muelleri	40	0	280	40	0	0	0	0	600	2200	0
Dinophysis acuminata	0	0	80	80	40	0	0	0	0	0	0
Dinophysis acuta	200	0	0	0	0	0	0	0	0	0	0
Dinophysis norvegica	0	0	80	0	40	0	0	0	0	900	0
Dinophysis rotundata	0	0	0	0	40	0	0	0	0	0	0
Dinophysis spp.	0	0	0	0	0	0	0	0	200	0	0
Gymnodinium spp.	4200	840	280	680	1280	5240	7000	49600	3800	0	2400
Gyrodinium fusiforme	5320	200	200	0	40	0	0	0	0	0	0
Prorocentrum micans	13000	200	0	0	0	0	0	0	0	0	4600
Prorocentrum minimum	0	0	0	0	280	0	62100	0	0	0	0
Prorocentrum spp.	0	0	0	0	0	0	0	354100	0	1300	0
Protoperidinium spp.	17840	320	280	240	1440	9520	1800	2300	2700	300	0
Scripsiella group	0	40	0	0	0	3840	0	0	4700	0	0
Others											

Dictyocha fibula	200	0	0	0	0	0	0	0	0	0	0
Dictyocha speculum	0	240	4760	800	9200	400	1400	0	0	0	0
Dinobryon spp.	160	0	0	0	0	0	0	0	4800	0	2500
Eutreptiella spp.	0	0	0	0	440	2520	0	0	0	400	0

Diatoms dominated in terms of cell numbers most of the year, the exception was in September when the dinoflagellates were more abundant (Figure 23). In May, an exceptional one billion *Pseudo-nitzschia* spp. cells were recorded (Figure 23).

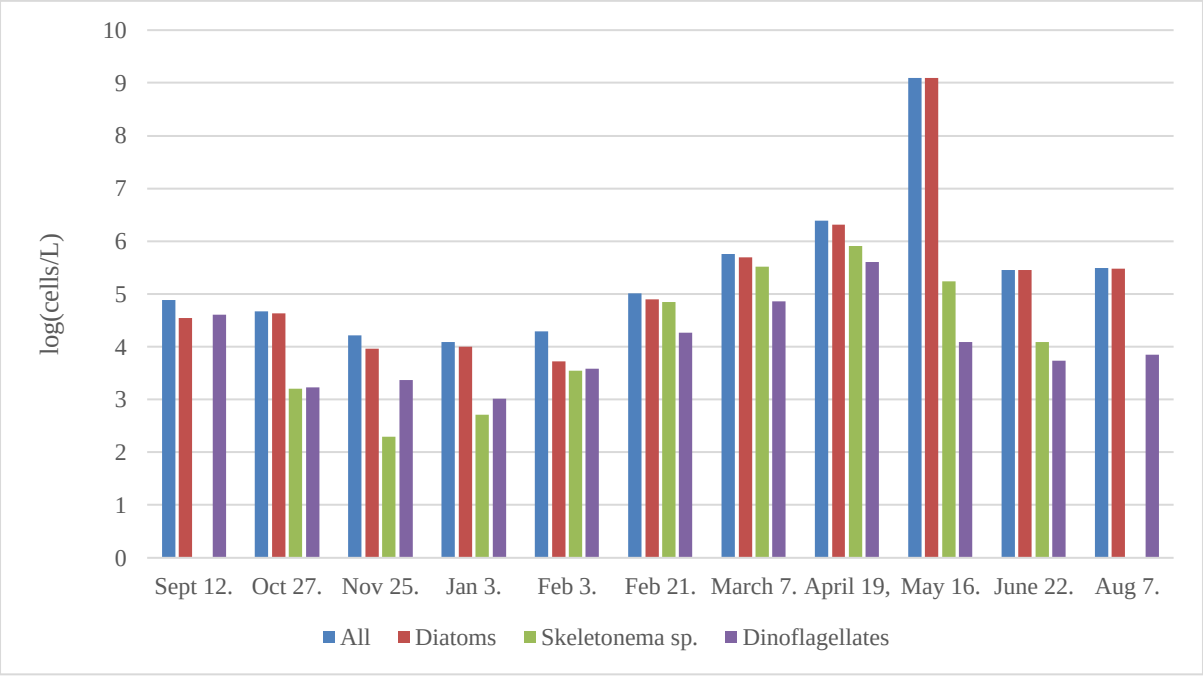

***Figure 23**: Abundance of total phytoplankton, diatoms,* Skeletonema *sp., and dinoflagellates.*

The number of counted cells peaked in March to May. The species that contributed most to the cell abundance were *Skeletonema* sp., *Pseudo-nitzschia* spp., *Thalassiosira* spp., *Thalassionema nitzschioides* and *Chaetoceros* spp. In September, there were high numbers of cells of *Prorocentrum micans, Gymnodiniales* spp., and *Protoperidinium* spp. that caused the increase of counted dinoflagellate cells.

There were some variations between the cell counts from 1957 – 1958 (Appendix 7) and those of 2016 – 2017 (Figure 24). To enable a comparison between the two investigations, some alternations were necessary. Hasle & Smayda sampled at Drøbak from February 1957 to May 1958. As the present study was conducted during fewer months than that of Hasle & Smayda, most of the selected cell count numbers used in comparison with the present study are from 1957. The exception is the cell counts from January 1958 that were included as there were no samples from January 1957. There were two samplings from February 2017 and only one in 1957. The Feb and Feb II from 1957 are results from the same sample.

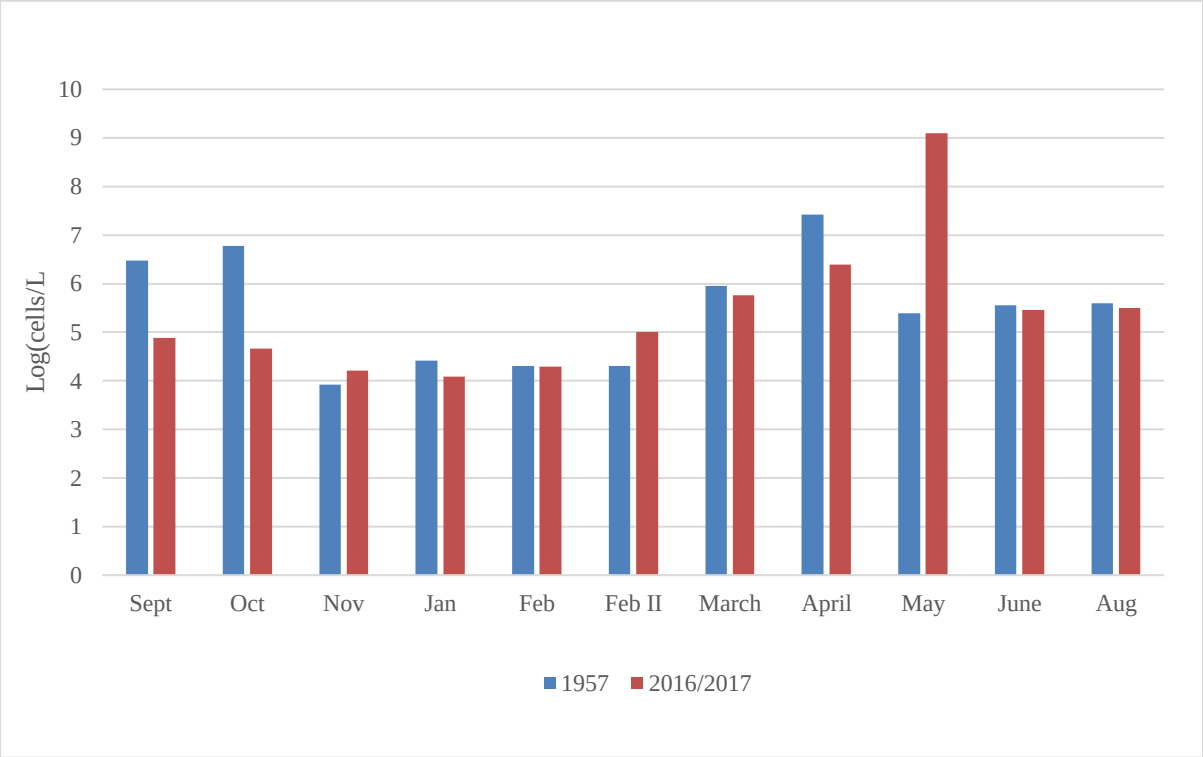

***Figure 24**: Comparison of phytoplankton cell abundance (note: logarithmic scale) between the present 2017 observations and those of Hasle & Smayda in 1957.*

There were some differences between the two investigations such as fewer cells per liter counted in 2017 (Figure 24). The exception was in November, February II and May. The taxa that contributed to the high cell counts were *Skeletonema* sp., *Chaetoceros* spp., *Thalassiosira* spp., *Pseudo-nitzschia* spp. and *Leptocylindrus* spp.

3.2.3 Biovolume

Diatoms dominated the samples in terms of biovolume (Figure 25). The values were especially high in April, May, and August. *Chaetoceros* spp., *Leptocylindrus danicus*, *Pseudo-nitzschia* spp., *Skeletonema* sp., and *Thalassionema nitzschioides* dominated the April sample. In

August, the high biovolume was due to *Dactyliosolen fragilissimus*, *Cerataulina pelagica*, and L*eptocylindrus danicus.* The excessive values in May were due to the amount of *Pseudo-nitzschia* spp. cells (1234596734 cells/L). Due to these extreme values the remaining biovolume data may appear small. However, in April the total biovolume of phytoplankton was at 3601.329 mm^3/L contra 592.86 mm^3/L the previous month.

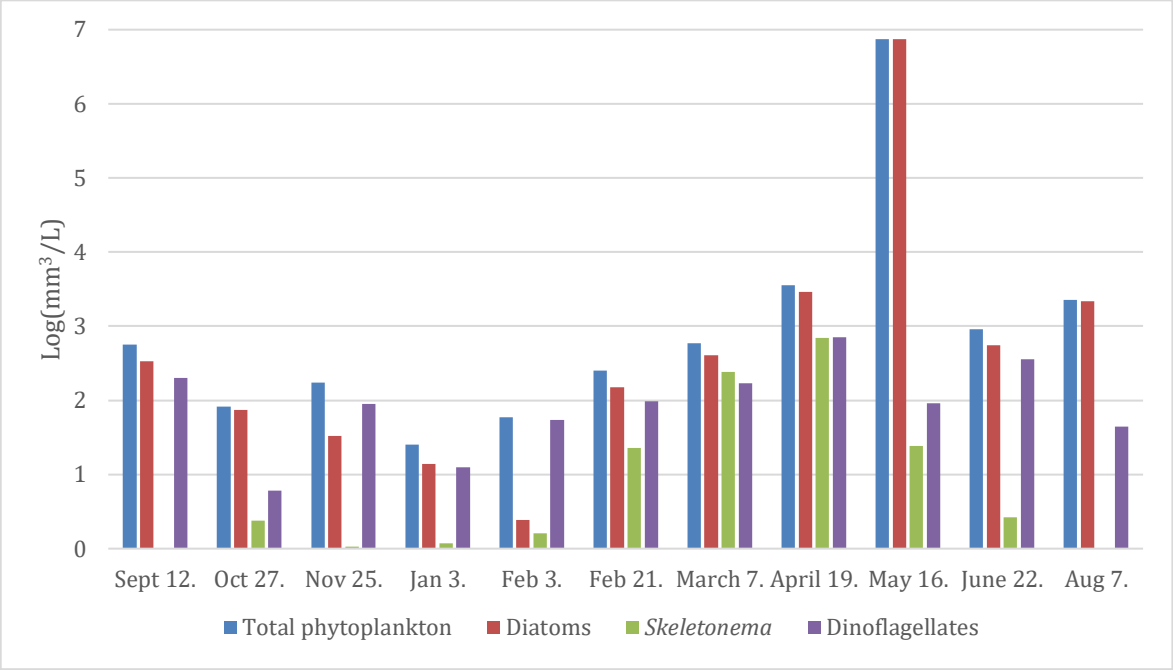

Figure 25*: Calculated biovolume in mm^3/L derived from cell counts of diatoms, dinoflagellates and* Skeletonema *over the sampling year (note: in logarithmic scale).*

The biovolume was at its lowest during winter and autumn. In January, the value for diatoms was at 12.7 mm^3/L and 11.5 mm^3/L for dinoflagellates. The biovolume of dinoflagellates remained lower than the value of diatoms throughout almost the entire year, except for two samplings on the 3rd of February with 53 mm^3/L versus 2.6 mm^3/L, and the 25th of November with 88.6 mm^3/L versus 31.9 mm^3/L.

The percentage of *Skeletonema* in all microalgae and all diatoms was calculated from the biovolume (Figure 26 – 27).

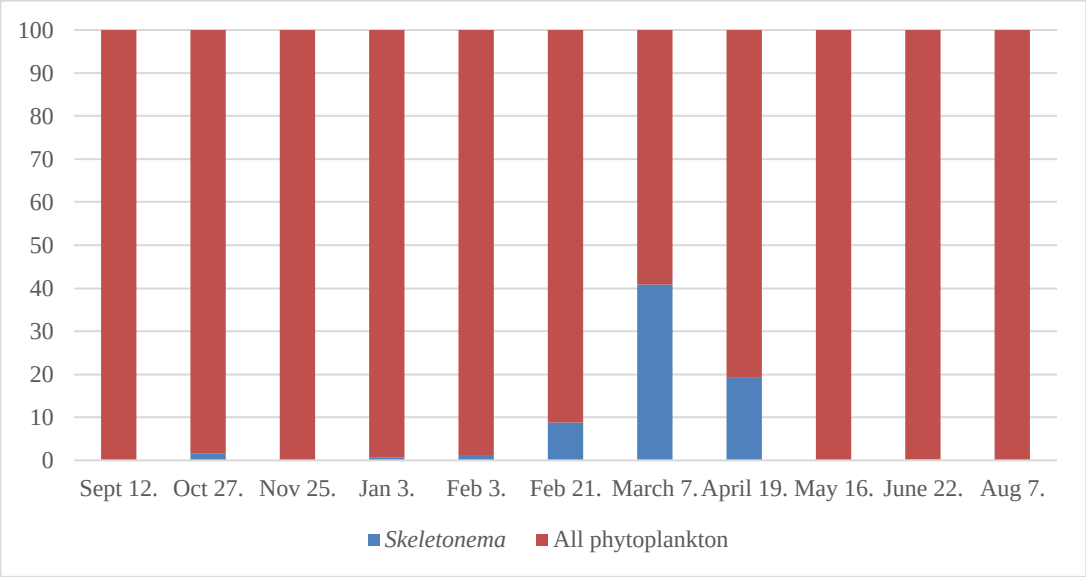

*Figure **26**: Percentage of* Skeletonema *to total biovolume of microalgae.*

Skeletonema contributed a significant part of the total phytoplankton biovolume during the spring. On the 21st of February the biovolume was at 10%, in March it was at 40% and in April it was at 20%. The May sample showed a dominance of *Pseudo-nitzschia* spp.

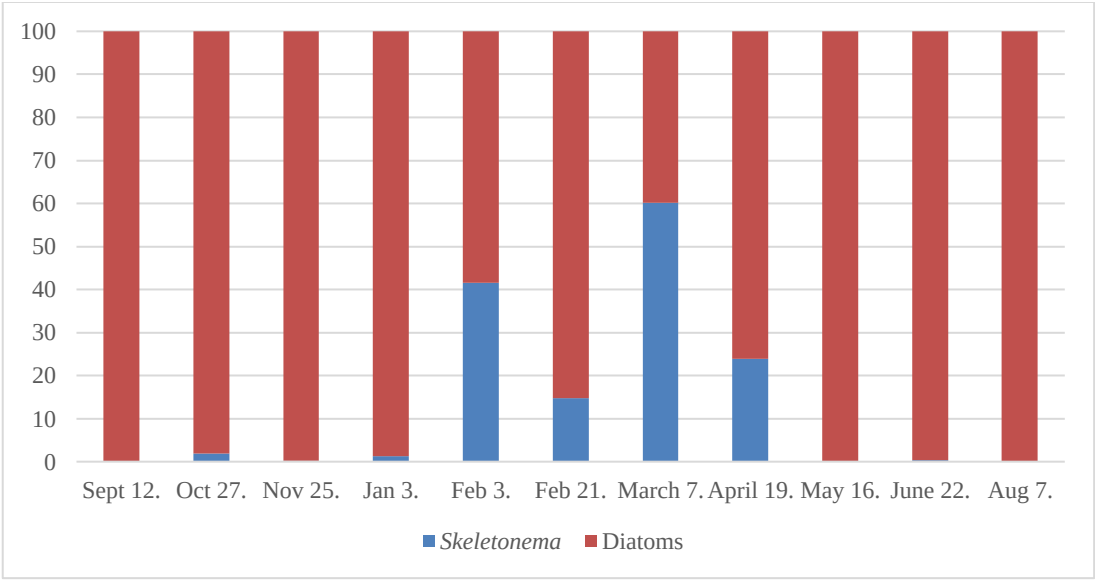

***Figure 27**: Percentage of* Skeletonema *to total biovolume of diatoms.*

The same trend appeared when comparing the biovolume of *Skeletonema* with that of diatoms. However, *Skeletonema* did contribute more to the total diatom biovolume than the total

phytoplankton biovolume. On the 3rd of February, *Skeletonema* biovolume was 40% of the total diatom biovolume versus 1% of the microalgae and in March 60% of the diatom biovolume belonged to *Skeletonema*.

3.3 *Skeletonema*

The same terms to describe morphological features in *Skeletonema* (Table 3) were used in the present study as used in the research of Sarno et al. (2005).

3.3.1 Historical material – what was previously in the fjord

Of the five cleaned samples from the Grethe Hasle collection, three contained cells of *Skeletonema* (Figure 28 – 29). The sample from April 4th,1930 had many cells. The linking of intercalary strutted processes was in a 1:2 zigzag formation with a plaint joint (Figure 28 left), the terminal valves had strutted processes with flared tips and the terminal labiate process was located sub-centrally. Together these morphological structures verify that the *Skeletonema* species found in Drøbak in 1930 was *Skeletonema marinoi.*

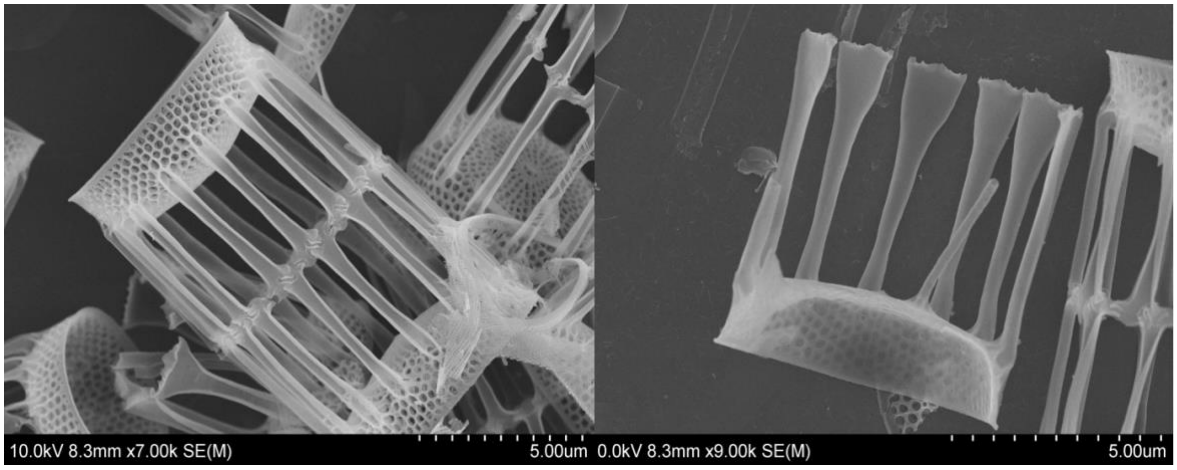

Figure 28*: Intercalary strutted processes (left) and terminal strutted processes (right)* Skeletonema marinoi *collected by Grethe Hasle at Drøbak the 04.04.1930.*

Fewer cells of *Skeletonema* were observed in the samples from March 22nd,1936 and December 1st,1936 (Figure 29). No terminal valves were found, but there were several intercalary valves. In the sample from 1936 the cells were a little damaged, and it was difficult to see important structures. It was still possible to observe the linking of processes that was in a 1:2 zigzag and plaint joint formation. This linking is found both in *S. costatum* and in *S.*

marinoi. It can be concluded that the sample from 1930 contains *S. marinoi*. This was not possible for the samples from 1936 and 1987.

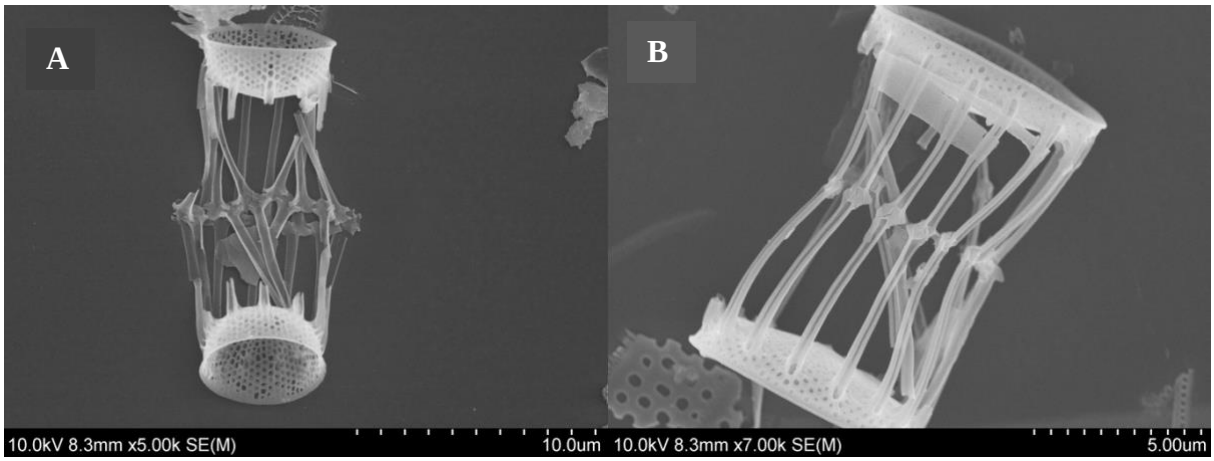

***Figure 29**: Skeletonema marinoi collected at Drøbak **A**: 22.03.1936 and **B**: 01.12.1987 (right).*

The amount of counted cells of *Skeletonema* differs between the present study and that of Hasle & Smayda (1960; Figure 30).

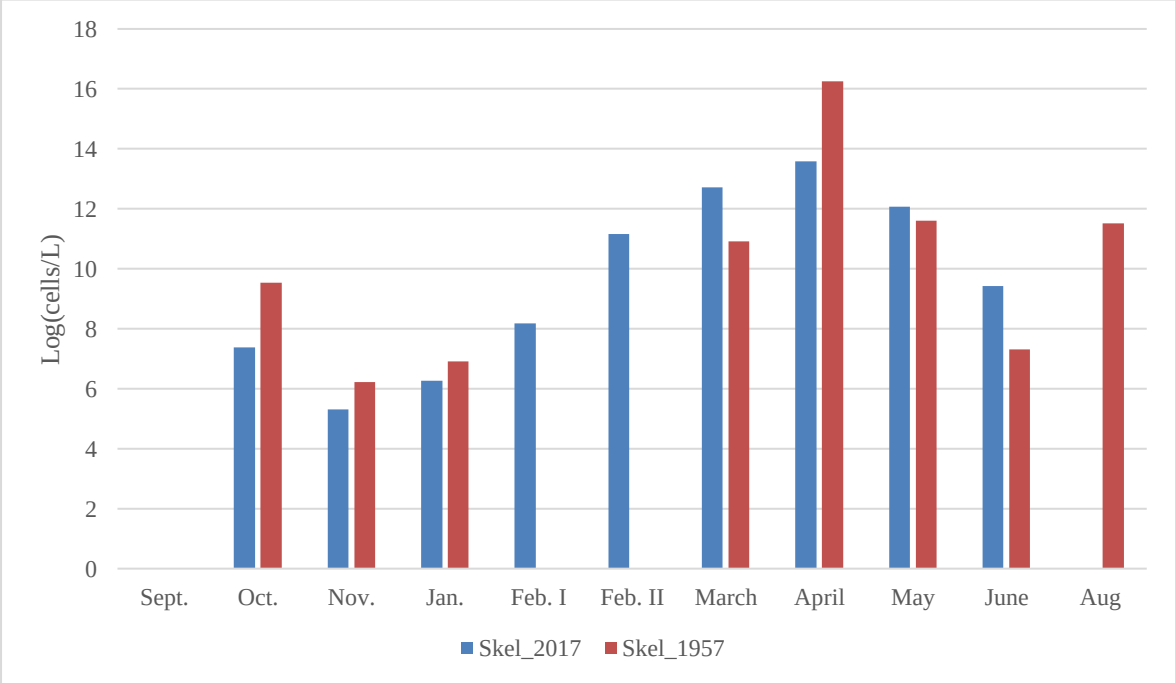

***Figure 30**: The difference in counted cell number of* Skeletonema *from the research of Hasle & Smayda (Red) in 1957 and the present study from 2016 – 2017 (blue).*

Hasle & Smayda documented more cell counts of *Skeletonema* from October to January, and in April and August, than the present study (Figure 30). However, there were more cell counts of *Skeletonema* documented in 2016/2017 between February to March and May to June, than

during the same months in 1957. There is a significant difference between the cell counts in April, with 0.8 million cells in 2017 and 11 million cells in 1957.

3.3.2 The identity of NIVA-Bac 1, *Skeletonema pseudocostatum*

There were many cells in the SEM prepared sample of the culture NIVA-Bac 1 (Figure 31 –33). There were only single cells and therefore no intercalary strutted processes that could be used in species identification. Some process-looking structures were visible. They were situated marginally and looked tubular at the basal part, with an oblique opening (Figure 33). It is the same formation which is found in the terminal strutted process of *Skeletonema pseudocostatum (*Figure 34; Sarno et al., 2005). There was also a structure that was located sub-centrally on the cell, which presumably is the terminal labiate process (arrow in Figure 31). It was located in the same area where it is found in *S. marinoi* and *S. pseudocostatum*.

Even though there was a resemblance between the culture and *S. pseudocostatum*, it is difficult to conclude that it is the same species as there are no intercalary strutted processes in the culture to study.

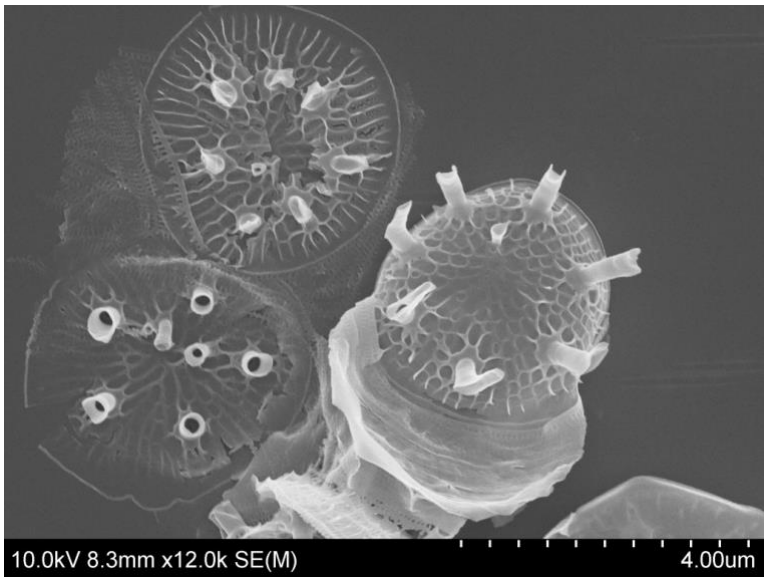

Figure 31*: SEM micrograph of the culture NIVA-Bac 1 showing valves and processes.*

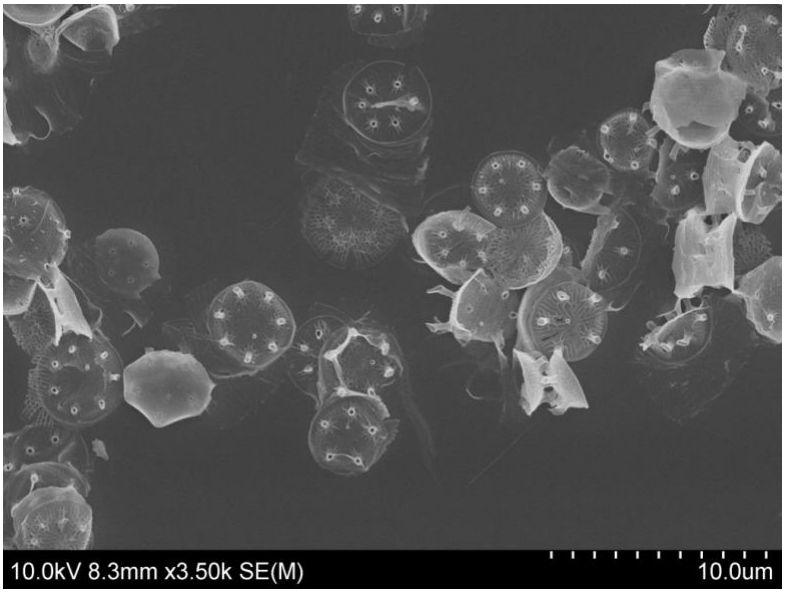

***Figure 32**: SEM micrograph of the culture NIVA-Bac 1 showing many single cells.*

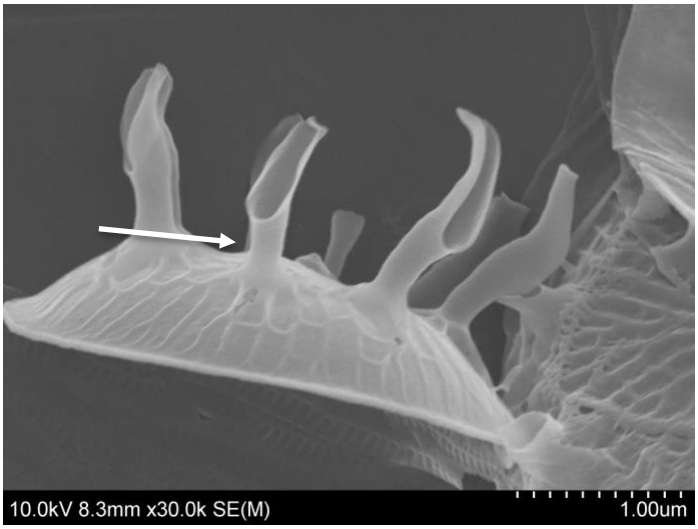

***Figure 33**: Structures that resembles terminal strutted processes in the valves of NIVA-Bac 1.*

***Figure 34**: Terminal strutted processes (arrow) in* Skeletonema pseudocostatum *(Sarno et al, 2005).*

Based on the analysis of the isolated LSU rDNA, the culture contained *S. pseudocostatum* sequence. The NIVA-Bac 1 sequence is located on the same branch in the phylogenetic tree as *S. pseudocostatum* identified by Sarno et al. (2005), which further confirms the species identity of the culture (Figure 35).

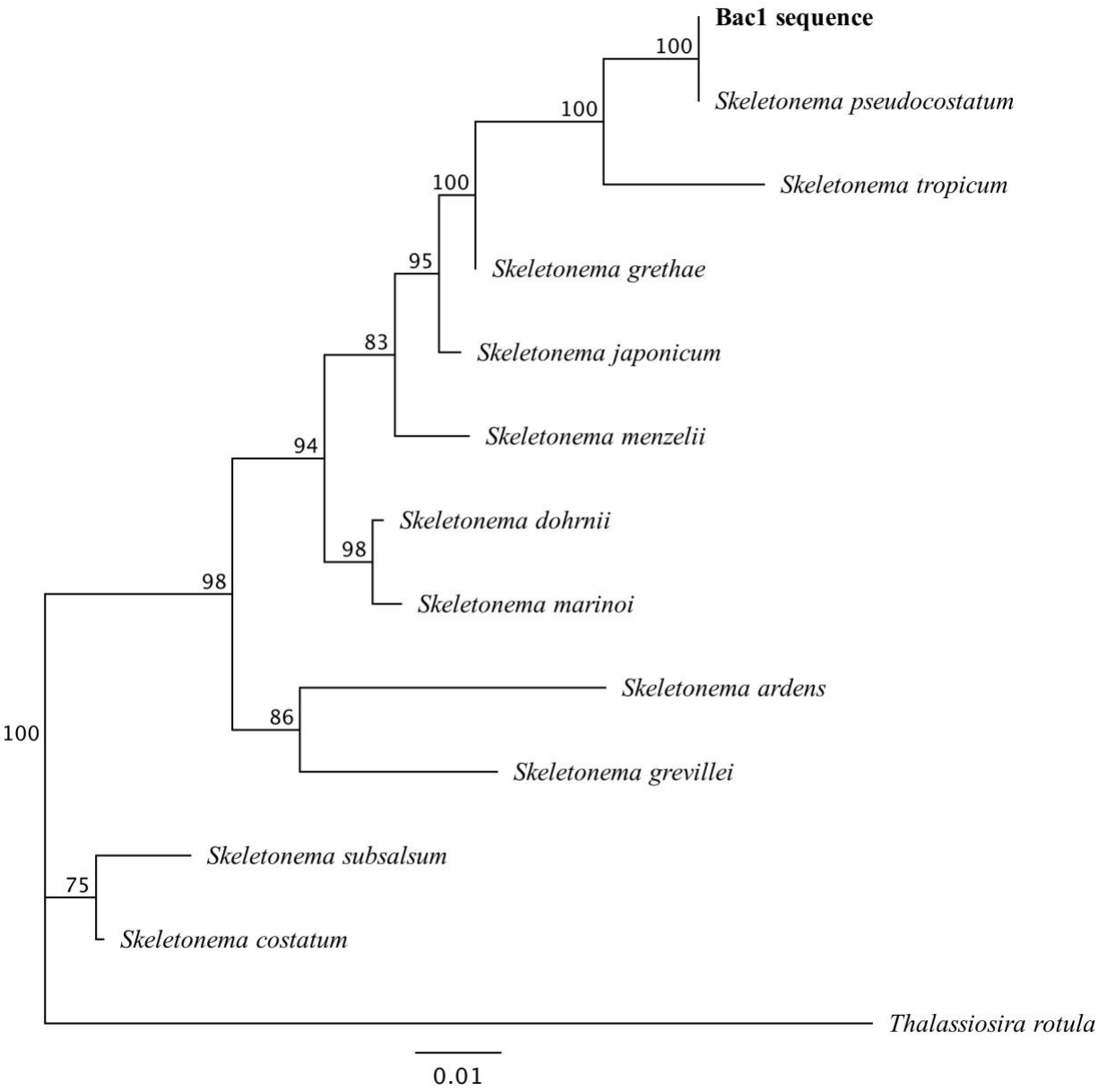

Figure 35*: Neighbor joining tree inferred from the nuclear rDNA LSU from* Skeletonema *sequences.*

3.3.3 New material – what was in the fjord between September 2016 and August 2017

The genus *Skeletonema* was present in all samples except the one from August. Species identification using morphological features is illustrated in SEM micrographs (Figure 36 – 43).

Both pictures from LM and SEM illustrate a variation in morphology (Figure 36). These differences were in cell size, both length and width, as well as in the number of cells in a chain and the chain length.

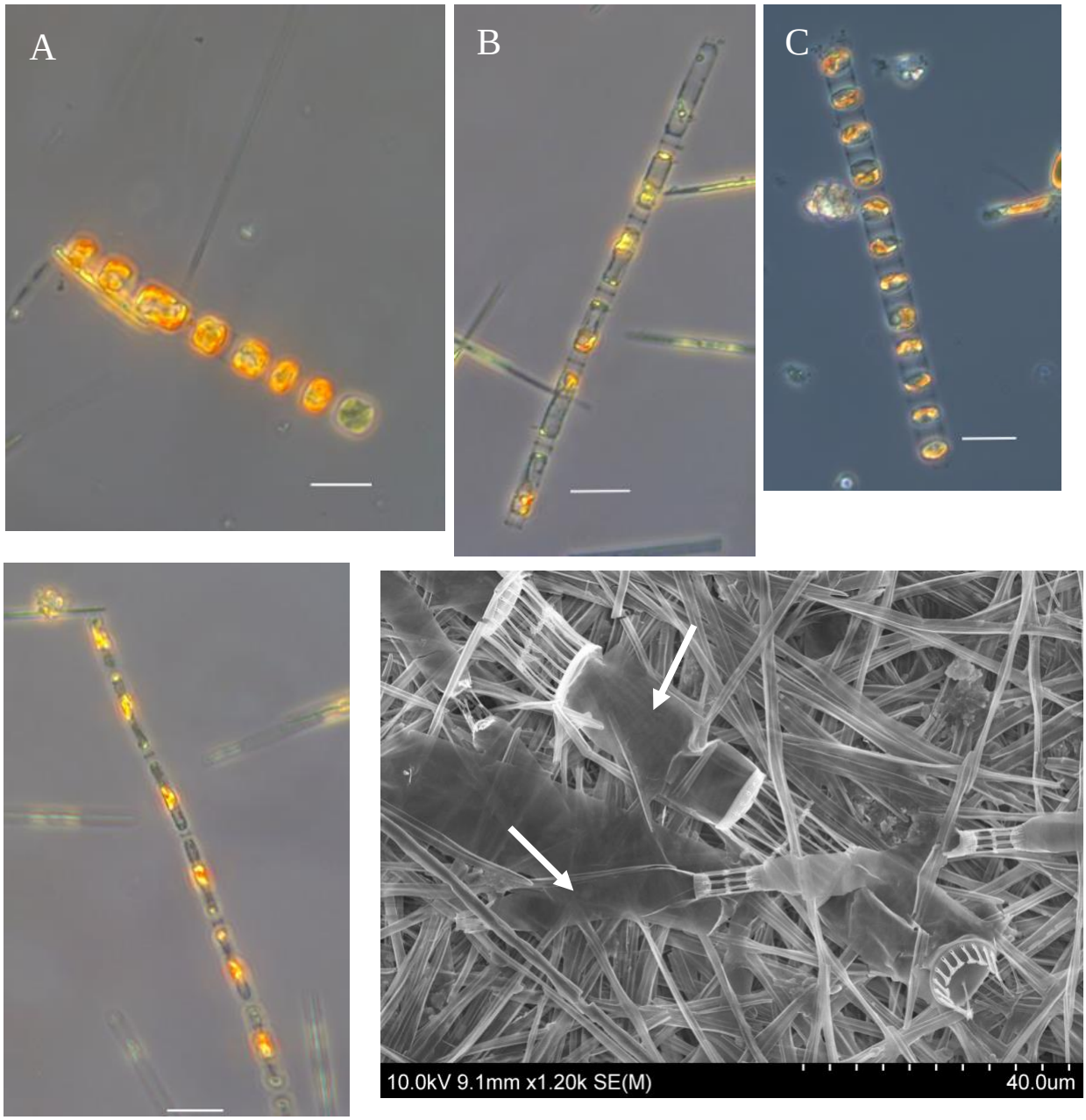

***Figure 36**: LM (**A-D**) and SEM micrographs (**E**) illustrate the variation in* Skeletonema *cell morphology found throughout the sampling year. A-D; scalebar 20µm. E: arrows pointing at two chains with visible width and process differences.*

In the picture taken in SEM, it is easy to see how different the cells might look (Figure 36 E). There are four chains lying next to and on top of each other. Two arrows are pointing at two different chains. These chains contain cells that have a different width. In addition, the chain

with the widest cells have longer and more intercalary strutted processes than the chain with smaller cells. These variations in cell and chain morphology could be found within a sampling month (e.g., October and May) as well as between the different sampling months. There were also visible differences in the frustule thickness. In some samples, newly formed processes were visible beneath the frustule, e.g., in samples from February (Figure 37). In others samples the frustule had a thicker appearance with band structures over the cell (Figure 38).

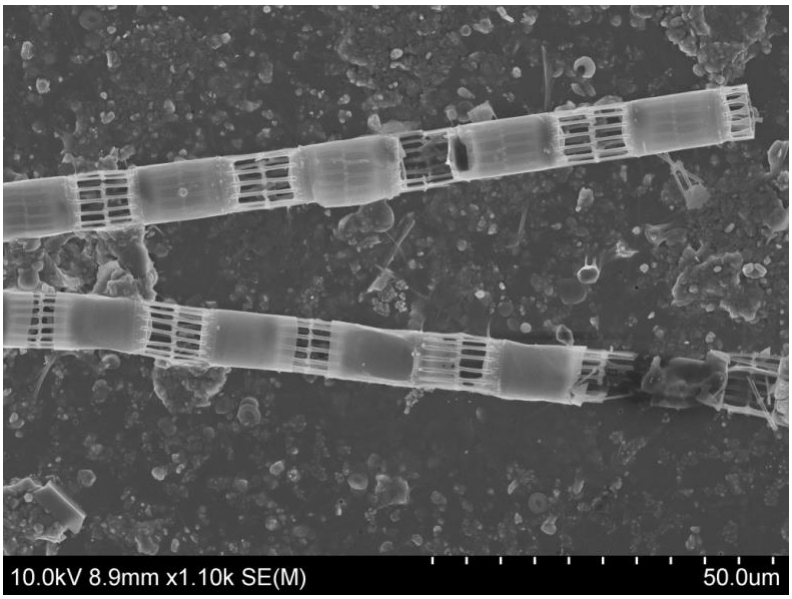

***Figure 37**: SEM micrograph of* Skeletonema *from 16.05.2017 with visible processes beneath the frustule.*

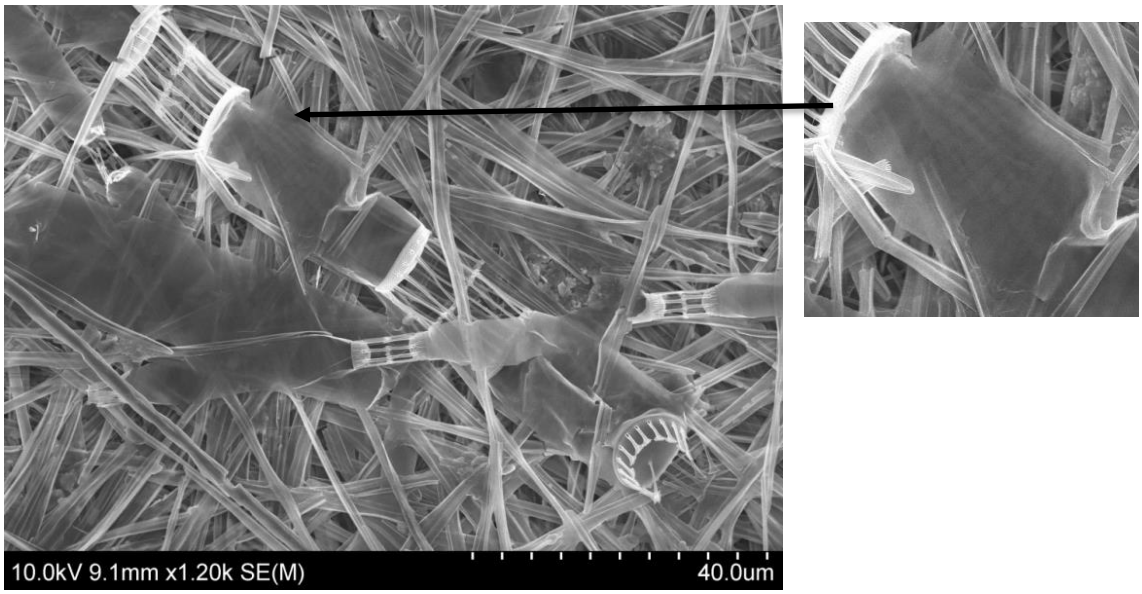

***Figure 38**: SEM micrograph of* Skeletonema *from 21.02.2017 with a zoom on the frustule with visible band structures.*

In SEM it was possible to see that the abovementioned variations did not lead to different species. In addition, it was possible to see that species-specific structures, as used to describe Hasle's findings, were the same in all the varying cells and chains. Three different methods were used to prepare stubs for SEM. The filtrated water from the Niskin bottles and Ruttner sampler were most used in the species identification as important structures were visible without acid cleaning. In the case of the acid cleaned net haul samples, it was necessary with the poly-L-lysine glass on the stubs too enable visualization of the phytoplankton.

Intercalary valves and processes

The intercalary strutted processes were aligned by two manners in all the samples with *Skeletonema*. Either the intercalary strutted processes were aligned in a 1:1 linkage, or they were displaced in a 1:2 linkage. The linkage resembles a zigzag connection line. The distal end of the intercalary strutted processes was flattened and flared, and the interlocking between two adjacent intercalary strutted processes was a plaint joint with flared tip against flared tip (Figure 39 – 40).

In all the samples, it was the 1:2 linkage that occurred the most. Some chains contained both 1:1 and 1:2 linkage types (Figure 39).

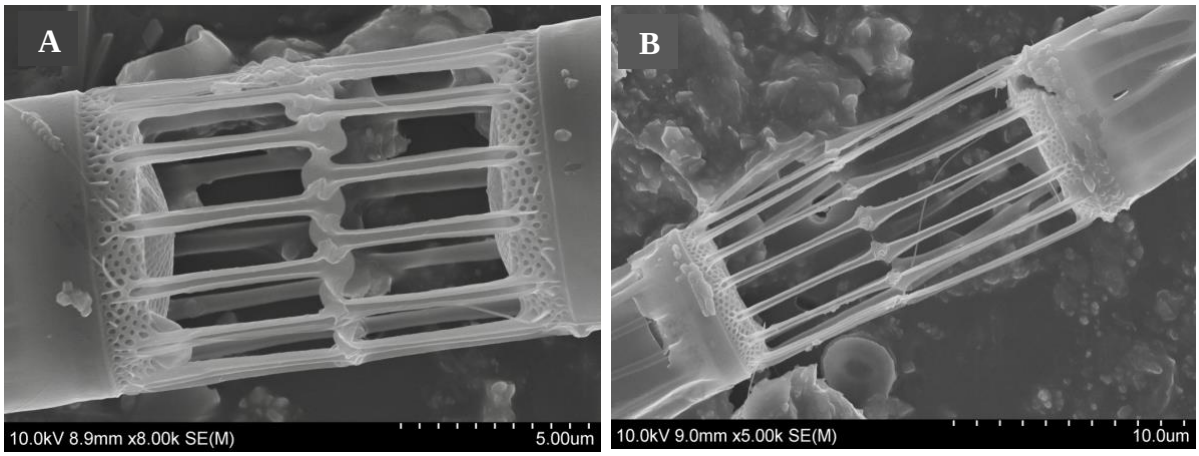

Figure 39*: SEM micrograph of interlocking of strutted processes from one chain in* ***A****: 1:2 formation in* Skeletonema*, and* ***B****: 1:1 formation.*

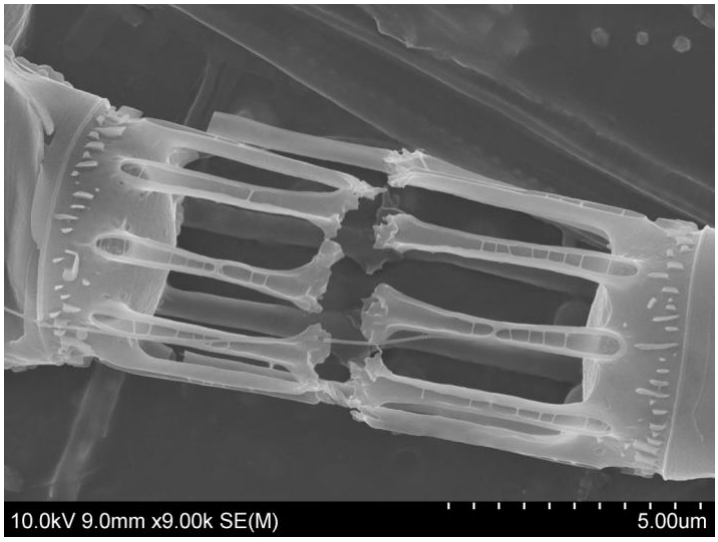

Figure 40*: SEM micrograph of intercalary strutted processes that have a disconnected meeting point. (November 2016) sample.*

The intercalary labiate process was short and located at the margin of the intercalary valves (Figure 41).

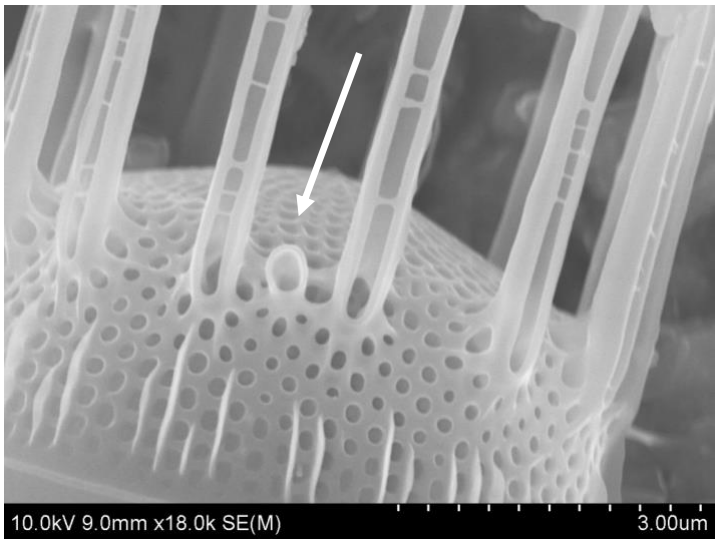

Figure 41: *SEM micrograph of intercalary labiate process (arrow) in* Skeletonema.

The terminal valves and processes

The strutted processes in terminal vales, found in samples containing *Skeletonema*, were open along their entire length and with a dentate margin at their distal end (Figure 42). The labiate process was located a little sub-centrally and had a long, truncate locking process (Figure 42 – 45, note arrows).

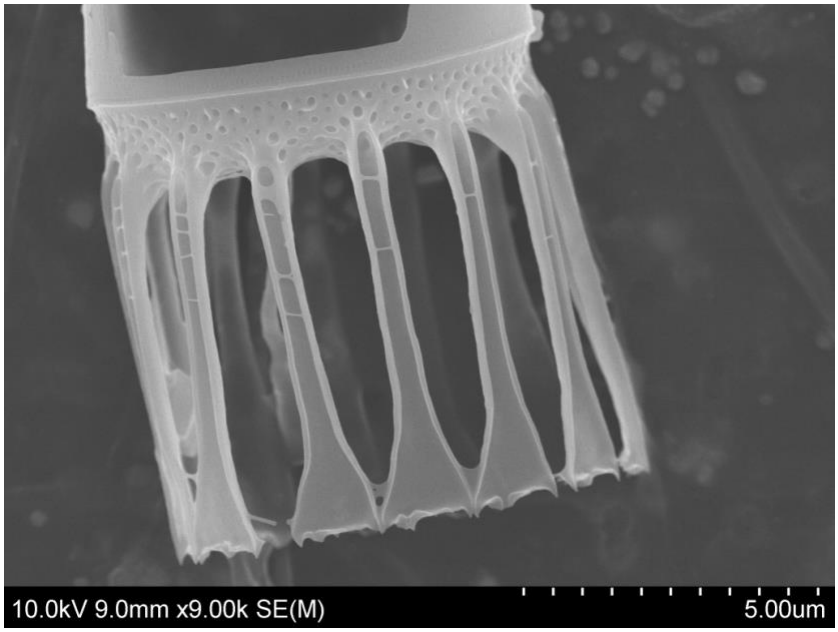

***Figure 42**: SEM micrograph of terminal strutted process.*

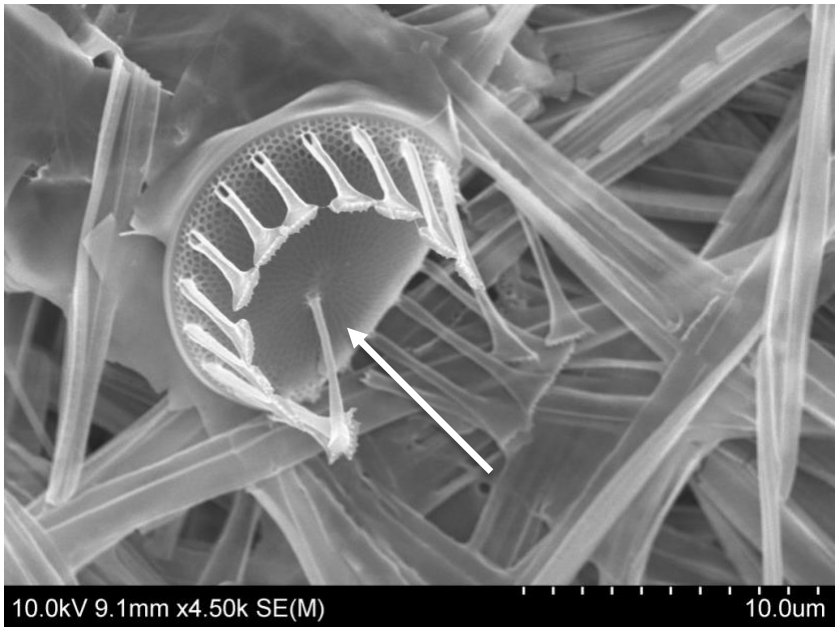

.

***Figure 43**: SEM micrograph of terminal valve of Skeletonema with arrow pointing at the terminal labiate process*

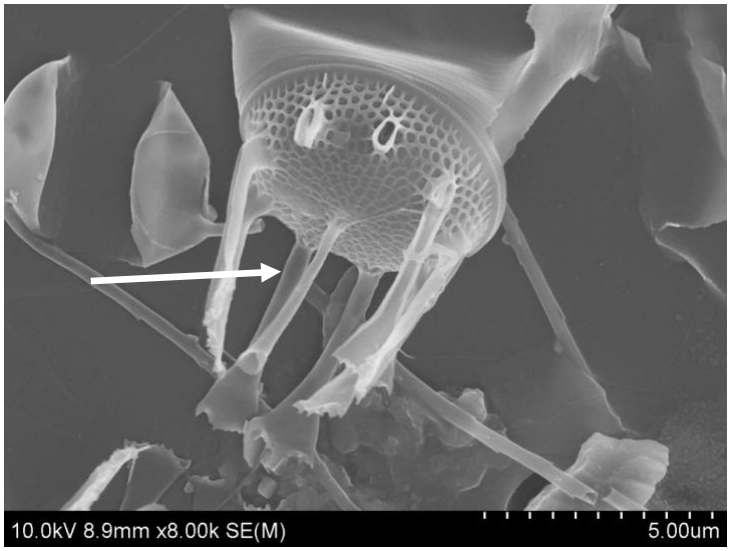

***Figure 44**: SEM micrograph of terminal valve of* Skeletonema *with arrow pointing at the terminal labiate process.*

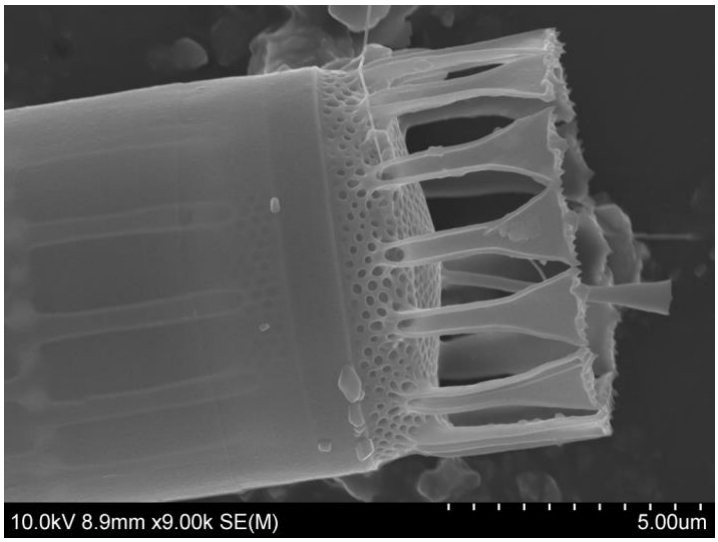

***Figure 45**: SEM micrographs of terminal valve with terminal strutted process and the terminal labiate process.*

Using all these identified structures, it is possible to conclude that the *Skeletonema* found at Drøbak from September 2016 to August 2017 is *Skeletonema marinoi.*

3.3.4 Variation in cell size and chain length

With a generalized additive model (GAM), it was possible to see that the cell length in *Skeletonema marinoi* varies over the sampling year (Figure 46). The variation in size

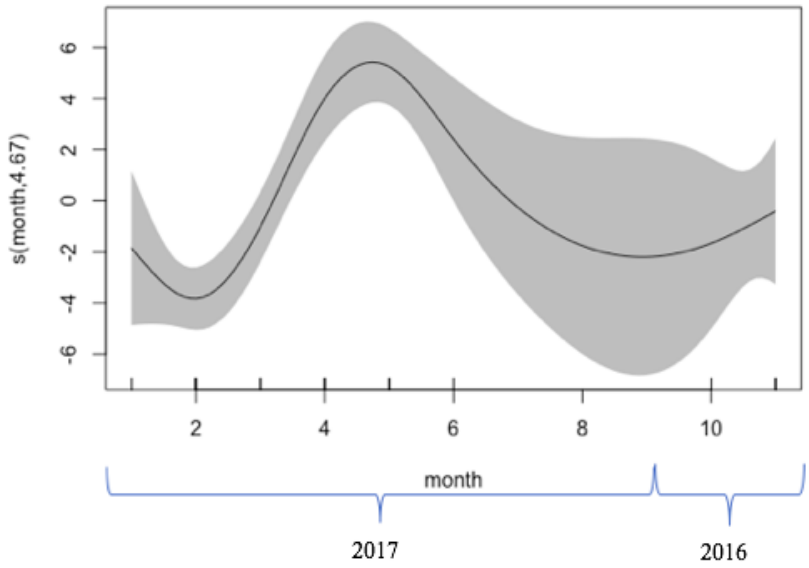

***Figure 46**: Variation of cell length in* Skeletonema marinoi *illustrated with GAM.*

correlated with the different months (Figure 46) (R^2 = 0.317, p-value > 0.001). The cell size increased from March to May with a length up to 19 µm, before it decreased until August to October where it varied from 7.5 µm to 15 µm.

The cell size also correlated with the variation in salinity (Figure 47) and temperature (Figure 48). Both analyses were justified with low p-values and high R^2 values (Table 8).

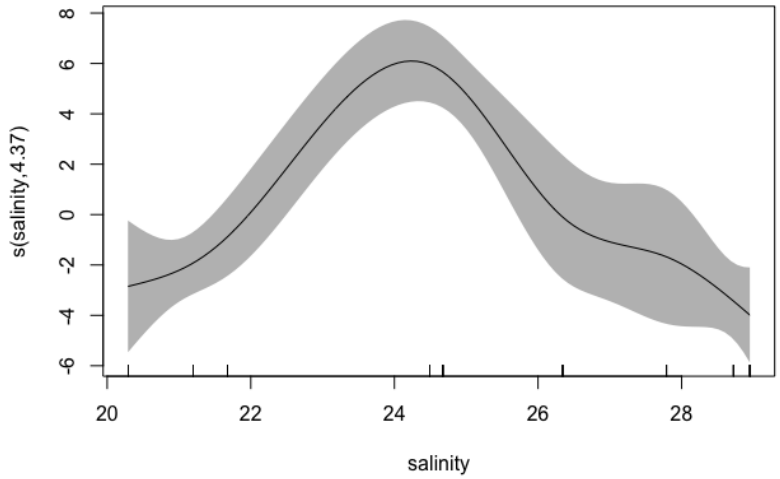

***Figure 47:** Variation of cell length with the variation of salinity over the sampling year.*

The largest cells were found at a salinity around 22 – 26 PSU and at a temperature between 5-11°C.

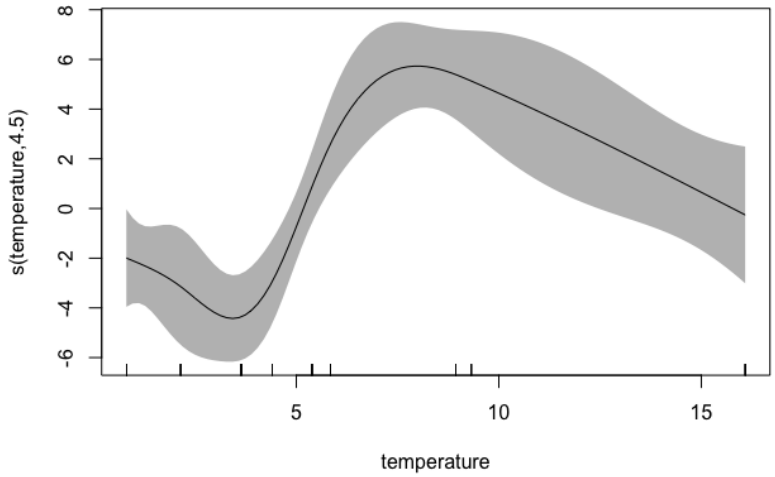

Figure 48: *Variation of cell length with the variation of temperature over the sampling year.*

The variation of number of cells in a chain as a function of temperature (Figure 49), salinity and month were also analyzed in GAM (Figure 49). These analyses, however did result in good R^2 or p-value (Table 8).

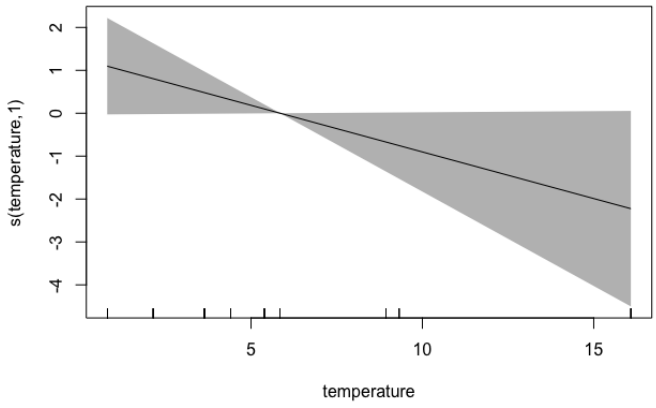

Figure 49: *Variation of the number of cells in a chain with the variation of temperature over the sampling year.*

***Table 8**: Model summary of GAM analysis on cell length and number of cells in chain.*

	Cell length/month	Cell length/PSU	Cell length/Temperature	Number of cells in chain/temperature
Estimated Std.	13.1484	13.1484	13.1484	7.1028
p-value	$4.13*10^{-8}$	$1.16*10^{-10}$	$2.34*10^{-8}$	0.0535
R^2	0.317	0.386	0.322	0.0258
Deviance explained	34.7%	41.1%	35.1%	3.5%

The variation of chain length correlated with the different months and the changing temperature and salinity (Figure 50, Table 9). As with the cell length, the largest chains were found during the spring, with a temperature between 5°C and 15°C, and with a salinity between 22 and 26 PSU.

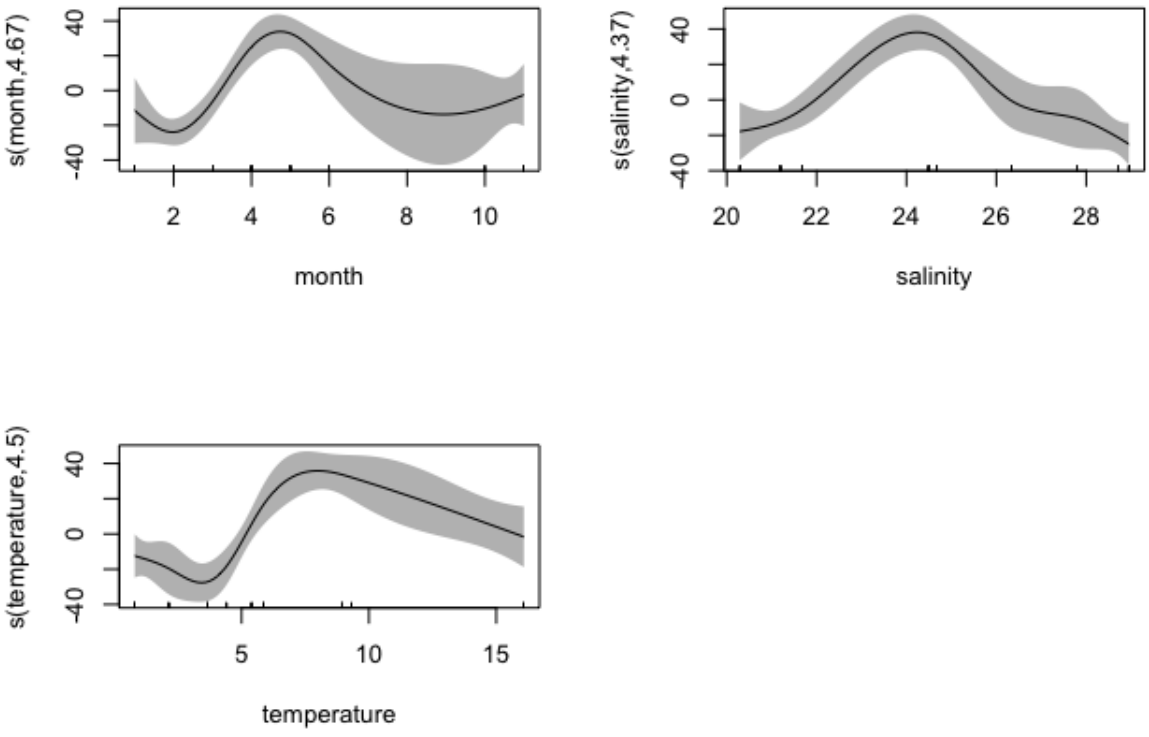

***Figure 50**: Variation of chain length with month, salinity and temperature.*

***Table 9**: Model summary of GAM analysis on chain length.*

	Chain length/month	Chain length/PSU	Chain length/temperature
Estimated Std.	82.177	82.177	82.177
p-value	$4.13*10^{-8}$	$1.16*10^{-10}$	$2.34*10^{-8}$
R^2	0.317	0.386	0.322
Deviance explained	34.7%	41.1%	35.1%

4 Discussion

This investigation at Drøbak showed a seasonal dynamic phytoplankton abundance similar to previous studies. It also revealed that *Skeletonema marinoi* is an annual species that occurs in Oslofjorden during all seasons. Further that *S. pseudocostatum* was found previously at Drøbak which leads to the belief that more than one species of *Skeletonema* may occur in Oslofjorden.

4.1 The seasonal cycle of phytoplankton at Drøbak 2016-2017

4.1.1 The observed hydrographical variations

The hydrographical data demonstrated seasonal changes as in previously reported trends (Braarud & Bursa, 1939; Hasle & Smayda, 1960; Walday et al., 2015). The variation in temperature over the year illustrates seasonal changes typical of temperate seas. The salinity fluctuates a bit more than the temperature, indicating that there might have been an input of different water masses. For instance, the sudden change in salinity from January 2017 to February 2017 can result from snow melting and an increase of freshwater, whereas the rise in salinity from late February to March can be a consequence of deep water mixing (Figure 16). The temperature from 2016/2017 illustrate the same variations as was found in 1957/1958 (Figure 17) which are typical for Oslofjorden (Walday et al., 2017). However, the salinity measurements from these two investigations were different (Figure 18). In total, the salinity was a bit higher in 1957/1958 than 2016/2017, which can be explained by differences in weather during the sampling year as this effects the salinity. The currents are wind driven and if there were more southern winds, or less northern winds, in 1957/1958, more heavy water from the Atlantic could be carried to the Drøbak area (Baalsrud & Magnusson, 2002). More rain and snow melting could also result in lower salinity in 2016/2017. It has been documented more rain at the Blindern weather station in 2017 than what is considered to be the standard amount (Table 10).

***Table 10**: The amount of rainfall from April-August 2017, and the average amount of rain the same period measured at Blindern, Oslo (yr.no).*

Month	Total amount of rain (mm)	Normal amount of rain (mm)
April	57	41
Mai	78.3	53
June	90.7	65
July	98.2	81
August	158.9	89

Nevertheless, there is no available weather data from 1957/1958, hence it is not possible to conclude on the reason behind the salinity difference.

Water transparency in terms of Secchi depth also varied throughout the year. A Secchi depth indicates how deep the light penetrates the water and consequently the location of phytoplankton. The deepest Secchi value was during the winter, and it peaked in the spring (Figure 19 – 20). The Secchi depths vary due to dissolved organic matter/carbon in the water and the amount of phytoplankton (Paasche, 2005). The number of particles in the water change with the current and amount of rainfall which changes the water visibility. A report by Norconsult documented fluctuating Secchi depth measurements sampled at Elle at a selected month over several years which illustrate its unpredictability (Norconsult, 2017). Yet the shallow Secchi depth values from the spring 2017 could be due to a phytoplankton bloom. The Secchi depth was also measured during one week at Elle by a field course from UiO. One day the Secchi depth was at 15 m depth, and a few days later it was at 6.5 m depth (personal observation, 13.06.2017). This quick change in Secchi depth further illustrates the unpredictability in Secchi measurements and difficulty to observe and document changes in phytoplankton growth as one day may be completely different then the next.

4.1.2 Investigation of net hauls, cell counts, and biovolume

The observed phytoplankton taxa from the present study were normal for the area and illustrated seasonal adaptations as in previous investigations (Hasle & Smayda, 1960; Hostyeva, 2011; Naustvoll et al., 2013; Walday et al., 2017). During the summer there was an increase of dinoflagellate taxa, e.g., *Tripos* spp., *Prorocentrum* spp., and *Protoperidinium* spp. (Figure 21 – 22). It was still diatoms that were dominant in the summer in terms of cell counts and biovolume (Figure 22 & 23). This dominance was due to high numbers of *Dactyliosolen fragilissimus, Proboscia alata, Pseudo-nitzschia* spp., and *Chaetoceros* spp. *Dactyliosolen fragilissimus* and *P. alata* were most abundant during the summer compared to the other seasons, as previously documented (Hostyeva, 2011; Lange et al., 1992; Walday et al., 2017).

During the autumn there was a higher abundance of dinoflagellate taxa compared to the other seasons (Figure 21). Several species of *Tripos* and *Prorocentrum,* like *P. micans*, bloomed along with other species of *Protoperidinium* and several *Gymnodiniales* taxa. Dinoflagellates

dominated the cell counts due to these taxa, but not in terms of biovolume. However, these values were low compared to the cell counts and biovolume of the other seasons. The higher abundance of dinoflagellate could be due to a decline in competitive species. When there are little nutrients left in the stable top layer, diatoms die and sink out. A trend in Oslofjorden has been that after a decrease of diatom cells, the amount of dinoflagellate cells increases (Paasche, 2005). There were fewer cell counts of diatoms during the autumn compared to values from the other seasons. Yet the diatoms dominated in biovolume and cell counts throughout the present study except the cell counts from the 12th of September 2016. Reasons behind this dominance can be due to an increase of nutrients carried along with runoff from land, which have been documented to increase since 2015 (Walday et al., 2016; Walday et al., 2017). For instance, during summer 2017 there was more rain measured at Oslo than average (Table 10). This abnormal rainfall can explain why diatoms dominated in all the samples, and why dinoflagellates did not peak after the spring bloom, which was the case in the outer part of Oslofjorden in 2010 (Hostyeva, 2011).

It was during the winter that the highest and lowest number of taxa were observed. The highest values were in January where some rarely observed species occurred, e.g., *Coscinodiscus* sp. and various species of *Protoperidinium*. It is possible that taxa were more thoroughly identified in the January samples, as there were few cells per liter and thus easier to observe each cell. More species of *Thalassiosira* and *Chaetoceros* were observed in January, wherein other samples the same taxa occur except that they were classified to genus level. Another explanation can be the slight increase in salinity from November to January which may imply that there also was an increase in nutrient concentration. However, it was also during the winter that the lowest number of taxa, along with the lowest number of cell counts and biovolume were documented (Figure 21, 23 & 25). There were presumably unfavorable conditions for algal growth as the winter in temperate seas is characterized by little sunlight and a decrease in pycnocline (Table 2). Density measurements provided by the CTD in November confirms a decrease in pycnocline (Appendix 6). There are unfortunately no density measurements from January the 3rd or February the 3rd, but as the density tends to follow the salinity gradient (Denny, 2008) it may appear that there was a small pycnocline in January and a weak one in February (Appendix 6). These measurements could have supported the low numbers of cell counts and biovolume in the winter samples.

In the spring there was a peak of diatom cells created by a few taxa: *Skeletonema* sp., *Chaetoceros* spp., *Pseudo-nitzschia* spp., *Thalassiosira* spp., and *Thalassionema nitzschioides*. These taxa have been documented as spring bloom dominating species (Dahl et al., 2007; Hostyeva, 2011). It is possible to presume that due to the observed taxa, as well as the peak in both cell counts and biovolume (Figure 23 & 25) there was a spring bloom at Drøbak between March to May. From the biovolume it is possible to conclude that *Skeletonema* sp. played a significant role during the spring bloom in both the total amount of phytoplankton and in the number of diatoms (Figure 26 & 27). In March *Skeletonema* sp. accounted for approximately 60% of the total diatoms biovolume and 40% of total phytoplankton. In April the biovolume of *Skeletonema* sp. was about 22% of total diatoms. Most of the other taxa peaked in cell number in April, except for *Pseudo-nitzschia* spp. that peaked in May. A bloom in April is later than what has been documented in previous years (Aure et al., 2014; Hostyeva, 2011; Naustvoll et al., 2010; Walday et al., 2011). Reasons for the late bloom may be due to hydrographical conditions, e.g., a weak pycnocline and low nutrient concentration prior to March/April. Nevertheless, judging from the hydrographical data, it is possible to assume that a bloom could have started in late February (Figure 16). A decrease in salinity can indicate that there has been an increase of freshwater. Freshwater has a lower density than the saltwater and thus forms a stable surface layer. In this stable surface layer, there were presumably available nutrients from both the freshwater input and from the prior vertical mixing of deep water. The Secchi depth values do not confirm a bloom in late February as it was at a deep depth. It does however illustrate a possible bloom in April, as the depth is very shallow in this month compared to the rest of the year (Figure 19 – 20).

Due to the delay in spring bloom compared to previous findings, it is interesting to investigate reasons behind. First, it is probable that an earlier bloom did occur, but not during the conducted cruises. It is possible to find the timing of the bloom due to a collaboration between NIVA and Color line. The cruise ship Color Fantasy tracks the fluorescence on its voyage from Oslo to Kiel. This collaboration and tracking system is called FerryBox. From the FerryBox data sampled in 2017, the spring bloom derived from the fluorescence max was in March at Drøbak (Appendix 9; Marit Norli at NIVA, personal communication), which means that this present study missed out on the spring bloom in 2017. Also, the presumption that the spring bloom would occur in February, as two cruises were planned that month to increase the chance to observe a bloom, was wrong.

Phytoplankton are found in patches (Martin, 2003). They also grow and die out fast. This growth pattern can be reasons why a phytoplankton bloom was not detected in March. The water sample was from one location in the fjord, once a month. Much can happen from day to day or location to location, for instance the Secchi values that changed rapidly in June 2017 (section 4.1). Measurements from Skagerrak in 2001 shows how chlorophyll a concentration can go from 2-4 μg/L in two days (Andersson et al., 2006). Further, it was the diatoms that dominate the spring blooms. They have a high surface/volume ratio and can therefore efficiently absorb the available nutrients. They do not have flagella and rely on currents and turbulence for water movement. If there is little turbulence, a depletion of nutrients may occur in the reachable surrounding area around the diatoms, which may lead to a rapid decrease in the number of diatoms. Additionally, the amount of zooplankton increases shortly after the increase in phytoplankton (Paasche, 2005). As zooplankton are grazers on phytoplankton, an increase might have an impact on growth and death of phytoplankton. Lastly it is important to note that in the present study it was microplankton (20 – 200 μm) that were counted and used to determine the spring bloom. By only looking at microplankton, smaller flagellates may be excluded, which for instance have been documented to be the dominating phytoplankton during summer periods in Oslofjorden (Walday et al., 2017). No bloom was visible in April from the FerryBox data, which illustrates how cell counts and biovolume may give a wrong interpretation of the seasonal dynamics. It is possible that the spring bloom was wrongly detected because of the excluding of smaller phytoplankton in the cell enumeration, which may have been detected if fluorescence was measured throughout the study.

There was also an indication of a summer bloom. The second highest biovolume concentration was in August 2017 with 2245.8 mm^3/L (Figure 25). The high biovolume was due to the high cell counts of *Dactyliosolen fragilissimus* (2024 mm^3/L and 312300 cells/L). Interestingly the total number of counted cells in August did not vary much from June (288300 cells/L). This difference in biovolume was because there were fewer counted cells of *D. fragilissimus* (67800 cells/L), and instead a high number of smaller cells of *Pseudo-nitzschia* spp. (166200 cells/L). This difference demonstrates how biovolume might give a different idea of the phytoplankton composition than the results from cell counts, as *D. fragilissimus* have a higher volume than *Pseudo-nitzschia* spp. Lastly it was dinoflagellates that had the highest number of taxa compared to the diatoms (Figure 21 – 22).

The present study shows that diatoms dominated over dinoflagellates and the other identified algae in both cells per liter and biovolume in 2016/2017 (Figure 23 & 25). As mentioned earlier, these three types of measurements can give different points of view. In April it was *Pseudo-nitzschia* spp. that dominated the cell counts and *Chaetoceros* spp. that had the most significant biovolume (Table 11).

Table 11: *Dominating species in April in means of cells/L and in biovolume taken from Table 7 and Appendix 8.*

	Chaetoceros spp	*Skeletonema* sp	*Pseudo-nitzschia* sp	*Prorocentrum* cf. *minimum*
Cells/L	96600	800300	1023000	354100
mm^3/L	1660	691,5	442	563

The biovolume is estimated from the volume of the shapes that resemble the different cells (Hillebrand et al., 1999). Whether the estimated biovolume represents reality or not, is debatable. Phytoplankton exist in a variety of shapes and can be solitary or in chains/colonies. *Pseudo-nitzschia* spp. can be short and thin but are often found in long stepped colonies/chains. In contrast, *Prorocentrum* cf. *minimum* are small cylindrical cells and exist solitary. Due to these differences in appearance, the biovolume can act as a mean to represent each cell equally. Nevertheless, looking at the April sample under a light microscope, *Skeletonema* sp. and *Pseudo-nitzschia* spp. were most noticeable and not *Chaetoceros* spp. which had the highest biovolume. With these different observations in mind one can speculate which of the measurements represent the phytoplankton composition most accurately. To count individual cells may give a false picture of the actual situation, for example diatoms commonly occur in chains or colonies. In comparison with dinoflagellates, the amount of diatom cells might appear much greater. However, dinoflagellates may have a greater total biovolume than diatoms. Biovolume and cell counts from the present study gave the illusion of a spring bloom. With the data from FerryBox it was possible to conclude that this was a wrong assumption. In light of these findings, the need of a better method or to combine the described methods from the present study is necessary for a more accurate picture about the phytoplankton composition.

4.2 Seasonal cycle of phytoplankton at Drøbak in 1957-1958 and 2016-2017.

There was little difference in the periods of annual maximum and minimum of phytoplankton between the data collected in 1957-1958 and 2016 – 2017. The most apparent differences were in the cell counts. Hasle & Smayda (1960) documented more cells per liter during the spring than what was found in 2016 – 2017. However, where there were more documented cells/L in 1957 – 1958, there were more documented taxa in 2016 – 2017 (Table 12).

***Table 12**: Number of different taxa found between March to May in 1957 and in 2017 from Appendix 7 and Table 5.*

	March	April	May
1957	17	17	8
2017	23	18	25

The same taxa dominated the spring in 1957 and 2017. This dominance constituted mainly of *Chaetoceros* spp., *Thalassiosira* spp., *Leptocylindrus danicus*, *Pseudo-nitzschia* spp., and *Skeletonema* sp. In May 2017, there was also an increase of *Dactyliosolen fragilissimus*, and a high number of *Pseudo-nitzschia* spp. cells which were not found in May 1957. Another difference was a high number of cells from September to October 1957 which might appear to have been an autumn bloom. Between 1957-1958, *Skeletonema costatum* was documented with the highest number of cells per liter (22450000). This number of cells was higher than what was documented in 2017 (800200 cells/L). *Skeletonema costatum* has earlier been used as an indicator for eutrophication (Braarud & Bursa, 1939). This is not the case any longer as the use of species as indicators might be dubious. However, there was ongoing eutrophication in the 1950s, and the increase of nutrients can be an important factor in explaining the high number of cells in 1957 compared to 2017. An increase in nutrients has been documented to result in an increase of cell numbers and a decrease in the number of taxa (Dragsund et al., 2006), which was an apparent difference between the present investigation and that of Hasle & Smayda. The same trend is noticeable in cell counts of dinoflagellates from the two investigations. In 2016/2017 there were documented a higher amount of dinoflagellate species and a lower number of cells, than what was found between 1957 – 1958. The most significant difference was in the summer data (Table 13).

***Table 13**: Variation in the amount of different dinoflagellate species in 1957 and in 2017 from Appendix 7 and Table 5.*

	June	August
1957	214700	57060
2017	5400	7000

The comparison between the results was possible as both studies were performed at Drøbak and the enumeration was by the Utermöhl method. However, use of this method may lead to the difference in the results. First, the phytoplankton identification is an ongoing modification. Some of the identified species from 1957-1958 have changed the taxonomical name. For instance, *Ceratium longipes* is now named *Tripos longipes*. The Utermöhl method also has its disadvantage as it is performed by a person. This method is time-consuming and requires a skilled person to perform the species identification (Karlson et al., 2010). The level of skills between the investigators will also influence the result. There is some difference in the level of identification between our investigations. Where there is documented *Pseudo-nitzschia* spp. in the present study, Hasle & Smayda identified two different species of *Pseudo-nitzschia*. Later investigations in Oslofjorden, such as e.g., Hostyeva (2011) documented the presence of 9 species.

To better enable comparison between years and to spot trends, it would have been beneficial if there were more extended time series of data as well as a standardized sampling method so that possible bias in method does not hinder the comparison.

4.3 *Skeletonema* species in Oslofjorden

4.3.1 *Skeletonema marinoi*

Skeletonema marinoi was the only observed species of *Skeletonema* found during the present investigations and in the old samples from the Natural History Museum (04.04.1939, 22.03.1936, and 01.12.1987). The species illustrated a broad variation in cell and chain morphology, which could lead to the confusion of believing that these variations distinguish different species (Figure 36). This misunderstanding may occur as cells in the present study could be long and elongated (Figure 36 D) to more quadrat looking (Figure 36 A & 36 C). For instance, Medlin et al. (1991) observed that *S. pseudocostatum* had shorter chain length then

S. costatum. Nevertheless, it had been known for some time that the cell morphology in *Skeletonema* is dubious to use in species identification (Hasle, 1973).

With the knowledge that *S. marinoi* also occurred in old samples (Figure 28 – 29) as stated previously, it is possible to speculate that *S. costatum* was wrongly identified in previous investigations like in those of Braarud & Bursa (1939) and of Hasle & Smayda (1960). This belief is further amplified by the investigation of Kooistra et al. (2008), where *S. costatum* was only documented in waters far from Europe. However, the fact that the culture NIVA-Bac 1 contained *S. pseudocostatum* collected at Drøbak in 1962 illustrates that other species may occur in Oslofjorden (Figure 35). *Skeletonema pseudocostatum* has been observed in the Baltic Sea, which is water that may influence Oslofjorden (Baalsrud & Magnusson, 2002; Kooistra et al., 2008). As the water in Oslofjorden is affected by water from the Atlantic Sea, the Baltic Sea, and the German Bight among others, currents may carry different species from these various areas. Investigations have documented that *S. marinoi* and *S. pseudocostatum* may tolerate a broad variation in salinity (Branda, 1984; Kooistra et al., 2008). Other factors as nutrient concentration and temperature may limit the growth of these species, yet in means of salinity both can occur in Oslofjorden. Godhe et al. (2006) have documented *S. marinoi* as the only *Skeletonema* species from genetic investigation along the west coast of Sweden, which is an area that is affected by the same currents as Oslofjorden. These finding along with the present research may illustrate that *S. marinoi* is the typical species of *Skeletonema* in Oslofjorden.

4.3.2 Possible life cycle of *Skeletonema marinoi?*

Skeletonema marinoi illustrated an adaptation to the varying environmental conditions in Oslofjorden. It occurred in salinities from about 20 – 30 PSU, and temperatures ranging from about 0 – 15°C (Figure 16). The counted cells per liter peaked during the spring (Figure 23), but in contrast with other spring bloom dominating species, like *Chaetoceros decipiens*, there were still a number of cells during the remaining seasons. The exception was September 2016, and in August 2017 where *S. marinoi* was found only in the net hauls (Table 5). Takabayashi et al. wrote that "each shape and size of diatoms has apparent advantages and disadvantages" (2006, p. 831). These advantages may be adjustments to increase nutrient uptake, buoyancy or light absorption among other factors. The adaptation to environmental changes, or phenology, have been investigated by several researchers (Ji et al., 2010; Marchese et al., 2017). In the

present research, cells of *S. marinoi* varied depending on the month, salinity and temperature (Figure 46 – 48). They were small in January and started to increase in size from March to April, before they decreased in size again in September. In October the confidence interval was wide, signifying that there were both small and larger cells. The variation in size may illustrate life cycle strategies found in diatoms with a size reduction-restitution cycle (Figure 10).

Autumn: September to October 2016

There were no cell counts of *S. marinoi* in September 2017. In October there was an increase in cells which had varying cell length (Figure 48 & 49). As September 2016, the first sampling month in the present study, it is not possible to see if there was an increase from summer cell counts to those from the autumn. However, Hasle & Smayda (1960) documented a peak in *Skeletonema* cells in October (Figure 30), and the same was documented in the outer part of Oslofjorden in September 2010 (Hostyeva, 2011). With the slight increase of salinity in October, there might have been an increase in available nutrient leading to an autumn bloom, which could explain the rapid increase in number of cells. Hasle also found the variation in cell size of *S. costatum* in Oslofjorden during the autumn and debated if it was a preparation for auxosporulation or resting spores (Hasle, 1973). Further, Sicko-Goad et al. (1989) found that a decrease in light availability together with lower temperature could lead to resting- spore and cell formation. Resting cells might be difficult to observe in diatoms, as it develops under the frustule cover and resembles a vegetative cell (Montresor et al., 2013). There were no visible resting cells or spores in the collected samples from October 2016. Reasons behind the lack of observed resting cells can be due to errors in method. Smetacek (1985) stated that the frustule would get more silicified during resting cell formation and act as ballast. Water samples from the CTD and horizontal net hauls were collected at 2 m depth. Only the vertical net haul sampled water below 2 m depth. It might be that the resting cells would have been found deeper in the water column.

Winter: November 2016 to early February 2017

During the winter period, there was a decrease in *S. marinoi* cells. They did not disappear entirely but remained at a low number (200 to 800 cells per liter). The winter in temperate seas is characterized by a decrease in sunlight and the breaking down of the pycnocline creating unfavorable conditions for algal growth. Some species are overwintering in small numbers. Godhe & Härnström (2010) found a low number of *S. marinoi* in Gullmar Fjord and classified them as overwintering cells. These overwintering cells are also known as "fugitive" cells that

are left behind at the surface during a mass sinking of resting-spores and -cells (Smetacek, 1985). In order to not sink out, it would be favorable to have a small size to increase the buoyancy. It would also be beneficial to be small so that the surface/volume ratio increases and hence increase the nutrient uptake when there is a low nutrient concentration in the surrounding environment. The observed cells of *S. marinoi* that were found at Drøbak between November 2016 to early February 2017 had small cell sizes and short chains. It may be one of the reasons why some cells were observed at the surface during harsh winter conditions due to the characteristics mentioned above.

Spring: Late February to May 2017

Reasons behind diatoms success during blooms are partly due to the ability to absorb nutrients with a large surface/volume ratio, and partly due to the capacity to increase rapidly in biomass (Fawcett & Ward, 2011). High nutrient conditions at the surface in the present study were likely found during the spring, as described earlier, and therefore when it would be an advantage to increase cell size as documented with *S. marinoi* (Figure 46). Smayda & Boleyn (1966) stated that chain formation could aid in buoyancy and decrease the sedimentation rate during favorable conditions for growth. The chain length of *S. marinoi* was at its maximum during the spring and could be an explanation for its success together with the large cell size. Saravanan & Godhe (2010) discovered that *S. marinoi* could be influenced by salinity and temperature, where the large cells were a response to lower salinity and temperature. This trend was somewhat found during the present study. The largest cells of *S. marinoi* occurred with salinity at 24 PSU and the temperature at 9°C (Figure 46-47). In May, the cell size and chain length started to decrease along with the cell counts (Figure 46, 50, and 23). This may be due to the decrease in nutrients, as what has been documented in several studies (Smetacek, 1985; Takabayashi et al., 2006). Later research has suggested that the increase in zooplankton may also affect the chain length, where smaller chains are favorable under the circumstances of high abundance of zooplankton (Bergkvist et al., 2012; Bjærke et al., 2015). Zooplankton abundance was not investigated during the present research. It would have been interesting to compare the variations of *Skeletonema* cell and chain morphology with the amount of zooplankton during the sampling year as the GAM analysis of these variations compared to salinity and temperature did not correlate 100% and thus not the sole explanation (Table 8 – 9). It was also possible to see some morphological differences in the cells from the SEM investigation. In samples from February 2017 newly formed processes were visible beneath the frustule during what was

presumably cell division (Figure 37). Whereas in the May 2017 sample the frustule looks thicker and had band structures across the entire cell (Figure 38). As mentioned earlier, a thicker frustule might aid in sedimentation as it increases the weight and might be a reason behind the thicker looking frustule (Smetacek, 1985).

Summer: June-August 2017

There was a decrease in counted cells, cell size and chain length of *S. marinoi* in June and August, which could be explained by a possible increase in grazers or due to unfavorable environmental conditions. The surface temperature was higher with 16°C (Figure 16), and the nutrient concentration was probably low after a high nutrient consumption in the spring bloom. The low abundance of cells could be a result of resting cell formation, with a low number of "fugitive" cells at the surface.

This present investigation has documented that *S. marinoi* was an annual occurring species which showed indications of different strategies correlating with the seasonal variations. By looking at the variation in cell counts, cell size, and chain length compared with the observed seasonal variations of hydrographical data, it is possible to suggest an *S. marinoi* life cycle with various strategies to increase survival. However, there are some missing data to be certain of these strategies. First, more frequent cruises after blooms would be useful to increase the chance of observing strategies applied by *S. marinoi* for persistence during harsh conditions. It would also be useful to collect water at different depths and investigate if there was a difference in cell and chain morphology of *S. marinoi* corresponding to these depths in an attempt to observe resting cells.

4.4 Conclusion and suggestions for further study

The observed phytoplankton during this investigation illustrated seasonal adaptations. The same taxa were observed during the present study as previous documented in Oslofjorden. There were some differences between the findings from 1957 – 1958 with those of the present study. This difference occurred in the registered salinity that was slightly higher in 1957 – 1958 and the number of counted cells that also was higher in 1957/1958. This difference could be due to an alteration in environmental conditions, as there was ongoing eutrophication in the 1950s. These differences justify the need to monitor the seasonal changes in phytoplankton, as it may give an idea of potential environmental changes in Oslofjorden. The necessity to observe

phytoplankton and environmental changes is further amplified as there has been documented an increase in surface temperature and more heavy rainfall by the European Environment Agency, in addition to the observed increase of nutrient concentration in Oslofjorden the last years by NIVA and IMR. However, it has been difficult to observe trends in the seasonal cycle of phytoplankton as the present study only compared two annual investigations and some reports from NIVA and IMR. The phytoplankton documentation was fragmented in the various reports of NIVA and IMR, which made it difficult to perform a thorough comparison. It would be beneficial to investigate longer time intervals of data. With increasing knowledge about phytoplankton, genetics monitoring could be standardized. With genetic analysis it would be possible to get a more precise idea about the species composition according to season. However, to quantify the occurrence of different taxa, it is the Utermöhl method that is the most accurate as other methods are not yet specific or quantitative enough (Karlson et al., 2010). Even though this method is time-consuming, it would be beneficial as more standardized and occurring monitoring could give a baseline for later investigations and abnormalities could be detected.

Skeletonema marinoi was documented in every season and had a maximum of cell numbers and biovolume during the spring bloom where it had a significant role both in the total amount of diatoms and of phytoplankton (March to May 2017). The present study also established that *S. marinoi* occurred in Oslofjorden in the 1930s and that *S. pseudocostatum* can be found even though it was not the case during this year-long investigation. It was only possible to species identify one sample from the NHM. It would therefore be interesting to investigate more samples, to see if there are other species to be found, especially summer samples as this is when the culture was isolated. A genetic investigation along with the performed morphological investigations could have been useful. If other species of *Skeletonema* occurred in low numbers, they might have been detected by genetic analysis. However, with morphological studies, it was possible to observe the changing morphology of *S. marinoi* with the different environmental conditions and thus observe possible strategies for survival. In the present study there were little investigations concerning variation in strutted processes, apart from the species identification. It could have been interesting to study the thickness, quantity and length of intercalary strutted processes in regards to different environmental circumstances. Knowledge about possible life cycle strategies can be advantageous in predicting changes in phytoplankton composition, and thus a possible alternation higher up in the food web.

References

Andersson, P., Axe, P., Eilola, K., Hansson, M., Håkansson, B., Karlson, B., … II, F. S. (2006). *Monitoring the pelagic system in the Skagerrak*. (B. Karlson, Ed.). Uddevalla: Forum Skagerrak II.

Armbrust, E. V., Chisholm, S. W., & Olson, R. J. (1990). Role of light and the cell cycle on the induction of spermatogenesis in a centric diatom. *Journal of Phycology*, *26*(3), 470–478. https://doi.org/10.1111/j.0022-3646.1990.00470.x

Aure, J., Danielssen, D. S., & Naustvoll, L. J. (2014). *Miljøundersøkelser i norske fjorder: Ytre Oslofjord 1937-2011*. *Fisken og Havet* (Vol. 5). Bergen.

Bergkvist, J., Thor, P., Jakobsen, H. H., Wängberg, S.-Å., & Selander, E. (2012). Grazer-induced chain length plasticity reduces grazing risk in a marine diatom. *Limnology and Oceanography*, *57*(1), 318–324. https://doi.org/10.4319/lo.2012.57.1.0318

Bjærke, O., Jonsson, P. R., Alam, A., & Selander, E. (2015). Is chain length in phytoplankton regulated to evade predation? *Journal of Plankton Research*, *37*(6), 1110–1119. https://doi.org/10.1093/plankt/fbv076

Branda, L. E. (1984). The Salinity Tolerance of Forty-six Marine Phytoplankton Isolates. *Estuarine, Coastal and Shelf Science*, *18*, 543–556.

Braarud, T., & Bursa, A. (1939). The Phytoplankton of the Oslo Fjord 1933–1934. *Hvalrådet Skr.*, *19*.

Baalsrud, K., & Magnusson, J. (2002). *Indre Oslofjord, Natur og Miljø*. Fagråder for vann- og avløpsteknisk samarbeid i indre Oslofjord.

Cleve, P. T. (1873). Examination of diatoms found on the surface of the Sea of Java. *Bihang till Kongliga Svenska Vetenskaps-Akademiens Handlingar*.

Dahl, E., Gustad, E., & Naustvoll, L. (2007). Overvåkning av alger langs norskekysten. *Fisken Og Havet*, (Kyst og havbruk 2), 28–31.

Denny, M. (2008). *How the Ocean Works*. New Jersey: Princeton University Press.

Dragsund, E., Aspholm, O., Tangen, K., Bakke, S. M., Heier, L., & Jensen, T. (2006). *Overvåking av Eutrofitilstanden i Ytre Oslofjord. Femårsrapport 2001 - 2005*. Horten.

Edwards, M., & Richardson, A. J. (2004). Impact of climate change on marine pelagic phenology and trophic mismatch. *Nature*, *430*(7002), 881–884. https://doi.org/10.1038/nature02808

Fawcett, S. E., & Ward, B. B. (2011). Phytoplankton succession and nitrogen utilization during the development of an upwelling bloom. *Marine Ecology Progress Series*, *428*, 13–31. https://doi.org/10.3354/meps09070

Füssel, H.-M., Jol, A., Marx, A., Hildén, M., Aparicio, A., Bastrup-Birk, A., … van der Linden, P. (2017). *Climate change, impacts and vulnerability in Europe 2016 - An indicator-based report* (Vol. 1/2017). Luxenbourg: European Environment Agency. https://doi.org/citeulike-article-id:14262052 doi: 10.2800/534806

Gallagher, J. C. (1982). Physiologial variation and electrophoretic banding patterns of genetically different seasonal populations of *Skeletonema costatum* (*Bacillariophyceae*). *Journal of Phycology*, *18*(1), 148–162. https://doi.org/10.1111/j.1529-8817.1982.tb03169.x

Godhe, A., & Härnström, K. (2010). Linking the planktonic and benthic habitat: Genetic structure of the marine diatom *Skeletonema marinoi*. *Molecular Ecology*, *19*(20), 4478–4490. https://doi.org/10.1111/j.1365-294X.2010.04841.x

Godhe, A., McQuoid, M. R., Karunasagar, I., Karunasagar, I., & Rehnstam-Holm, A. S. (2006). Comparison of three common molecular tools for distinguishing among geographically separated clones of the diatom *Skeletonema marinoi* Sarno et Zingone

(*Bacillariophyceae*). *Journal of Phycology*, *42*(2), 280–291. https://doi.org/10.1111/j.1529-8817.2006.00197.x
Godhe, A., & Rynearson, T. (2017). The role of intraspecific variation in the ecological and evolutionary success of diatoms in changing environments. *Philosophical Transactions of the Royal Society of London*, *8*(372). https://doi.org/10.1098/rstb.2016.0399
Greville, R. K. (1866). Descriptions of new and rare diatoms. Series XVI. *Transactions of the Microscopical Society, New Series, London*, *13*, 43–57.
Gaarder, T., & Gran, H. H. (1927). *Investigations of the production of plankton in the oslo fjord*. *Conseil Intebational pour l'exploration de la Mar. Rapports et Proces-Verbaux* (Vol. 42). Copenhague Høst en comm.
Hasle, G. R. (1973). Morphology and Taxonomy of *Skeletonema Costatum* (*Bacillariophyceae*). *Norwegian Journal of Botany*, *20*, 109–137.
Hasle, G. R., & Smayda, T. J. (1960). The Annual Cycle of Phytoplankton at Drøbak, Oslofjord. *Nytt Magasin for Botanikk*, *8*, 53–75.
Hasle, G. R., Syvertsen, E. E., Steidinger, K. A., & Tangen, K. (1996). *Identifying Marine Diatoms and Dinoflagellates*. (C. R. Tomas, Ed.). Academic Press.
Hillebrand, H., Dürselen, C.-D., Kirschtel, D., Pollingher, U., & Zohary, T. (1999). Biovolume calculation for pelagic and benthic microalgae. *Journal of Phycol*, *35*, 403–424. https://doi.org/10.1046/j.1529-8817.1999.3520403.x
Horner, R. A. (2002). *A Taxonomic Guide To Some Common Marine Phytoplankton*. Bristol: Biopress Limited.
Hostyeva, V. (2011). *Seasonal Cycle of Phytoplankton in Outer Oslofjorden with Emphasis on Pseudo-nitzschia Species*. University of Oslo.
Ji, R., Edwards, M., Mackas, D. L., Runge, J. A., & Thomas, A. C. (2010). Marine plankton phenology and life history in a changing climate: current research and future directions. *Journal of Plankton Research*, *32*(10), 1355–1368. https://doi.org/10.1093/plankt/fbq062
Kaczmarska, I., Poulíčková, A., Sato, S., Edlund, M. B., Idei, M., Watanabe, T., & Mann, D. G. (2013). Proposals for a terminology for diatom sexual reproduction, auxospores and resting stages. *Diatom Research*, *28*(3), 263–294. https://doi.org/10.1080/0269249X.2013.791344
Karlson, B., Cusack, C., & Bresnan, E. (2010). Microscopic and molecular methods for quantitative phytoplankton analysis. *IOC Manuals and Guides*, *55*, 110.
Kooistra, W. H. C. F., Sarno, D., Balzano, S., Gu, H., Andersen, R. A., & Zingone, A. (2008). Global Diversity and Biogeography of *Skeletonema* Species (B*acillariophyta*). *Protist*, *159*(177). https://doi.org/10.1016/j.protis.2007.09.004
Lange, C. B., Hasle, G. R., & Syvertsen, E. E. (1992). Seasonal cycle of diatoms in the Skagerrak, North Atlantic, with emphasis on the period 1980-1990. *Sarsia*, *77*, 173–187. https://doi.org/10.1080/00364827.1992.10413503
Marchese, C., Albouy, C., Tremblay, J., Dumont, D., D'Ortenzio, F., Vissault, S., & Bélanger, S. (2017). Changes in phytoplankton bloom phenology over the North Water (NOW) polynya: a response to changing environmental conditions. *Polar Biology*, *40*(9), 1721–1737. https://doi.org/10.1007/s00300-017-2095-2
Martin, A. P. (2003). Phytoplankton patchiness: the role of lateral stirring and mixing. *Progress in Oceanography*, *57*, 125–174. https://doi.org/10.1016/S0079-6611(03)00085-5
McQuoid, M. R., & Hobson, L. A. (1996). Diatom resting stages. *Journal of Phycology*, *32*, 889–902. https://doi.org/10.1111/j.0022-3646.1996.00889.x
Medlin, L. K., Elwood, H. J., Stickel, S., & Sogin, M. L. (1991). Morphological and genetic variation within the diatom *Skeletonema costatum* (*Bacillariophyta*): evidence for a new

species, *Skeletonema pseudocostatum*. *Journal of Phycology*, *27*, 514–524.
Medlin, L. K., & Kaczmarska, I. (2004). Evolution of the diatoms: V. Morphological and cytological support for the major clades and a taxonomic revision. *Phycologica*, *43*(3), 245–270. Retrieved from http://rep4-vm.awi.de/12139/1/Med2004a.pdf
Montresor, M., Di Prisco, C., Sarno, Di., Margiotta, F., & Zingone, A. (2013). Diversity and germination patterns of diatom resting stages at a coastal Mediterraneansite. *Marine Ecology Progress Series*, *484*, 79–95. https://doi.org/10.3354/meps10236
Naustvoll, L.-J., Selvik, J. R., & Sørensen, K. (2013). *Overvåking Ytre Oslofjord - tilførsler og undersøkelser i vannmassene i 2012.* Oslo.
Naustvoll, L.-J., Selvik, J. R., Sørensen, K., & Walday, M. (2010). *Overvåking av Ytre Oslofjord - tilførsel og vannmasseundersøkelser 2009.* Oslo.
Nelson, D. M., Tréguer, P., Brzezinski, M. A., Leynaert, A., & Quéguiner, B. (1995). Production and dissolution of biogenic silica in the ocean: Revised global estimates, comparison with regional data and relationship to biogenic sedimentation. *Global Biogeochemical Cycles*, *9*(3), 359–372. https://doi.org/10.1029/95GB01070
Norconsult. (2017). *Toktrapport kombitokt - Miljøovervåkning Indre Oslofjord*. Oslo.
Paasche, E. (2005). *Forelesninger i marin biologi botanisk del*. (J. Throndsen, Ed.). Oslo: Jahn Throndsen.
Paasche, E., & Kristiansen, S. (1982). Nitrogen Nutrition of the Phytoplankton in the Oslofjord. *Estuarine, Coastal and Shelf Science*, *14*, 237–249.
Saravanan, V., & Godhe, A. (2010). Genetic heterogeneity and physiological variation among seasonally separated clones of *Skeletonema marinoi* (*Bacillariophyceae*) in the Gullmar Fjord, Sweden. *European Journal of Phycology*, *45*(2), 177–190. https://doi.org/10.1080/09670260903445146
Sarno, D., Kooistra, W. H. C. F., Balzano, S., Hargraves, P. E., & Zingone, A. (2007). Diversity in the genus *Skeletonema* (*Bacillariophyceae*): III. Phylogenetic position and morphological variability of *Skeletonema costatum* and *Skeletonema grevillei*, with the description of Skeletonema ardens sp. nov. *Journal of Phycology*, *43*(1), 156–170. https://doi.org/10.1111/j.1529-8817.2006.00305.x
Sarno, D., Kooistra, W. H. C. F., Medlin, L. K., Percopo, I., & Zingone, A. (2005). Diversity in the genus *Skeletonema* (*Bacillariophyceae*). II. An assessment of the taxonomy of S. costatum-like species with the description of four new species. *Journal of Phycology*, *41*(1), 151–176. https://doi.org/10.1111/j.1529-8817.2005.04067.x
Scholin, C. A., Herzog, M., Sogin, M., & Anderson, D. M. (1994). Identification of group- and strain-specific genetic markers for globally distributed *Alexandrium* (*Dinophyceae*). II. Sequence analysis of a fragment of the LSU rRNA gene. *Journal of Phycology*, *30*, 999–1011.
Sicko-Goad, L., Stoermer, E. F., & Kociolek, J. P. (1989). Diatom resting cell rejuvenation and formation: Time course, species records and distribution. *Journal of Plankton Research*, *11*(2), 375–389. https://doi.org/10.1093/plankt/11.2.375
Skjevik, A.-T. (2012). *Algerapport nummer 2, 2012*. Gothenburg.
Smayda, T. J., & Boleyn, B. J. (1966). Experimental observations on the floatation of marine diatoms. II. *Skeletonema costatum* and *Rhizosolenia setigera*. *Limnology and Oceanography*, *11*, 18–34.
Smetacek, V. S. (1985). Role of sinking in diatom life-history cycles: ecological, evolutionary and geological significance. *Marine Biology*, *84*, 239–251.
Sætre, R. (2007). Driving forces. In *The Norwegian Costal Current* (pp. 45–58). Tapir Academic Press.
Takabayashi, M., Lew, K., Johnson, A., Marchi, A., Dugdale, R., Wilkerson, F. P., & Flynn, K. J. (2006). The effect of nutrient availability and temperature on chain length of the

diatom, Skeletonema costatum. *Journal of Plankton Research*, *28*(9), 831–840. https://doi.org/10.1093/plankt/fbl018
Throndsen, J. (1978). Preservation and storage. In: Sournia A (ed.): Phytoplankton manual. UNESCO, Paris, pp. 69-74.
Throndsen, J., Hasle, G. R., & Tangen, K. (2007). *Phytoplankton of the Norwegian Coastal Waters*. Oslo: Almater forlag as.
Utermöhl, H (1958) Zur vervollkommung der quantitativen phytolankton-methodik. *Mitteilungen-Internationale Vereinigung für Theoretische und Angewandte Limnologie*, 9 (1958), pp. 1–39
Walday, M., Beylich, B. A., Fagerli, C. W., Gitmark, J. K., Naustvoll, L.-J., & Selvik, J. R. (2015). *Overvåking av Ytre Oslofjord 2014-2018.*Oslo
Walday, M., Borgersen, G., Naustvoll, L.-J., & Selvik, J. R. (2016). *Overvåkning av Ytre Oslofjord 2014-2018. Årsrapport for 2015*. Oslo.
Walday, M., Gitmark, J. K., Naustvoll, L. J., & Selvik, J. R. (2017). *Overvåkning av Ytre Oslofjord 2014-2018. Årsrapport for 2016*. Oslo.
Walday, M., Gitmark, J., Naustvoll, L. J., Norlig, K., Selvik, J. R., & Sørensen, K. (2012). *Overvåkning av Ytre Oslofjord 2007-2011. 5-årsrapport*. Oslo.
Walday, M., Gitmark, J., Naustvoll, L., Norling, K., Selvik, J. R., & Sørensen, K. (2011). *Overvåkning av Ytre Oslofjord 2010. Årsrapport*. Oslo.
Wood, S. N. (2011). Fast stable restricted maximum likelihood and marginal likelihood estimation of semiparametric generalized linear models. *Journal of the Royal Statistical Society (B) 73,* 3-36.

Appendix

Appendix 1: Cell enumeration of *Pseudo-nitzschia* spp. from the May 2017 sample

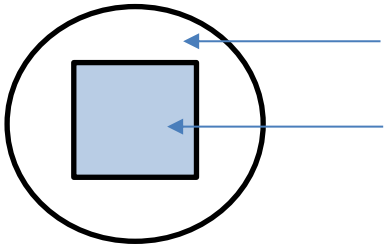

a: the sedimentation chamber (10 ml)

b: the field of view in the microscope (Gird in ocular)

The cell enumeration was performed at x10 magnification in LM

1. Circumference of the sedimentation chamber and the field of view

Radius of **a** is 130 mm

A: Circumference of **a**: Πr^2=53066 mm^2

Length and width of **b** is 0.7 mm

B: Circumference of **b**: 0.7 * 0.7 = 0.49 mm^2

2. Calculation to get number of cells of *Pseudo-nitzschia* spp. per liter:

$$\frac{cells}{L} = x * \frac{A}{n * B} * \frac{1}{0.01}$$

- A is the circumference of the sedimentation chamber = 53066 mm^2

- B is the circumference of the field of view = 0.49 mm^2
- x is the number of counted cells = 570
- n is the number of counted fields of view = 5
- 1/0.01 is to convert the number of cells counted in 10 ml (the sedimentation chamber) to cells per liter

$$\frac{cells}{L} = 570 * \frac{53066\ mm^2}{5 * 0.46\ mm^2} * \frac{1}{0.01\ L} = 123459634\ cells/L$$

Appendix 2: Procedure for acid cleaning (Adil Al Handal, personal communication)

1. Remove fixative by washing 3x in distilled water (place sample in conical centrifuge tube and centrifuge for 5 min to form pellet, remove supernatant. Repeat 2 times). Depending on the concentration of diatoms, volume of the sample may be adjusted.
2. Transfer material (adjust volume to 10 ml with distilled water) to beaker and add about 20 ml H_2O_2. (be careful when working with this highly oxidative chemical, always use gloves).
3. Heat on a hotplate set at 100-150°C in a fume cupboard until all organic material has been oxidized. This may take 30 minutes. Color of the sample changes to white (clear) unless sediment particles are present in the sample.
4. Remove the beakers from the heat. To ensure removal of all H_2O_2 residue and any carbonates, add a few drops of 50% HCl.
5. Allow samples to cool. Rinse 4x in distilled water (place sample in conical centrifuge tube and centrifuge at full speed for 5 min to form pellet, remove supernatant. Repeat 3 times to remove all salts).
6. Samples are now ready for mounting on SEM-stubs or to be stored in 70% ethanol.

Appendix 3: Qiagen blood and tissue kit for DNA isolation

Procedure:

1. Cultured microalgal cells: Centrifuge 50-2 mL culture in exponential growth at ca. 1000-3000 x g for 5-10 min, depending on cell size, to get a pellet. Remove the supernatant by decanting or pipetting. If strong cell covering, freeze the pellet (or use bead beater). Resuspend the pellet in **200 µl PBS** and transfer the solution to a 1.5 mL Eppendorf tube**. Add 20 µl proteinase K**. Phytoplankton on polycarbonate filter: **Add 20 µl proteinase K and 200 µl PBS** and continue to point 2. Optional: If RNA-free genomic DNA is required, add 4 µl RNase A (100 mg/ml) and incubate for 2 min at room temperature before continuing with step 2.
2. Add **200 µl Buffer AL** (without added ethanol). Mix thoroughly by vortexing and incubate at 56˚C for 10min. If filter, pipet out the liquid and transfer to new tube, press the filter together in the bottom with the tip and pipet up the rest of the liquid and transfer to new tube.

3. Add **200 µl ethanol** (96–100%), to the sample. and mix again by vortexing.
4. It is important that the sample and ethanol are mixed thoroughly by vortexing or pipetting to yield a homogeneous solution.
5. Pipet the mixture from step 3 into the DNeasy Mini spin column placed in a 2 ml collection tube (provided). Centrifuge at ≥**6000 x g (8000 rpm) for 1 min**. Discard flow-through and collection tube.
6. Place the DNeasy Mini spin column in a new 2 ml collection tube (provided), add **500 µl Buffer AW1**, and centrifuge for **1 min at ≥6000 x g (8000 rpm).** Discard flow-through and collection tube.
7. Place the DNeasy Mini spin column in a new 2 ml collection tube (provided), **add 500 µl Buffer AW2**, and centrifuge for **3 min at 20,000 x g (14,000 rpm)** to dry the DNeasy membrane. Discard flow-through and collection tube.
8. Place the DNeasy Mini spin column in a clean 1.5 ml or 2 ml microcentrifuge tube (not provided), and pipet **50 µl Buffer AE** directly onto the DNeasy membrane. Incubate at room temperature for 1 min, and then centrifuge for **1 min at ≥6000 x g** (8000 rpm) to elute

Recommended: For maximum DNA yield, repeat elution once as described in step 8.

Appendix 4: Picture of the electrophoresis gel with band of LSU

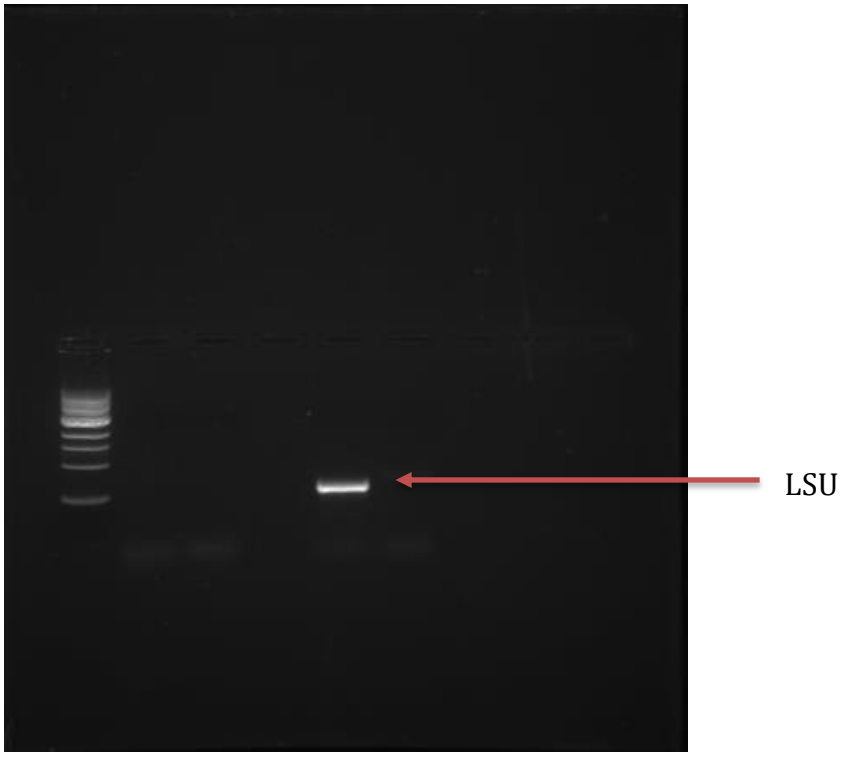

Appendix 5: Selected species of *Skeletonema* and their accession numbers used to construct a phylogenetic tree with the sequenced NIVA-Bac 1 culture.

Paper	Species	Accession number
Sarno *et al.*, 2005	*S. dohrni*	AJ633537
Sarno *et al.*, 2005	*S. grethae*	AJ633523
Sarno *et al.*, 2005	*S. japonicum*	AJ633521
Sarno *et al.*, 2005	*S. marinoi*	AJ633530
Sarno *et al.*, 2005	*S. menzelii*	AJ633526
Sarno *et al.*, 2005	*S. pseudocostatum*	AJ633508
Sarno *et al.*, 2005	*S. subsalsum*	AJ633539
Sarno *et al.*, 2005	*S. tropicum*	AJ633515
Sarno *et al.*, 2005	*Thalassiosira rotula* (outgroup)	AJ633505
Sarno *et al.*, 2007	*S. costatum*	DQ396524
Sarno *et al.*, 2007	*S. grevillei*	CCMP1685

Appendix 6: CTD and STD – salinity, temperature, depth, density, and fluorescence.
September 12th 2016

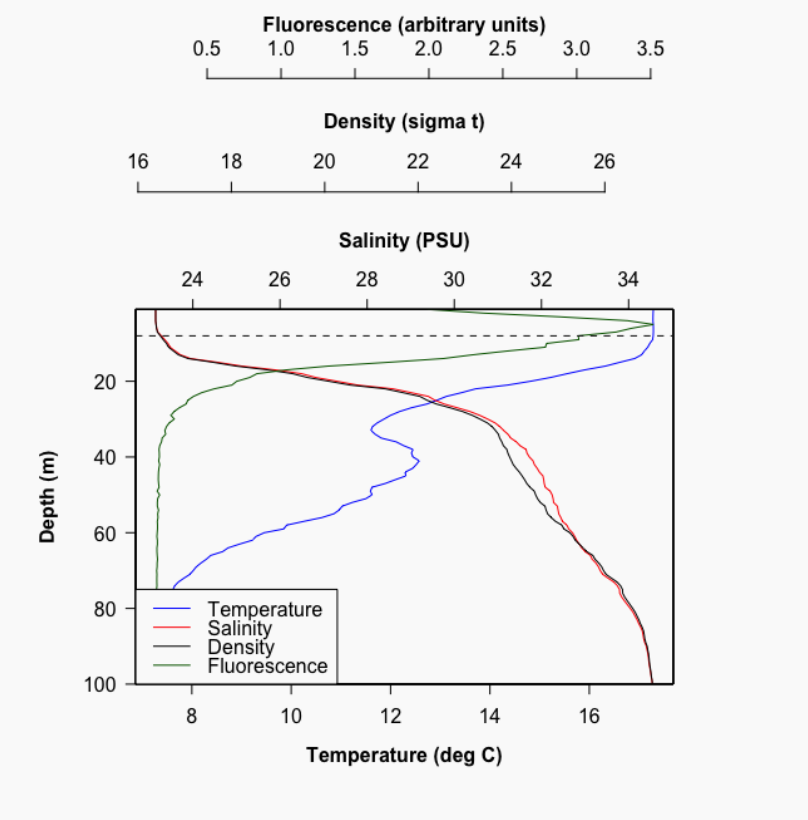

October 27th 2016

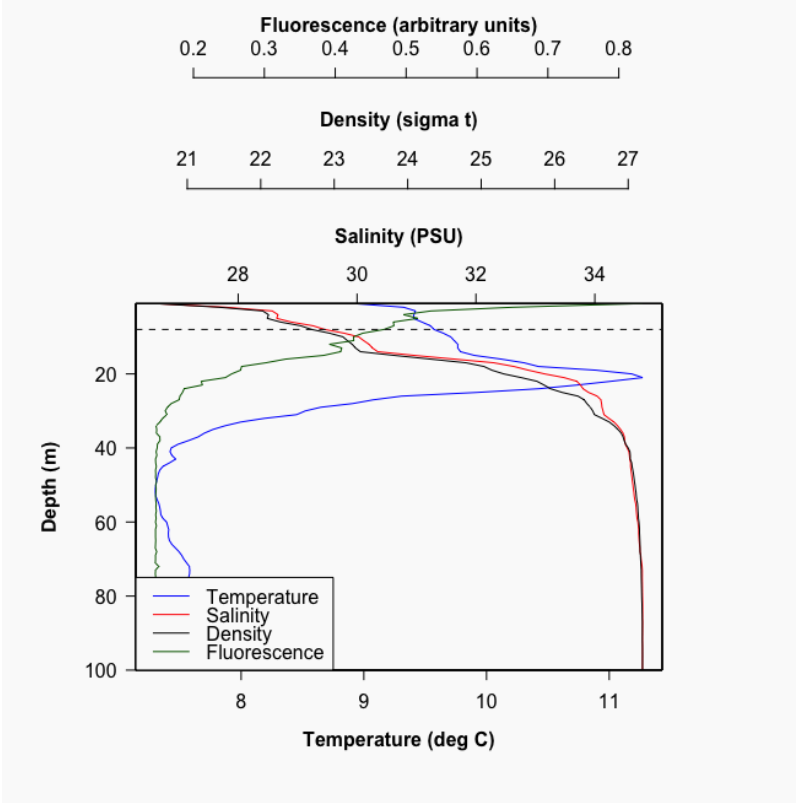

November 28th 2016

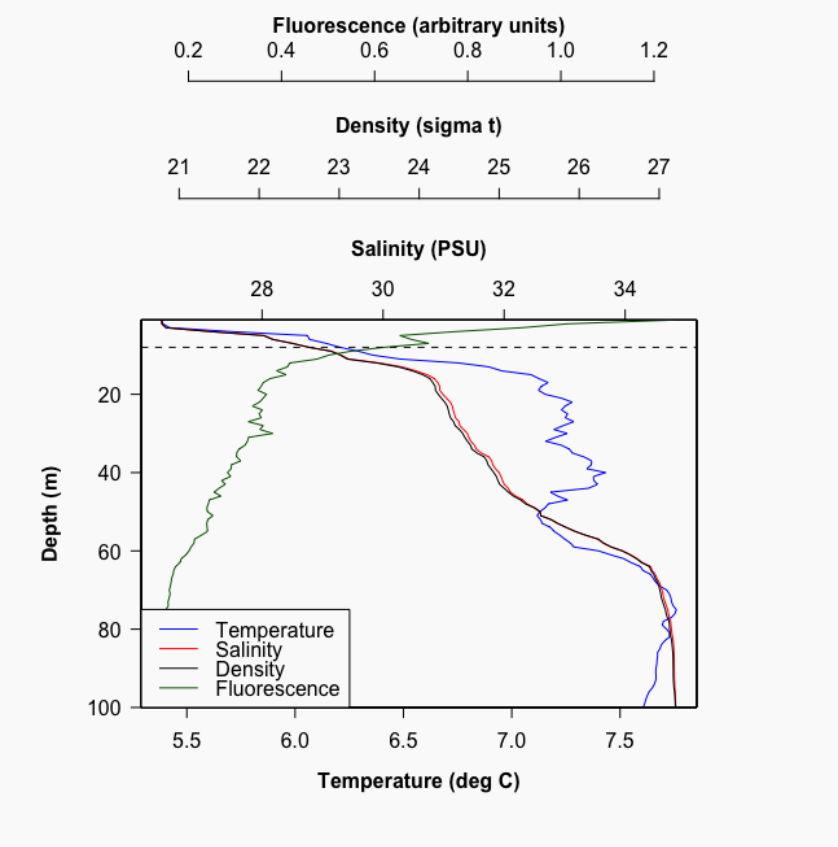

January 3rd 2017

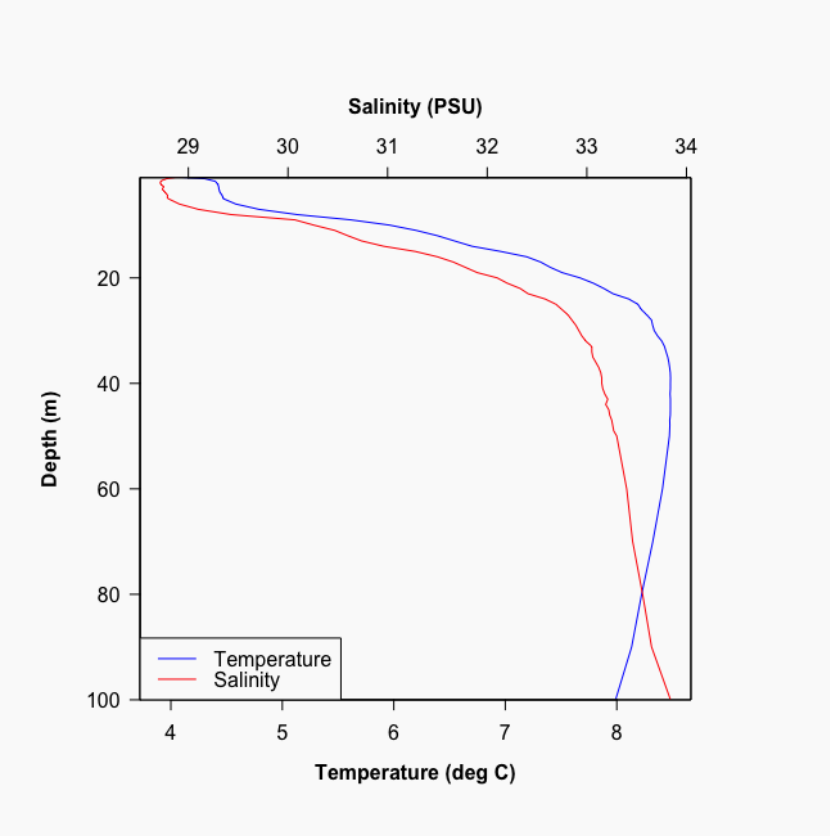

February 3rd 2017

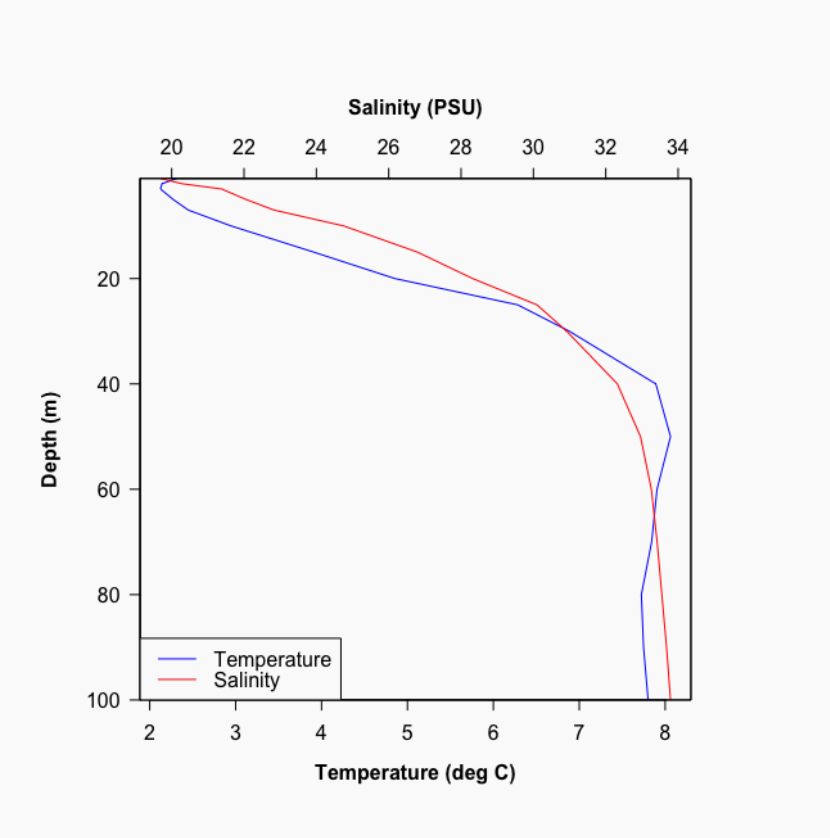

February 21st 2017

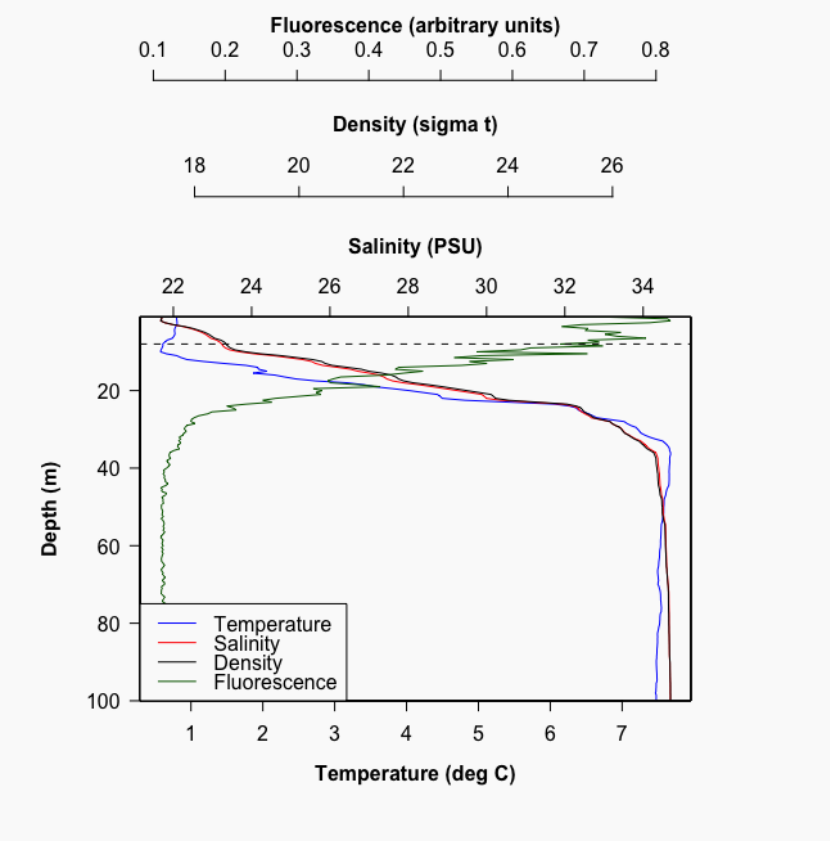

March 7th 2017

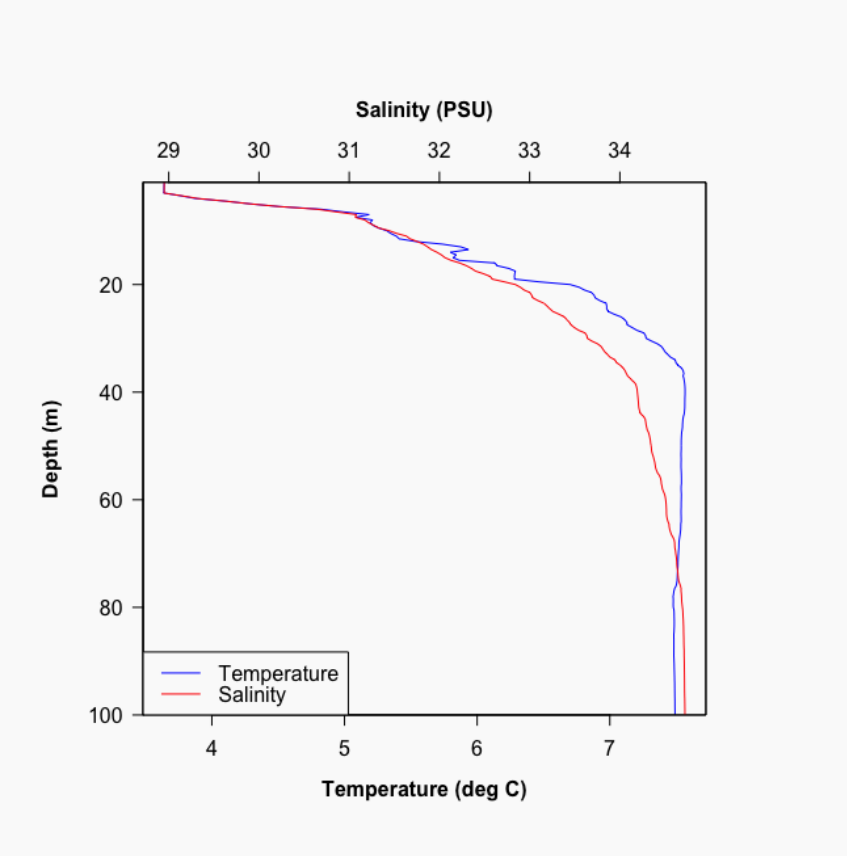

April 19th 2017

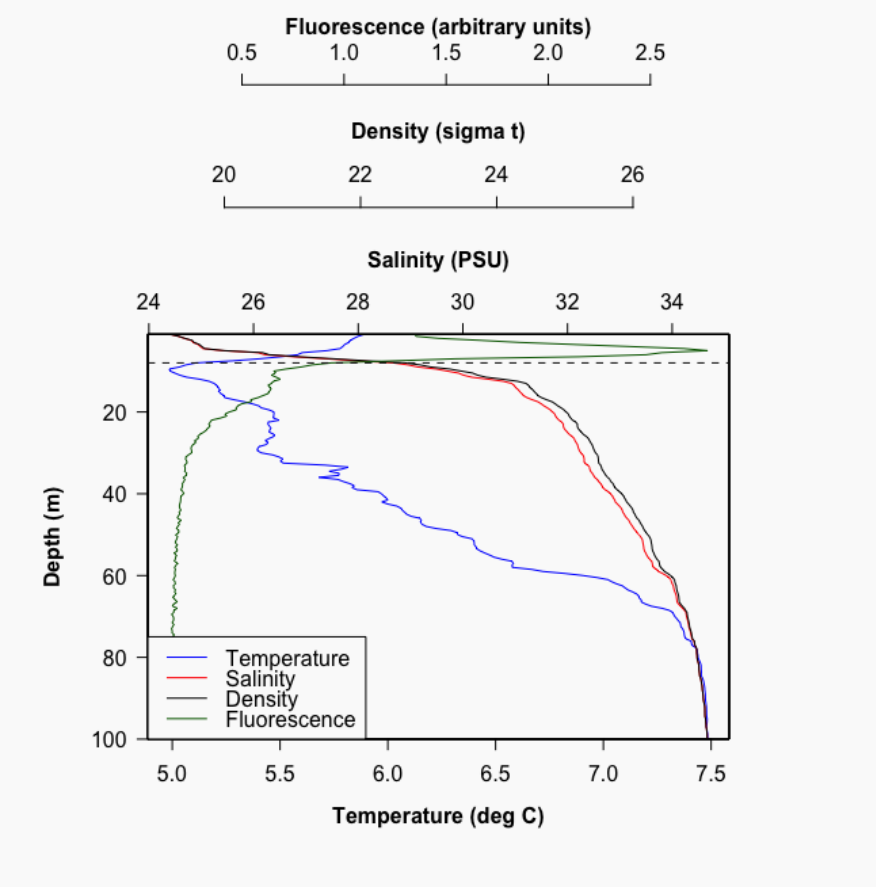

May 16th 2017

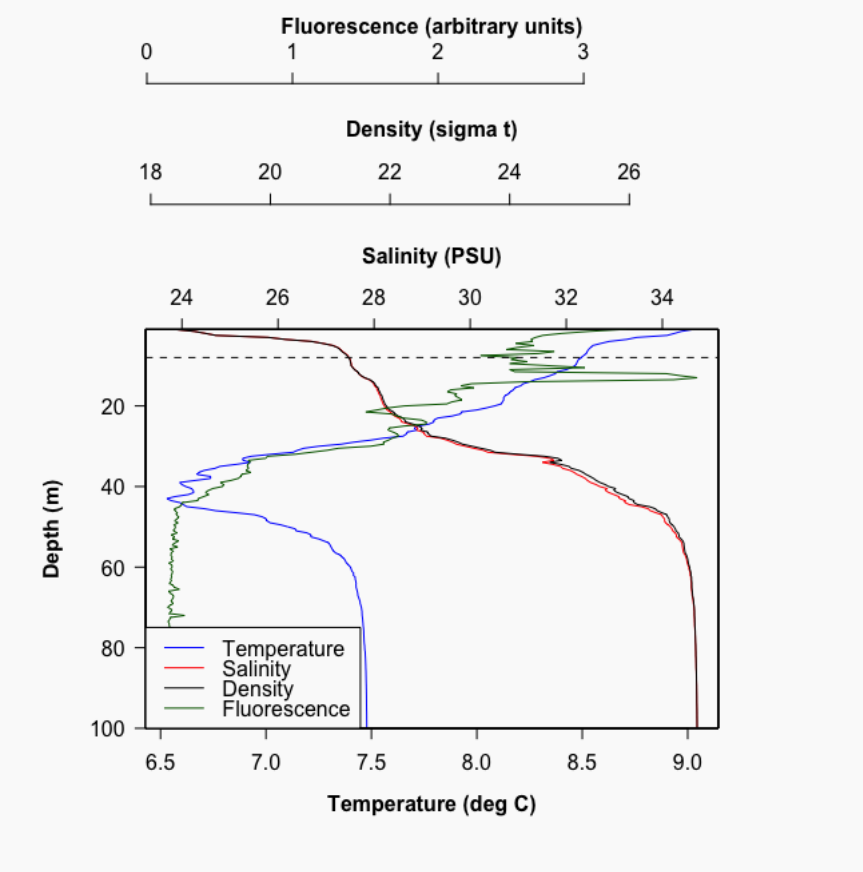

June 8th 2017

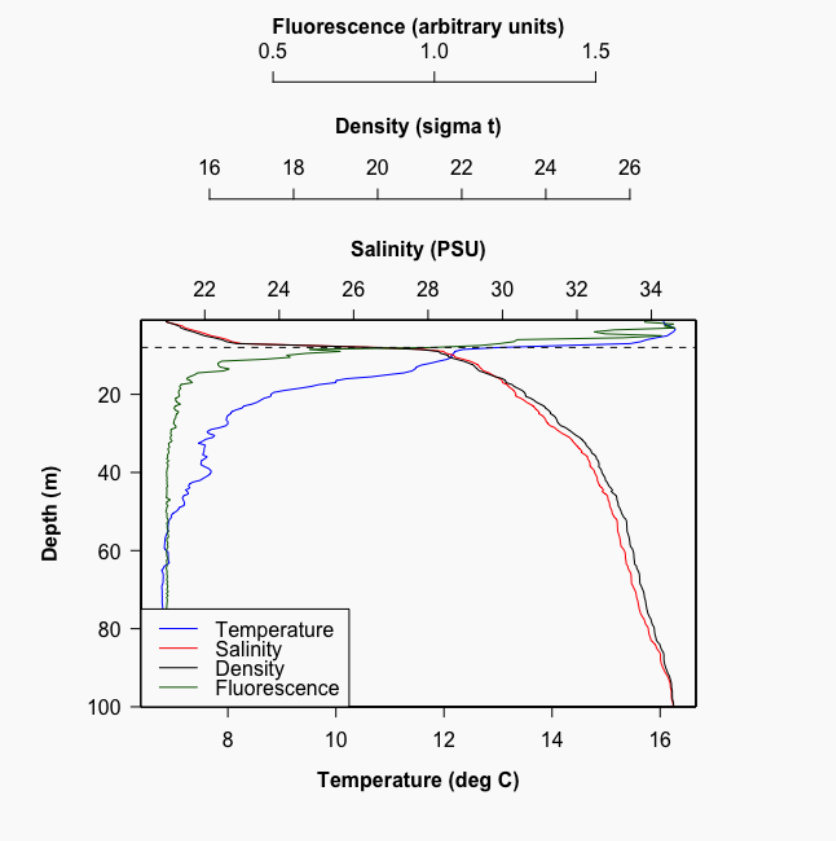

August 7th 2017

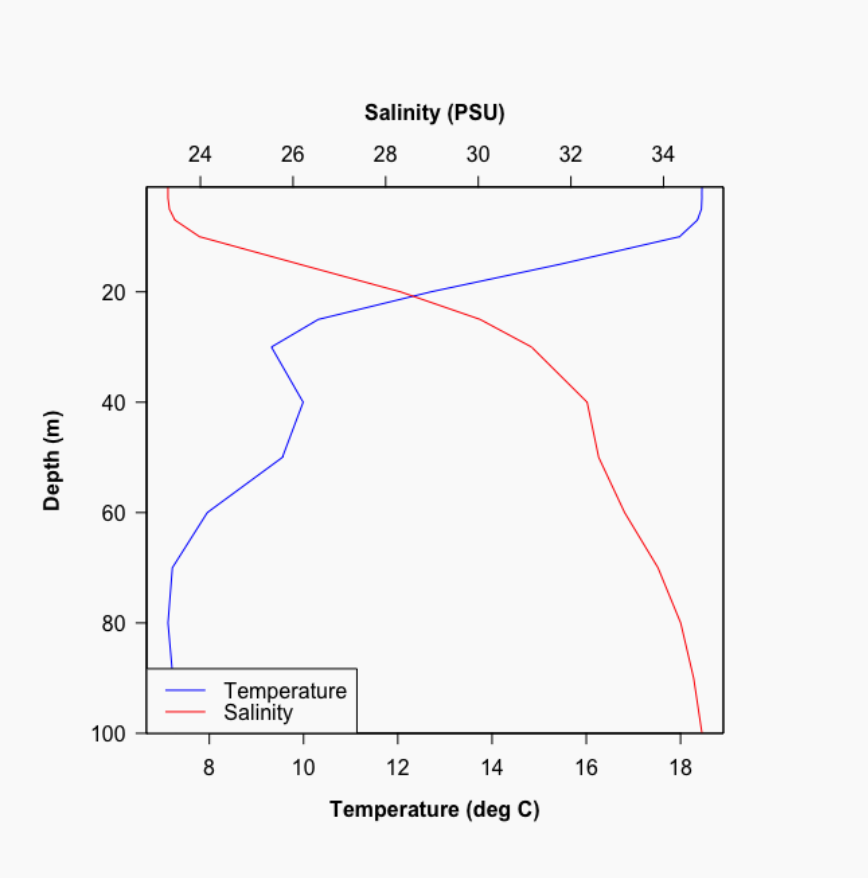

Appendix 7: Cell enumeration from the study of Hasle & Smayda (1960**)**

Species list from 1957:

Species	Feb	Marc h	April	May	June	July	Aug	Sept	Oct	Nov	Dec
DIATOMS											
Cosinosira polychorda	0	<500	0	0	0	0	0	0	0	0	0
Cerataulina pelagica	<500	<500	8000	0	<500	0	2000	22100	45830	0	0
Chaetoceros affinis	0	0	<500	0	0	0	8200	<500	0	0	0
Chaetoceros calcitrans	1500	500	30710	1200	0	0	7000	0	3500	0	0
Chaetoceros compressus	0	0	0	0	0	0	1440	500	0	0	0
Chaetoceros constrictus	0	0	2240	0	0	0	0	0	0	0	0

Chaetoceros curvisetus	0	0	0	0	0	0	2500 0	18000	<500	0	0
Chaetoceros debilis	<500	16500	640	0	0	0	0	0	0	0	0
Chaetoceros decipiens	0	6560	2320	0	<500	0	0	0	0	0	0
Chaetoceros laciniosus	0	24500	5500	0	0	0	0	0	0	0	0
Chaetoceros septentrionalis	0	0	0	0	0	0	0	0	0	0	0
Chaetoceros socialis	0	44000	279000	0	0	0	26500	0	0	0	0
Cyclotella caspia	0	0	0	0	0	5000	60000	0	120000	0	0
Cylindrotheca closterium	<500	500	3500	<500	<500	0	26000	5000	59000	<500	0
Lauderia annulata	0	<500	0	0	0	0	0	670000	67000	0	0
Leptocylindrus danicus	0	14500	3000	<500	0	0	0	0	63000	0	<500
Leptocylindrus minimus	3500	86000	14200	2450	0	0	0	0	11000	0	0
Pseudo-nitzschia delicatissima	<500	9500	27000	<500	500	0	11000	3000	<500	0	<500
Pseudo-nitzschia seriata	800	12450	38500	<500	0	0	500	0	0	0	<500
Skeletonema costatum	0	55500	224500	11000	15000	10000	0	14000	<500	<500	1000
Thalassionema nitzschioides	0	<500	500	<500	14500	600	3800	620	<500	<500	0
Thalassiosira gravida	0	500	<500	0	0	0	0	0	1600	<500	<500
Thalassiosira nordenskioldii	0	12000	206000	0	0	0	0	0	0	<500	<500
DINOFLAGELLATES											

Alexandrium tamarense	<100	0	580	140	0	0	<100	0	0	0	0
Amylax triacantha	0	0	<100	<100	<100	<100	0	0	0	0	<100
Dinophysis acuminata	1660	900	1100	220	140	880	<100	<100	<100	<100	0
Dinophysis acuta	0	180	200	<100	<100	0	0	0	180	200	<100
Dinophysis norvegica	<100	0	320	100	<100	0	<100	<100	<100	<100	0
Gymnodinaceae	9500	<100	34450	33000	3000	4000	5000	4000	6000	4220	<100
Gymnodinium gracile	480	<100	1040	19000	0	0	540	0	4040	100	<100
Heterocapsa triquetra	0	0	860	5000	4500	10000	<100	8000	120	0	0
Lingulodinium polyedra	0	0	0	0	0	<100	18500	800	<100	0	0
Peridinium minusculum	0	0	4500	26000	<100	13000	0	<100	9500	0	0
Prorocentrum balticum	<100	<100	<100	<100	201000	5500	<100	5000	0	0	0
Prorocentrum micans	0	0	0	<100	<100	<100	22000	3200	5540	<100	0
Protoceratium reticulatum	0	0	720	140	0	<100	0	0	0	0	0
Protoperidinium brevipes	<100	0	6000	3100	0	0	<100	0	<100	<100	<100
Protoperidinium pellucidum	0	0	720	640	0	200	0	160	220	0	0
Pyrophacus steinii	0	0	0	0	0	0	860	600	0	0	0
Scripsiella acuminata	<100	0	41000	4000	300	3500	5500	720	540	<100	0
Tripos furca	0	0	0	1180	820	160	2040	12160	2340	320	<100

Tripos fusus	0	0	0	210	<100	<100	1380	2480	220	<100	0
Tripos lineatus	0	0	0	780	0	0	<100	0	0	0	0
Tripos longipes	0	<100	<100	800	480	0	0	0	<100	<100	<100
Tripos macroceros	0	0	0	140	0	0	0	<100	100	<100	<100
Tripos muelleri	<100	380	100	1280	3860	1840	540	320	180	0	<100

*some names have been changes to current accepted taxonomic names

Species list from 1958:

Species	**Jan**	**Feb**	**March**	**April**	**May**
DIATOMS					
Cosinosira polychorda	0	0	69500	920	0
Cerataulina pelagica	0	0	62000	2500	18000
Chaetoceros affinis	0	<500	2040	1000	0
Chaetoceros calcitrans	0	0	0	0	0
Chaetoceros compressus	0	<500	0	4500	0
Chaetoceros constrictus	<500	0	45000	1640	12500
Chaetoceros curvisetus	0	0	0	0	<500
Chaetoceros debilis	<500	<500	177000	162000	1120000
Chaetoceros decipiens	0	<500	<500	<500	31000
Chaetoceros laciniosus	0	0	115000	17000	65000
Chaetoceros septentrionalis	0	0	3000	500	110000
Chaetoceros socialis	0	<500	67000	1500	3000
Cyclotella caspia	0	600	0	0	0
Cylindrotheca closterium	<500	0	0	<500	3000
Lauderia annulata	0	0		0	0
Leptocylindrus danicus	7000	<500	220	2500	9000
Leptocylindrus minimus	0	0	3000	5500	11000
Pseudo-nitzschia delicatissima	<500	2320	172000	7000	61000
Pseudo-nitzschia seriata	<500	<500	7320	13000	<500
Skeletonema costatum	1640	150000	12000	974000	
Thalassionema nitzschioides	9480	1600	560	0	<500
Thalassiosira gravida	0	<500	17300	1088	0
Thalassiosira nordenskioldii	<500	0	1308500	11620	780
DINOFLAGELLATES					

Alexandrium tamarense	0	0	<100	<100	1120
Amylax triacantha	0	0	0	<100	2680
Dinophysis acuminata	100	220	<100	660	1720
Dinophysis acuta	0	0	0	0	0
Dinophysis norvegica	<100	<100	<100	<100	<100
Gymnodinaceae	3500	3000	22000	8940	54000
Gymnodinium gracile	<100	<100	480	700	960
Heterocapsa triquetra	0	<100	0	<100	3000
Lingulodinium polyedra	0	0	<100	<100	0
Peridinium minusculum	<100	0	<100	0	6000
Prorocentrum balticum	<100	0	<100	3000	3000
Prorocentrum micans	0	0	0	0	<100
Protoceratium reticulatum	0	0	0	140	280
Protoperidinium brevipes	<100	<100	180	600	12000
Protoperidinium pellucidum	<100	0	<100	1360	1200
Pyrophacus steinii	0	0	0	0	0
Scripsiella acuminata	<100	<100	120	<100	10000
Tripos furca	0	0	<100	0	<100
Tripos fusus	0	0	<100	0	<100
Tripos lineatus	<100	0	0	0	0
Tripos longipes	<100	0	0	<100	200
Tripos macroceros	<100	0	0	0	0
Tripos muelleri	100	0	0	<100	<100

*some names have been changes to current accepted taxonomic names

Appendix 7: Biovolume raw data from Plankton toolbox

Month	Species	abundance_units_l	volume_mm3_l	volume_um3_unit
Sept 12.	*Ceratium lineatum*	160	2.886	18040
Sept 12.	*Ceratoneis closterium**	8880	1.598	180
Sept 12.	*Chaetoceros*	5720	1.848	323
Sept 12.	*Gymnodiniales*	4200	3.772	898
Sept 12.	*Gyrodinium fusiforme*	5320	87.44	16440

Sept 12.	*Peridiniales*	17840	30.81	1727
Sept 12.	*Prorocentrum micans*	13000	105.2	8095
Sept 12.	*Pseudo-nitzschia*	20320	12.44	612
Sept 12.	*Rhizosolenia*	4520	319.3	70650
Oct 27.	*Cerataulina pelagica*	560	1.539	2748
Oct 27.	*Ceratium lineatum*	80	1.02	12750
Oct 27.	*Ceratoneis closterium*	4000	0.72	180
Oct 27.	*Chaetoceros curvisetus*	3480	4.611	1325
Oct 27.	*Chaetoceros decipiens*	1360	5.739	4220
Oct 27.	*Chaetoceros*	4440	1.434	323
Oct 27.	*Dictyocha speculum*	240	2.693	11220
Oct 27.	*Guinardia flaccida*	1400	30.77	21980
Oct 27.	*Gymnodiniales*	840	0.7543	898
Oct 27.	*Gyrodinium fusiforme*	200	3.287	16440
Oct 27.	*Leptocylindrus danicus*	5400	11.53	2135
Oct 27.	*Melosira*	80	0.08904	1113
Oct 27.	*Navicula*	1720	0.645	375
Oct 27.	*Pseudo-nitzschia*	22960	14.05	612
Oct 27.	*Skeletonema marinoi*	1600	1.382	864

Oct 27.	*Thalassiosira*	280	0.8792	3140
Nov 25.	*Akashiwo sanguinea*	800	35.9	44880
Nov 25.	*Ceratium lineatum*	360	6.493	18040
Nov 25.	*Ceratium tripos*	280	37.46	133800
Nov 25.	*Chaetoceros*	120	0.1448	1207
Jan 3.	*Ceratium tripos*	40	3.486	87140
Jan 3.	*Ceratoneis closterium*	360	0.0648	180
Jan 3.	*Chaetoceros*	160	0.09008	563
Jan 3.	*Dactyliosolen fragilissimus*	160	1.064	6649
Jan 3.	*Dictyocha speculum*	800	3.271	4089
Jan 3.	*Dinophysis acuta*	80	3.133	39170
Jan 3.	*Ditylum brightwellii*	80	2.205	27560
Jan 3.	*Gymnodiniales*	680	1.574	2314
Jan 3.	*Leptocylindrus danicus*	4520	3.96	876
Jan 3.	*Peridiniales*	240	3.293	13720
Jan 3.	*Pseudo-nitzschia*	4360	2.668	612
Jan 3.	*Skeletonema marinoi*	520	0.17	327
Jan 3.	*Thalassiosira*	800	2.512	3140
Feb 3.	*Akashiwo sanguinea*	640	28.72	44880
Feb 3.	*Ceratoneis closterium*	480	0.0864	180
Feb 3.	*Chaetoceros*	320	0.1034	323
Feb 3.	*Dictyocha speculum*	920	3.762	4089
Feb 3.	*Dinophysis acuminata*	40	0.3206	8014

Feb 3.	*Dinophysis norvegica*	40	1.171	29290
Feb 3.	*Dinophysis*	40	0.08024	2006
Feb 3.	*Eutreptiella*	440	0.3318	754
Feb 3.	*Gymnodiniales*	1280	1.613	1260
Feb 3.	*Gyrodinium fusiforme*	40	0.6574	16440
Feb 3.	*Leptocylindrus danicus*	200	0.157	785
Feb 3.	*Peridiniales*	1440	20.35	14130
Feb 3.	*Prorocentrum balticum***	280	0.2898	1035
Feb 3.	*Pseudo-nitzschia*	800	0.4896	612
Feb 3.	*Skeletonema marinoi*	3560	0.5945	167
Feb 21.	*Chaetoceros*	1680	8.902	5299
Feb 21.	*Dictyocha speculum*	400	1.636	4089
Feb 21.	*Ditylum brightwellii*	80	4.608	57600
Feb 21.	*Eutreptiella*	2520	1.068	424
Feb 21.	*Gymnodiniales*	5240	66.64	12720
Feb 21.	*Peridiniales*	9520	29.39	3087
Feb 21.	*Rhizosolenia*	1520	107.4	70650
Feb 21.	*Skeletonema marinoi*	70840	22.03	311
Feb 21.	*Thalassionema nitzschioides*	3840	5.76	1500
Feb 21.	*Thalassiosira*	1680	5.275	3140
March 7.	*Akashiwo sanguinea*	400	17.95	44880

March 7.	*Ceratium lineatum*	200	2.549	12750
March 7.	*Ceratoneis closterium*	2300	0.414	180
March 7.	*Chaetoceros decipiens*	5300	71.15	13420
March 7.	*Chaetoceros socialis*	10600	3.328	314
March 7.	*Chaetoceros*	10700	2.45	229
March 7.	*Coscinodiscus*	200	10.01	50070
March 7.	*Dictyocha speculum*	4700	19.22	4089
March 7.	*Gymnodiniales*	7000	46.07	6582
March 7.	*Leptocylindrus danicus*	1500	0.9045	603
March 7.	*Navicula*	3000	1.125	375
March 7.	*Peridiniales*	1800	5.557	3087
March 7.	*Proboscia alata*	500	3.454	6908
March 7.	*Prorocentrum balticum*	62100	98.74	1590
March 7.	*Pseudo-nitzschia*	12400	5.357	432
March 7.	*Rhizosolenia*	3000	3.768	1256
March 7.	*Skeletonema marinoi*	330900	241.9	731
March 7.	*Thalassionema nitzschioides*	8300	12.45	1500
March 7.	*Thalassiosira*	14800	46.47	3140
April 19.	*Ceratoneis closterium*	12400	2.232	180

April 19.	*Chaetoceros decipiens*	45600	1654	36270
April 19.	*Chaetoceros tenuisimus*	25000	0.325	13
April 19.	*Chaetoceros*	26000	5.954	229
April 19.	*Gymnodiniales*	49600	114.8	2314
April 19.	*Leptocylindrus danicus*	66600	40.16	603
April 19.	*Peridiniales*	2300	31.55	13720
April 19.	*Proboscia alata*	1000	6.908	6908
April 19.	*Prorocentrum balticum*	354100	563	1590
April 19.	*Pseudo-nitzschia*	1023000	442	432
April 19.	*Skeletonema marinoi*	800300	691.5	864
April 19.	*Thalassionema nitzschioides*	32600	48.9	1500
May 16.	*Ceratium fusus*	200	4.755	23770
May 16.	*Ceratium tripos*	600	52.28	87140
May 16.	*Chaetoceros*	6200	2.003	323
May 16.	*Dactyliosolen fragilissimus*	12200	161.6	13250
May 16.	*Dinobryon*	4800	0.0912	19
May 16.	*Dinophysis*	200	0.7238	3619
May 16.	*Guinardia flaccida*	1100	13.41	12190
May 16.	*Gymnodiniales*	3800	8.793	2314

May 16.	*Peridiniales*	2700	4.663	1727
May 16.	*Pseudo-nitzschia*	4938000000	2133000	432
May 16.	*Scripsiella*	4700	19.68	4187
May 16.	*Skeletonema marinoi*	173100	23.2	134
May 16.	*Thalassionema nitzschioides*	53900	21.83	405
June 22.	*Ceratium horridum*	700	34.16	48810
June 22.	*Ceratium tripos*	2200	294.3	133800
June 22.	*Ceratoneis closterium*	2500	0.45	180
June 22.	*Chaetoceros*	26500	9.063	342
June 22.	*Dactyliosolen fragilissimus*	67800	450.8	6649
June 22.	*Dinophysis norvegica*	900	26.36	29290
June 22.	*Leptocylindrus danicus*	4300	3.376	785
June 22.	*Proboscia alata*	1600	11.05	6908
June 22.	*Prorocentrum balticum*	1300	1.345	1035
June 22.	*Pseudo-nitzschia*	166200	71.8	432
June 22.	*Skeletonema marinoi*	12300	1.648	134
Aug 7.	*Cerataulina pelagica*	21600	127.2	5888
Aug 7.	*Ceratoneis closterium*	1200	0.216	180
Aug 7.	*Chaetoceros*	4000	0.916	229

Aug 7.	*Dactyliosolen fragilissimus*	246300	2024	8218
Aug 7.	*Gymnodiniales*	2400	5.554	2314
Aug 7.	*Leptocylindrus danicus*	49600	38.94	785
Aug 7.	*Proboscia alata*	1700	11.74	6908
Aug 7.	*Prorocentrum micans*	4600	37.24	8095

***Ceratoneis closterum* is used in Phytoplankton toolbox and is regarded as a synonym for *Cylindrotheca closterum* (algeabase.org)

***Prorocentrum balticum* was the only *Prorocentrum* in Phytoplankton toolbox which matched the size of *P. minimum* and *Prorocentrum* spp.

Appendix 9: Fluorescence measurements from Oslofjorden 2017 provided by Marit Norli, NIVA. Drøbak is at 59.66 (black line).